VOLUME 83 NUMBER 2

THE ASTROPHYSICAL JOURNAL

AN INTERNATIONAL REVIEW OF SPECTROSCOPY AND ASTRONOMICAL PHYSICS

Founded in 1895 by GEORGE E. HALE *and* JAMES E. KEELER

Edited by

HENRY G. GALE
Ryerson Physical Laboratory of the University of Chicago

FREDERICK H. SEARES
Mount Wilson Observatory of the Carnegie Institution of Washington

OTTO STRUVE
Yerkes Observatory of the University of Chicago

MARCH 1936

THE UNIVERSITY OF CHICAGO PRESS
CHICAGO, ILLINOIS, U.S.A.

March 1936 Vol. 83, No. 2

THE ASTROPHYSICAL JOURNAL

AN INTERNATIONAL REVIEW OF SPECTROSCOPY AND ASTRONOMICAL PHYSICS

The Astrophysical Journal is published by the University of Chicago at the University of Chicago Press, 5750 Ellis Avenue, Chicago, Illinois, during each month except February and August. ¶The subscription price is $6.00 a year; the price of single copies is 75 cents. Orders for service of less than a half-year will be charged at the single-copy rate. ¶Postage is prepaid by the publishers on all orders from the United States, Mexico, Cuba, Porto Rico, Panama Canal Zone, Republic of Panama, Dominican Republic, Canary Islands, El Salvador, Argentina, Bolivia, Brazil, Colombia, Chile, Costa Rica, Ecuador, Guatemala, Honduras, Nicaragua, Peru, Hayti, Uruguay, Paraguay, Hawaiian Islands, Philippine Islands, Guam, Samoan Islands, Balearic Islands, Spain, and Venezuela. ¶Postage is charged extra as follows: for Canada and Newfoundland, 30 cents on annual subscriptions (total $6.30); on single copies, 3 cents (total 78 cents); for all other countries in the Postal Union, 80 cents on annual subscriptions (total $6.80), on single copies, 8 cents (total 83 cents). ¶Patrons are requested to make all remittances payable to The University of Chicago Press, in postal or express money orders or bank drafts.

The following are authorized agents:

For the British Empire, except North America, India, and Australasia: The Cambridge University Press, Fetter Lane, London, E.C. 4. Prices of yearly subscriptions and of single copies may be had on application.

For Japan: The Maruzen Company, Ltd., Tokyo.

For Chnia: The Commercial Press, Ltd., 211 Honan Road, Shanghai. Yearly subscriptions, $6.00; single copies, 75 cents, or their equivalents in Chinese money. Postage extra, on yearly subscriptions 80 cents, on single copies 8 cents.

Claims for missing numbers should be made within the month following the regular month of publication. The publishers expect to supply missing numbers free only when losses have been sustained in transit, and when the reserve stock will permit.

Business correspondence should be addressed to The University of Chicago Press, Chicago, Illinois.

Communications for the editors and manuscripts should be addressed to: Otto Struve, Editor of THE ASTROPHYSICAL JOURNAL, Yerkes Observatory, Williams Bay, Wisconsin.

The cable address is "Observatory, Williamsbay, Wisconsin."

The articles in this journal are indexed in the *International Index to Periodicals*, New York, N.Y.

Applications for permission to quote from this journal should be addressed to The University of Chicago Press, and will be freely granted.

Entered as second-class matter, January 17, 1895, at the Post-Office, Chicago, Ill., under the act of March 3, 1879.
Acceptance for mailing at special rate of postage provided for in Section 1103, Act of October 3, 1917, authorized on July 15, 1918.

PRINTED IN THE U.S.A.

THE ASTROPHYSICAL JOURNAL

AN INTERNATIONAL REVIEW OF SPECTROSCOPY AND ASTRONOMICAL PHYSICS

VOLUME 83 MARCH 1936 NUMBER 2

DARKENING AT THE LIMB AND COLOR INDEX OF AN ECLIPSING VARIABLE (U Cephei)

H. O. ROSENBERG

ABSTRACT

A method is described whereby it is possible to derive color indices for two effective wave-lengths from simultaneous exposures on one plate, in the focal plane of a Newtonian reflector.

This method was used for the eclipsing variable U Cephei at λ 4015 and λ 6165. The total change in color index between the phase of constant light and that of primary minimum amounts to 1.51 mag. The greater part of this change is caused by the difference in spectral type between the bright star (Ao) and the fainter component (G6). A study of the individual light-curves obtained in different wave-lengths reveals an effect of darkening at the limb, which increases with decreasing wave-length and which is comparable to the darkening observed in the sun. However, the total range in the amount of darkening between λ 4015 and λ 6165 is smaller for the Ao star than for the sun.

THE PROBLEM

Spectrophotometric measures on the surface of the sun have lead to the conclusion[1] that the amount of darkening at the limb increases with decreasing wave-length. It would not be unreasonable to expect that a similar relation between darkening and wave-length would exist in the stars, but heretofore no observational evidence has been found in support of this assumption. From theoretical considerations it would seem probable that the amount of darkening would vary with the effective temperature or with the spectral type of the star. As a first approximation,[2] the darkening is a function of $\lambda \cdot T_{abs}$; hence, for a constant temperature the darkening will decrease with increasing wave-length, and for a constant wave-length it will increase with decreasing temperature.

[1] Vogel; Abbot and Fowle; Very; Moll, van der Bilt, and Burger; Schwarzschild and Villiger; *et al.*

[2] Milne, *Phil. Trans.* (A), **223**, 201, 1923; Lindblad, *Nova Acta Upsala*, **6**, No. 1, 1923.

The effect of darkening at the limb in stars can be observed only in the case of eclipsing variables where the shape of the light-curve depends upon the amount of darkening. In the simple case of a central total eclipse the "darkened curve" shows, as Shapley has stated,[3] a somewhat slower change in light at the beginning of the eclipse and just preceding the beginning of totality than would be observed in the case of uniformly illuminated disks. The opposite occurs in that phase of the variable in which the edge of the eclipsing star moves over the center of the eclipsed star: here, where the change of light is most rapid, the "darkened curve" is steeper than the "uniform curve." In practice, both curves are usually made to coincide in their steepest parts. Accordingly, the difference in shape between the two curves consists of a longer duration of the darkened eclipse and a shorter duration of the phase of constant minimum. The greatest difference occurs just before totality; at that point it corresponds to nearly the full amount of the darkening.

In the case of an annular or a partial eclipse, the problem is more complicated. The theory of the effect has been discussed by various authors.[4]

There is, however, another effect caused by darkening that has not heretofore been observed. Since the amount of darkening increases with decreasing wave-length, the color index of an eclipsing variable must increase near the minimum; and it is not improbable that this change of color index would be large enough to be detected. Thus, if we compute the loss of light in the sun for a hypothetical annular eclipse, at λ 4150 and λ 6500 and for different radii of the eclipsing dark body, we find:

Radius of Eclipsing Body	Loss of Light		Δ Color Index
	λ 4150	λ 6500	
0.50	$0^{M}.56$	$0^{M}.43$	$+0^{M}.13$
.60	0.84	0.65	.19
.70	1.20	0.96	.24
.80	1.75	1.45	.30
0.90	2.80	2.41	+0.39

[3] *Princeton Contr.*, No. 3, 107, 1915.

[4] Russell and Shapley, several papers in *Ap. J.*, **35** and **36**, 1912; Blažko, *Ann. Obs. Moscow*, **2**, **94**, 1911; Harzer, *Pub. Kiel*, **16**, 1927.

Even if the darkening effect in most eclipsing variables having spectral types earlier than that of the sun should be less than was found above, an attempt to investigate the change in color index would be well worth while.

The influence of darkening upon the color index of an eclipsing variable may be masked by a change in color index that is caused by the differences in the spectral types of the components. Most of the eclipsing binaries which have large ranges of variation in light are composed of a bright primary body and a fainter but larger companion. Accordingly, the effective temperature of the companion must be lower than that of the primary star. When the light is constant, the color of the principal star outweighs that of the companion; at primary minimum the observed color index is largely that of the component. The problem is to separate the darkening effect and the effect caused by the difference in spectral type.

THE METHOD

Two wedge-shaped half-filters, one red and the other blue, were inserted in the light beam of the 24-inch reflector of the Yerkes

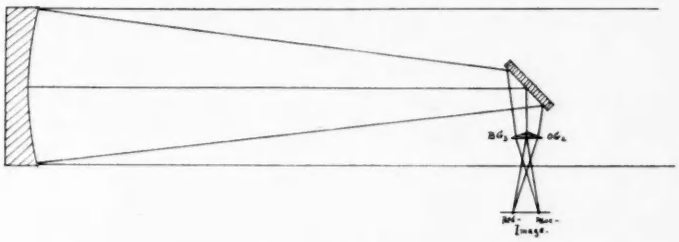

FIG. 1.—The optical arrangement

Observatory at a distance of about 20 cm in front of the focal plane. This method, suggested by me[5] some years ago, has the advantage of giving two focal images of the same star for each exposure. The distance between the blue image and the red image is about 1 mm. Since the refracting angle of the prismatic filters is only 15′, the prismatic dispersion may be neglected; even faint star images are quite round on the plates. The optical arrangement is shown in Figure 1.

[5] Führer, *Pub. Kiel Obs.*, **19**, 1933.

The filters and the photographic emulsions were chosen to give sufficiently strong star images with exposures of not more than 5 minutes for apparent magnitude 10. In order to obtain the highest possible precision, the blue image and the red image should be of approximately the same intensity for stars of average spectral class, and at the same time the difference between the effective wave-lengths of the two images must be as large as possible.

I finally decided to use Schott filters OG_2 and BG_3, in connection with Wratten and Wainwright Panchromatic plates, which have a

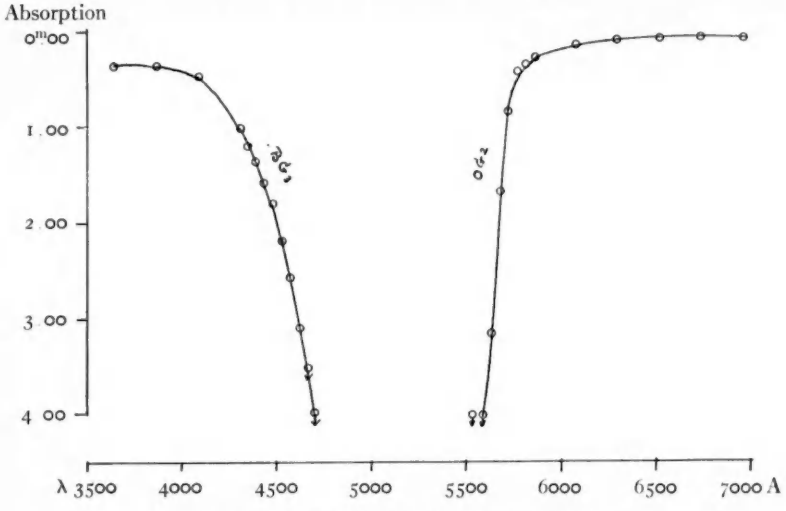

FIG. 2.—Absorption of filters BG_3 and OG_2

nearly constant sensitivity between the shortest wave-length transmitted by our atmosphere and λ 6300. All plates were backed. Table I gives the absorption and the corresponding loss of light for each filter (Fig. 2).

Each filter limits its range of wave-lengths on one side only. On the other side the limits are fixed for the blue image by the extinction in our atmosphere and for the red image by the end of the sensitivity of the plate. The effective wave-lengths for the two images are: λ 4015 and λ 6165. For stars of type Go the blue and the red images have the same intensity. For earlier types the blue image predominates, while for later types the red image prevails. Plate V shows a series of exposures for δ Scorpii (Bo), α Scorpii (Ma), and

PLATE V

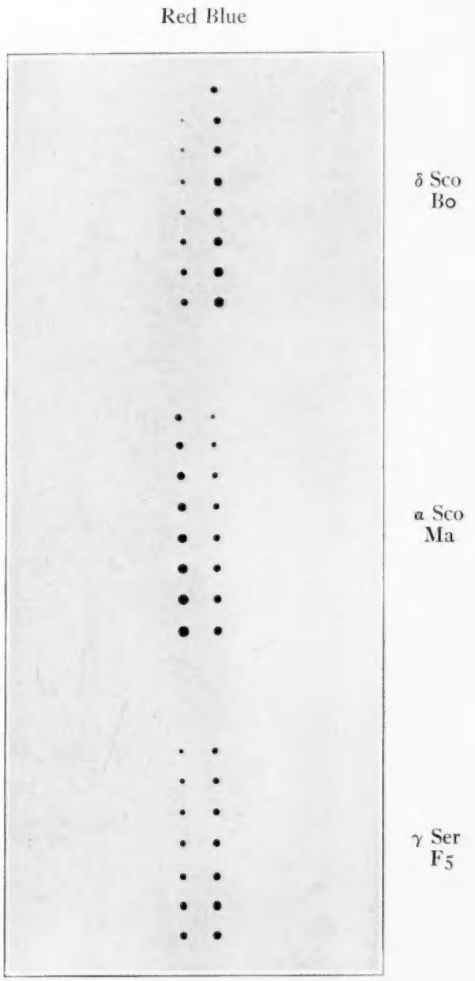

STAR IMAGES OBTAINED WITH WEDGE-SHAPED FILTERS, ATTACHED TO 24-INCH REFLECTOR

(Enlarged four times)

γ Serpentis (F5). Each step corresponds to half a magnitude. The difference in color index between the blue and the red images, for the Bo star and the Ma star, is approximately 4 mag.

TABLE I

BG_3			OG_2		
λ	Absorption	Loss of Light	λ	Absorption	Loss of Light
3641	0^M35	0.276	5543	4.0:	0.975
3862	0.34	.269	5588	4.0:	.975
4083	0.47	.351	5632	3.12	.944
4304	1.00	.602	5676	1.66	.783
4348	1.17	.660	5720	0.83	.534
4392	1.33	.706	5765	0.40	.308
4437	1.58	.767	5809	0.32	.255
4481	1.79	.808	5853	0.25	.206
4524	2.18	.866	6074	0.13	.113
4568	2.58	.907	6296	0.09	.080
4612	3.09	.942	6517	0.08	.071
4656	3.5:	.960	6738	0.07	.062
4700	4.0:	0.975	6959	0.07	0.062

Assuming the color index of an Ao star to be 0.00 mag., we obtain the relation between spectral class and color index shown in Table II.

TABLE II

Sp.	Color Index	Sp.	Color Index
		A1	$+0^M09$
Bo	-0^M81	A2	0.30
B2	.61	A3	0.40
B5	.38	F8	1.02
B8	− .09	K2	2.25
Ao	0.00	Ma	+3.12

By shifting the plateholder behind a small diaphragm, it was possible to obtain 120 single exposures on each plate. In order to obtain the scale of intensities, I adopted the method of variation of exposure time used by Dr. Führer.[6] The relation between exposure-time and intensity was carefully checked by means of exposures on the polar sequence and by exposures of stars obtained with and without a grating having a wickerwork of metallic wires, for which

[6] *Loc. cit.*

the absorption for the central diffraction disk was found to be $2^{M}.264 \pm 0^{M}.004$.

Because of the rapid changes in the transparency of the sky and in the seeing at Williams Bay, it was necessary to photograph the comparison stars simultaneously with the variable. This restricted the number of suitable objects, and the present discussion deals exclusively with the eclipsing variable U Cephei.

U CEPHEI

Earlier investigations[7] of U Cephei show that its eclipse is central and that the phase of totality lasts for about $0^{d}.08$. The range of the variation in light is large, being approximately 2.3 mag. for visual observations; and the brightness of the star at primary minimum, 9.2 mag., gives well-exposed blue and red images in 3 minutes. The Henry Draper spectral type is Ao; but according to a remark in the same catalogue the spectrum of the fainter star is of class Ko. This is in good agreement with an earlier statement by Blažko[8] and with the results of other observers, who had found that the variable is much redder at minimum than at constant light; hence, a considerable change in the color index of the variable was to be expected.

Table III gives the necessary data for the variable and the comparison stars used in this work. BD 81°30 has been used by many

TABLE III

U CEPHEI

BD	HD	α (1900)	δ (1900)	Ptm.	Ptg.	Sp.
81°25.....	5679	$0^{h}53^{m}.4$	+81°20′	var.	var.	Ao
81 26.....	.....	0 54.4	81 25	$10^{M}.51$	$10^{M}.60$	A2*
81 30.....	6006	0 56.3	+81 26	7.89	7.89	Ao

* According to my own measurements.

observers. Dugan found a sudden change of about $0^{M}.10$ for this star at about JD 242 1254 and suggested that some other comparison star be used in the future, although its magnitude seems to have been constant before and after that date.[9]

[7] Blažko, *op. cit.*, p. 94; Shapley, *op. cit.*, p. 36, and *Ap. J.*, **36**, 277, 1912; Dugan, *Princeton Contr.*, No. 5, 1920; Baker, *Laws Obs. Bull.* No. 30, 1921; Carpenter, *Ap. J.*, **72**, 212, 1930.

[8] *A.N.*, **181**, 298, 1909.

[9] Dugan, *op. cit.*, p. 5.

The elements of the variable used in this paper are taken from the *Katalog und Ephemeriden Veränderlicher Sterne*, by Prager.[10]

Epoch	JD 242 4253.6622	Secondary minimum	$6^{M}95$
Period	$2^{d}4929288$ (var.)	Duration of eclipse	$9^{h}1$
Constant light	$6^{M}85$	Duration of totality	$2^{h}1$
Primary minimum	$9^{M}19$		

Between October 25, 1934, and May 17, 1935, I obtained 1147 exposures of U Cephei, distributed over fifteen nights. Of these, 491 exposures on six nights were taken during primary minimum; the other exposures were taken at constant light or during secondary minimum. The plates were measured by means of photoelectric microphotometer of the writer's construction.[11]

On the nights of November 2 and November 11, 1934, two complete primary minima between phases $\pm 3^{h}5$ were observed, the light curves being symmetrical, except near minimum light. Deviations of $-0^{h}145$ and $-0^{h}147$ from Prager's epoch were derived. Accordingly, a correction of $-0^{d}0061$ was adopted for the epoch of my observations.

The photometric intensities of the comparison stars, given in Table III, permit us to reduce the magnitudes of U Cephei to the system of the *Henry Draper Catalogue*. As the effective wave-lengths used in this work do not coincide with either the photographic or the visual effective wave-lengths, these magnitudes have no great significance. They may, however, be compared with the magnitudes obtained by Shapley[12] from the visual observations of Wendell. It should be remembered that the spectra of the comparison stars are of approximately the same type as the spectrum of U Cephei in its phase of constant light.

The great difference in range for the three effective wave-lengths

	Blue λ 4015	Visual λ 5500	Red λ 6165
Constant light	$6^{M}73$	$6^{M}78$	$6^{M}81$
Primary minimum	10.18	9.17	8.75

[10] *Kleinere Veröffentlichungen der Univ. Sternwarte Berlin-Babelsberg*, No. 11, 1932.

[11] *Zs. f. Instrumentenkunde*, **45**, 313, 1925. [12] *Op. cit.*, p. 35.

TABLE IV

	Blue	Visual	Red
Constant light	$0^{M}00$	$0^{M}00$	$0^{M}00$
Primary minimum	$3^{M}45$	$2^{M}39$	$1^{M}94$
Secondary minimum	$0^{M}02$	$0^{M}07$	$0^{M}10$*
Semi-duration of primary eclipse	$0^{d}23$:	$0^{d}23$:	$0^{d}24$:
Semi-duration of totality	$0^{d}040$	$0^{d}043$	$0^{d}036$

* The secondary minimum is very flat, and some variations seem to be indicated in the observations for different epochs. The middle of the secondary minimum occurs at about $1^{d}40$ after the preceding primary minimum; this is $0^{d}15$ later than the mean of the two subsequent primary minima. The number of my observations during this phase is too small to derive the duration of the secondary minimum.

TABLE V

Phase	Red			Visual			Blue			Blue-Red
	Δ Mag.	C_u-O	C_d-O	Δ Mag.	C_u-O	C_d-O	Δ Mag.	C_u-O	C_d-O	Δ Color Index
$\pm 0^{d}2500$	$0^{M}00$	$0^{M}00$	$0^{M}00$	$0^{M}00$	$0^{M}00$	$0^{M}00$	$0^{M}00$	$0^{M}00$	$0^{M}00$	$0^{M}00$
± .2400	+0.01	− 1	− 1	+0.01	− 1	− 1	0.00	0	0	−0.01
± .2300	0.03	− 3	− 3	0.02	− 2	− 3	+0.02	− 2	− 2	−0.01
± .2200	0.05	− 5	− 4	0.04	− 4	− 4	0.04	− 4	− 3	−0.01
± .2100	0.07	− 4	− 4	0.06	− 4	− 4	0.06	− 4	− 4	−0.01
± .2000	0.08	− 3	− 3	0.08	− 4	− 4	0.09	− 4	− 4	+0.01
± .1900	0.11	− 2	− 3	0.12	− 3	− 5	0.12	− 3	− 4	+0.01
± .1800	0.14	0	− 2	0.16	− 2	− 4	0.17	− 3	− 5	+0.03
± .1700	0.18	+ 1	− 1	0.21	− 1	− 4	0.21	− 1	− 3	+0.03
± .1600	0.23	+ 3	0	0.26	+ 1	− 3	0.27	+ 1	− 2	+0.04
± .1500	0.29	+ 4	+ 2	0.34	+ 1	− 2	0.35	+ 2	− 2	+0.06
± .1400	0.38	+ 4	+ 2	0.43	+ 1	− 2	0.44	+ 2	0	+0.06
± .1300	0.48	+ 3	+ 2	0.54	0	− 2	0.56	+ 2	0	+0.08
± .1200	0.60	+ 1	+ 1	0.66	0	− 2	0.71	+ 1	+ 1	+0.11
± .1100	0.73	+ 1	+ 1	0.80	− 1	− 1	0.88	+ 1	+ 1	+0.15
± .1000	0.89	0	0	0.96	0	0	1.10	− 1	− 1	+0.21
± .0900	1.06	0	0	1.17	0	0	1.36	− 3	− 3	+0.30
± .0800	1.24	+ 1	+ 1	1.41	+ 1	+ 1	1.67	− 4	− 4	+0.43
− .0700	1.45	+ 2	+ 2	1.71	− 1	− 3	2.10	− 4	− 4	+0.65
− .0600	1.69	+ 4	0	2.02	0	− 6	2.59	+ 1	− 1	+0.90
− .0500	1.83	+ 8	+ 1	2.25	+ 11	− 1	3.02	+ 24	+ 1	+1.19
− .0400	1.92	+ 2	+ 2	2.38	+ 2	+ 1	3.39	+ 5	+ 3	+1.47
− .0300	1.93	+ 1	+ 1	2.39	+ 1	+ 1	3.41	+ 3	+ 3	+1.48
− .0200	1.93	+ 1	+ 1	2.40	0	0	3.42	+ 2	+ 2	+1.49
− .0100	1.93	+ 1	+ 1	2.40	0	0	3.43	+ 1	+ 1	+1.50
.0000	1.94	0	0	2.41	− 1	− 1	3.44	0	0	+1.50
+ .0100	1.94	0	0	2.42	− 2	− 2	3.46	− 2	− 2	+1.52
+ .0200	1.95	− 1	− 1	2.43	− 3	− 3	3.47	− 3	− 3	+1.52
+ .0300	1.95	− 1	− 1	2.44	− 4	− 4	3.48	− 4	− 4	+1.53
+ .0400	1.93	+ 1	+ 1	2.44	− 4	− 5	3.41	+ 3	+ 1	+1.48
+ .0500	1.84	+ 7	0	2.33	+ 3	− 7	3.04	+ 22	− 1	+1.20
+ .0600	1.68	+ 5	+ 1	2.04	− 2	− 8	2.59	+ 1	− 1	+0.91
+ .0700	+1.45	+ 2	+ 2	+1.71	− 1	− 1	+2.10	− 4	− 4	+0.65

indicates that the variation in color index amounts to $1^{M}.51$. Although other photographic observations have been available for

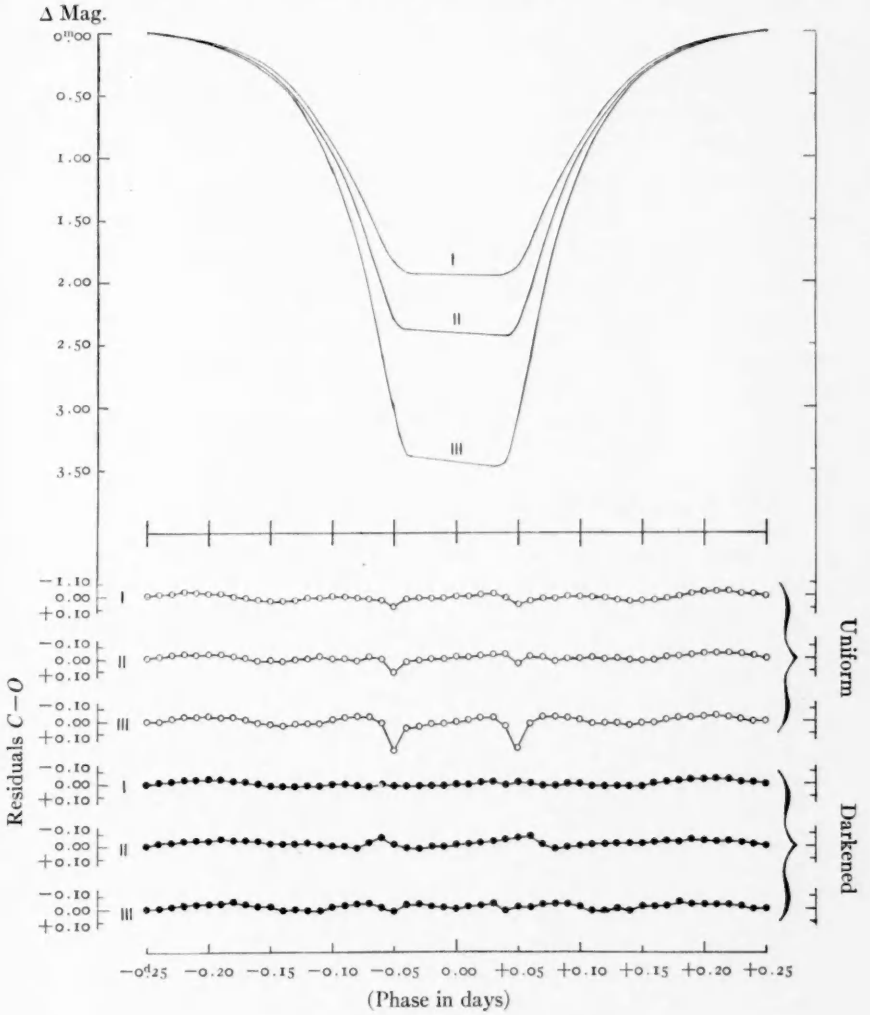

FIG. 3.—Light-curves of U Cephei
I Red (λ 6165)
II Visual (λ 5500)
III Blue (λ 4015)

some time,[13] no attention seems to have been given to this large change in color index.

[13] Baker, *loc. cit.;* Jordan and Parkhurst, *Ap. J.*, **23**, 81, 1906.

It is convenient in the following discussion to refer all intensities of U Cephei to the mean value of constant light. Table IV gives the characteristic data.

The smooth light-curves for the blue and red images seem to be symmetrical at primary eclipse. The departures between the descending and ascending branches amount to $0^{M}.01$ and $0^{M}.02$. In the vicinity of totality the curves are unsymmetrical; the brightness, instead of being at a constant minimum, gradually decreases by $0^{M}.09$ for the blue images, by $0^{M}.06$ for the visual observations of Wendell, and by $0^{M}.03$ for the red images. For all phases which are $0^{d}.06$ or more removed from the middle of the eclipse, I have taken the mean values for the descending and ascending branches.[14] The lack of symmetry at the time of totality seems to be common to stars of large range.[15] Table V gives the final light-curves for the blue and the red images, as well as for Wendell's observations (Fig. 3).

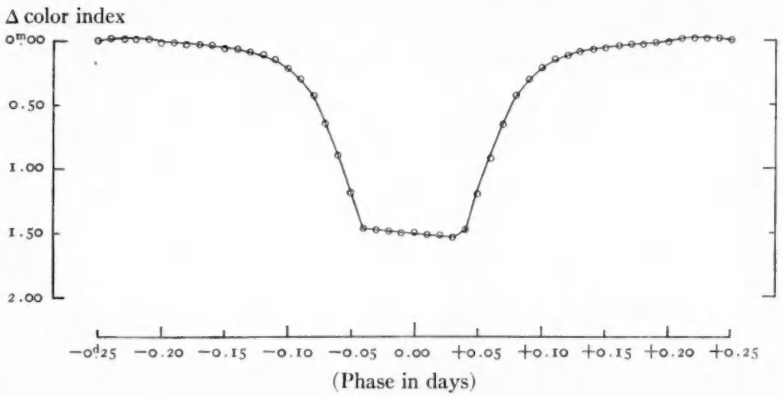

FIG. 4.—Δ color index of U Cephei

The differences in color index (Fig. 4) reveal a close correlation with the light-curve and are mostly due to the difference in spectral type of the two components. In order to isolate the small change of color index which might be expected to result from the darkening at the limb, I adopted the following procedure: Each individual light-curve was separately reduced in accordance with the theory of Russell and Shapley,[16] giving a uniform and a darkened solution. The

[14] Dugan's observations give evidence of a somewhat asymmetrical curve.

[15] Shapley, *op. cit.*, p. 35.

[16] *Ap. J.*, **35** and **36**, 1912.

visual observations by Wendell have been treated in the same way by Shapley.[17]

TABLE VI

α	l	θ	$\sin\theta$	$\sin^2\theta$	$\phi(k, \alpha)$	k_{dark} (*IV x*)	Weight	k_{unif} (*IV*)	Weight
	BLUE								
0.00	0.250:	0.6301	0.5892	0.3472	4.822	0.779	0	0.730	0
.10	.1920	.4839	.4652	.2164	3.006	.751	1	.663	1
.20	.1664	.4194	.4072	.1658	2.303	.726	1	.629	1
.30	.1472	.3710	.3625	.1314	1.825	.700	1	.598	1
.40	.1327	.3345	.3283	.1078	1.497	.687	1	.590	1
.50	.1198	.3019	.2973	.0884	1.228	.673	1	.600	1
.60	.1078	.2717	.2684	**.0720**	1.000	.....	.....	.....	....
.70	.0959	.2417	.2393	.0573	0.794	.672	1	.604	1
.80	.0827	.2084	.2069	.0428	0.594	.683	2	.615	2
.90	.0693	.1747	.1738	.0302	0.419	.661	2	.610	2
.95	.0600	.1512	.1506	.0227	0.315	.669	1	.628	1
.98	.0524	.1321	.1317	.0173	0.240	.677	1	.643	1
0.99	.0470	.1185	.1182	.0140	0.194	.676	1	.672	1
1.00	0.040:	0.1008	0.1006	0.0101	0.140	0.684	0	0.700	0
Mean	.....	.....	.....	.....	.....	0.685	.....	0.622	.....
	RED								
0.00	0.250:	0.6301	0.5892	0.3472	4.660	0.765	0	0.716	0
.10	.1956	.4930	.4733	.2240	3.007	.754	1	.663	1
.20	.1664	.4194	.4072	.1658	2.225	.700	1	.606	1
.30	.1478	.3725	.3640	.1325	1.779	.674	1	.575	1
.40	.1338	.3372	.3309	.1095	1.470	.645	1	.557	1
.50	.1216	.3065	.3017	.0910	1.221	.670	1	.590	1
.60	.1097	.2765	.2730	**.0745**	1.000	.....	.....	.....	.....
.70	.0968	.2440	.2416	.0584	0.784	.710	1	.623	1
.80	.0835	.2105	.2090	.0437	0.587	.692	2	.625	2
.90	.0682	.1719	.1711	.0293	0.393	.696	2	.640	2
.95	.0594	.1497	.1491	.0222	0.298	.694	1	.649	1
.98	.0484	.1220	.1217	.0148	0.199	.725	1	.686	1
0.99	.0438	.1104	.1102	.0121	0.162	.721	1	.704	1
1.00	0.036:	0.0907	0.0906	0.0082	0.110	0.725	0	0.742	0
Mean	.....	.....	.....	.....	.....	0.698	.....	0.630	.....

Since previous investigations had shown that the eclipse of U Cephei is central, the ratio of the diameters of the components, k, was derived[18] by means of the function $\phi(k, \alpha)$; the function[19]

[17] *Op. cit.*, p. 37.

[18] *Ap. J.*, **36**, 254, 1912.

[19] *Ibid.*, **35**, 321, 1912.

$\psi(k,a)$ gives a negative value for $\cot^2 i$. Table VI contains the results of the computations.

Since the ratio of the diameters cannot depend upon the method of observation, the values of k, determined for each effective wave-length, are in close agreement. Accordingly, I have adopted for the uniform solution a mean k of 0.626 and for the darkened solution

TABLE VII

	System I (Uniform)			System II (Darkened)		
	Blue	Red	Visual	Blue	Red	Visual
k	0.626	0.626	0.63	0.692	0.692	0.69
Primary minimum	3^M44	1^M94	2^M40	3^M44	1^M94	2^M40
Secondary minimum	0^M018	0^M071	0^M049	0^M022	0^M087	0^M077
Semi-duration of eclipse	0^d219	0^d220	0^d221	0^d227	0^d227	0^d225
Semi-duration of totality	0^d0479	0^d0480	0^d0447	0^d0390	0^d0392	0^d0395
L_b	0.9579	0.8325	.....	0.9579	0.8325	.....
L_f	0.0421	0.1675	.....	0.0421	0.1675	.....
L_b/L_f	22.76	4.97	.....	22.76	4.97	.....
I_b/I_f	57.9	12.6	20	47.5	10.4	17
r_b	0.202	0.203	.....	0.221	0.222	.....
r_f	0.323	0.324	.....	0.319	0.320	.....
r_b (mean)	0.2025		0.205	0.2215		0.221
r_f (mean)	0.3235		0.324	0.3195		0.320
$\bar{\rho}_b$	0.129		0.126	0.099		0.101
$\bar{\rho}_f$	0.032		0.032	0.033		0.033

0.692. The elements computed with these values of k are given in Table VII.

The values of I_b/I_f give for the difference between the color index of the primary star and that of the component, $-2.5\{\log I_b/I_f \text{ (blue)} - \log I_b/I_f \text{ (red)}\}$. The result is 1^M65 from the darkened and from the uniform solutions. Since the spectral type of the brighter star is A0, we find from Table II that the spectral type of the fainter star is G6. This is slightly earlier than the value given in the *Henry Draper Catalogue*.

DARKENING TOWARD THE LIMB

The residuals between the theoretical light-curves obtained from our elements and the observed intensities listed in Table V are shown in Figure 3. A similar treatment was made for Dugan's photometric observations, and the curve of the residuals closely resembles that

TABLE VIII

Phase	I		ΔI		$\pm o^{M}.01$
	$Red_{reduced}$	Blue	Blue-Red	$C_{dark} - C_{unif}$	
±0.250	**10000**	**10000**	0	0	±92
± .240	9894	10000	+106	0	91
± .230	9686	9817	+131	0	89
± .220	9482	9638	+156	+ 92	88
± .210	9282	9462	+180	0	85
± .200	9183	9205	+ 22	0	84
± .190	8891	8954	+ 63	− 85	82
± .180	8608	8551	− 57	−164	79
± .170	8242	8241	− 1	−155	75
± .160	7803	7798	− 5	−218	71
± .150	7303	7244	− 59	−168	69
± .140	6602	6668	+ 66	−124	61
± .130	5889	5970	+ 81	− 84	55
± .120	5114	5152	+ 38	0	47
± .110	4368	4446	+ 78	0	40
± .100	3563	3631	+ 68	0	35
± .090	2828	2858	+ 30	0	26
± .080	2167	2148	− 19	0	20
− .070	1520	1445	− 75	0	14
− .060	920	920	0	− 69	9
− .050	627	619	− 8	−116	5
− .040	457	441	− 16	− 4	5
− .030	438	432	− 6	0	4
− .020	438	428	− 10	0	4
− .010	438	425	− 13	0	4
.000	**421**	**421**	0	0	4
+ .010	421	413	− 8	0	4
+ .020	404	409	+ 5	0	4
+ .030	404	405	+ 1	0	4
+ .040	438	432	− 6	− 4	4
+ .050	607	608	+ 1	−116	5
+ .060	942	920	− 22	− 69	9
+0.070	1520	1445	− 75	0	±14

found from my own observations. An examination of the three curves of residuals obtained from the uniform solution shows marked departures at phase $\pm 0^{d}.050$. *The range of this departure increases with decreasing wave-length.* This is exactly what would be ex-

pected from the effect of darkening at the limb. The correctness of this interpretation is confirmed by the fact that the three curves for the darkened solution show no such departures. In fact, the residuals here seem to show a very slight departure in the opposite direction, indicating that the darkening may not be complete at the limb, as is assumed for the theoretical curve of darkening.[20]

The construction of the theoretical light-curves depends to some extent upon the weights attached to the different values of k, and these are always somewhat arbitrary. Therefore, it would be of interest to check our result by a method that depends directly upon

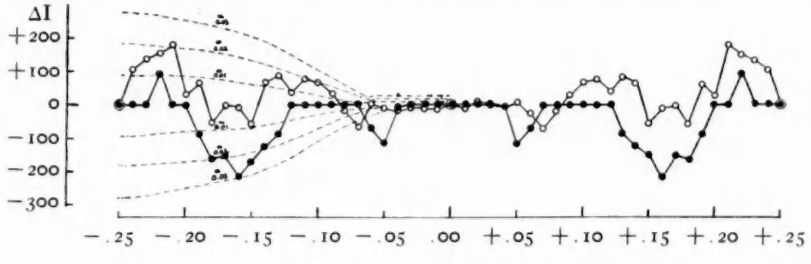

FIG. 5. $\Delta I_{\text{blue-red}}$ and $\Delta I_{\text{dark}-\text{uniform}}$
○ blue-red
● $C_{\text{dark}} - C_{\text{unif.}}$

the observations and does not involve a hypothesis. Following a suggestion made to me by Professor H. N. Russell, I have converted the two light-curves, for the red and for the blue images, into curves of intensities reduced to the same scale. Table VIII gives these intensities and their differences. The corresponding values computed by taking the differences of the intensities from the darkened and from the uniform solution are also shown in the table. The last column gives the variation in ΔI that corresponds to the variation in brightness of $0^{M}.01$. The observed and the computed values of ΔI are shown graphically in Figure 5. The dotted lines show the variations in ΔI that would correspond to a change in brightness equal to $0^{M}.01$, $0^{M}.02$, and $0^{M}.03$. The general appearance of the observed

[20] Dugan (*op. cit.*, p. 26) obtained a good representation of his observations, assuming that the limb brightness is one-third of the central brightness.

curve closely resembles that of the computed curve, and there can be no doubt that the interpretation of the phenomenon as being due to darkening at the limb is essentially correct.

If we assume that the residuals $C_u - O$ at phase $0^d.05$ are numerically equal to the amount of darkening, we obtain the following results:

	Darkening	Loss of Light	I*
Blue (λ 4015)	$0^M.24$	0.198	0.802
Visual (λ 5500)	.11	.096	.904
Red (λ 6165)	0.06	0.054	0.946

* I is expressed in fractions of the central intensity.

It will be of interest to derive the distance from the center of the star for which these values of the darkening hold. The mean phase of the beginning of the eclipse obtained from the observations and from the darkened curve is $0^d.2316$, and the mean phase for the beginning of the totality is $0^d.0390$. The difference, $0^d.1926$, is the interval required for the limb of the eclipsing body to pass over the

TABLE IX

Abbot and Fowle		Moll, van der Bilt, and Burger		Schwarzschild and Villiger	
λ	$I_{(0.89)}$	λ	$I_{(0.89)}$	λ	$I_{(0.89)}$
3860	0.52	4500	0.595	3225	0.483
4560	.57	5000	.642	.....	.....
5340	.64	5500	.668	.....	.....
6700	0.71	6000	.700	.....	.....
.....	.....	6500	0.716	.....	.....

entire diameter of the brighter component. The interval from the beginning of the eclipse to phase $0^d.050$ is $0^d.1816$; hence, at phase $0^d.050$ the fraction of the diameter of the eclipsed star that is covered is $0.1816/0.1926 = 0.943$. Accordingly, at this phase 0.114 of the radius was uneclipsed. If we should wish to compare the darkening

effect in U Cephei with that of the sun, we should take for the latter the value $R=0.89$.

The best values for the darkening of the sun are given by Abbot and Fowle,[21] by Moll, van der Bilt, and Burger,[22] and by Schwarz-

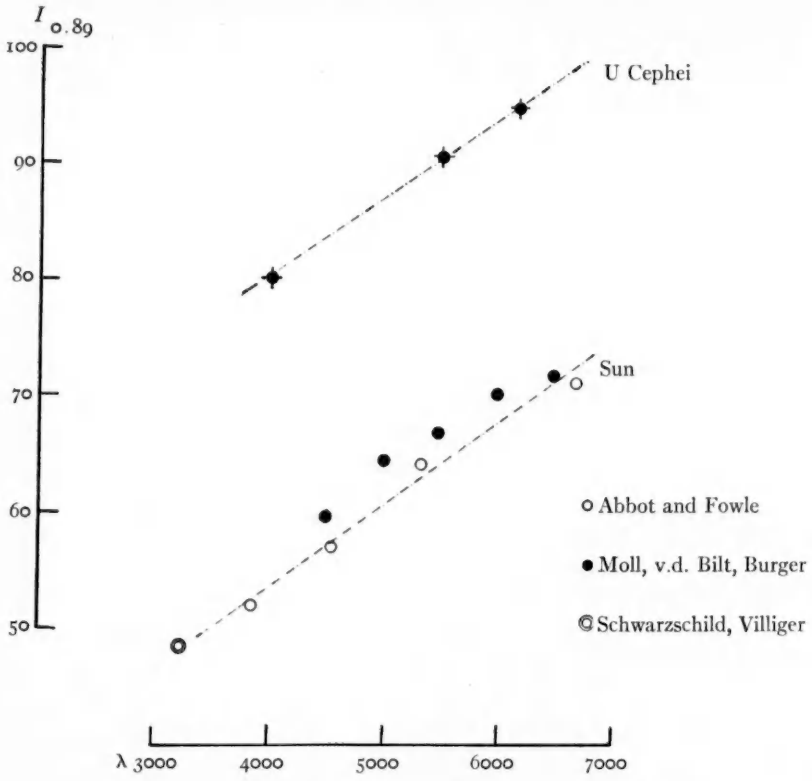

FIG. 6.—Darkening of U Cephei and of the sun at $R=0.89$

schild and Villiger.[23] Table IX gives the values for the sun interpolated from the original results for $R=0.89$.

Figure 6 shows that the slope of the curves for U Cephei and for the sun are the same, but that the absolute amount of darkening for the Ao star is much less than that for the sun. This result is in good

[21] *Ann. Ap. Obs. of the Smithsonian Institution*, **4**, 220, 1922.

[22] Moll, van der Bilt, and Burger, *B.A.N.*, **91**, 83, 1925.

[23] Schwarzschild and Villiger, *Ap. J.*, **23**, 284, 1906.

agreement with the theory. If the function of $\lambda \cdot T_{abs}$ is the same for all stars, we should be able to compute the temperature of the brighter component of U Cephei by comparing its darkening effect with that of the sun. Assuming for the sun a temperature of 6000°, we find for U Cephei 15,000°, or perhaps even a somewhat higher temperature.

YERKES OBSERVATORY
October 10, 1935

RADIATION FROM THE PLANET MERCURY*

EDISON PETTIT AND SETH B. NICHOLSON

ABSTRACT

Method of measurement.—The measurements of radiation from Mercury were made in 1923–1925 in the usual manner with the vacuum thermocouple at the Newtonian focus of the 100-inch telescope when the planet was near the meridian. They include observations of the transmissions of a microscope cover-glass, a water-cell, and a fluorite screen. The entire image was effective on the thermocouple junctions. It was not feasible to make detailed measurements over the planet's surface.

Reduction of the measurements.—The reductions were similar to those already developed for the moon. The reflected light, however, was separated from the planetary heat, not by the cover-glass, but by correcting the water-cell magnitude for losses suffered by transmission through the cell. Four magnitudes were then found: m_{rR}, the radiometric magnitude of the reflected light; m_{rB}, the radiometric magnitude of all the planetary heat; m_{rCg} and m_{rFl}, the radiometric magnitudes of the planetary heat transmitted by the cover-glass and by the fluorite screen, respectively. These results were all reduced to standard conditions: Mercury at the zenith, unit ρ, and mean r.

Radiation as a function of phase.—Both the planetary heat and reflected light were reduced to no atmosphere and plotted against phase angle i. The curves are much like those for the moon, the reflected light being nearly identical with that from the moon, although the planetary heat is somewhat higher than for the moon, at least for western elongations. At the extreme crescent phases Mercury seems to radiate a little less planetary heat relative to full phase than does the moon. The theoretical curve of planetary heat is in general higher than the observed curve for Mercury, and the discrepancy for the moon is a little larger still.

Apparent temperatures.—The temperature corresponding to the average radiation over the illuminated disk outside our atmosphere was obtained for each phase from m_{rB}, m_{rCg}, and m_{Tr}, the last quantity being the absorption of planetary heat by the cover-glass. These temperatures agree best if the atmospheric transmission between 1.3 and 6.6 μ is increased 40 per cent over that formerly given.

Temperature of the subsolar point.—The planetary heat radiated from the whole disk at full phase, read from the plot against phase angle, was reduced to the subsolar point by the formula $E = a \cos^{\frac{3}{4}} \theta$ found for the moon. With the aid of the fourth-power law this leads to a temperature of 600° K at the subsolar point for the planet at mean distance. If we assume a solar constant of 1.95 cal cm^{-2} min^{-1} and allow for the reflected radiation, amounting to 291×10^{-12} cal cm^{-2} min^{-1}, the temperature comes out 617° K. If we adopt $T = 610°$ K, the resulting temperatures at perihelion and aphelion are 685° and 550° K, respectively.

Radiometric albedo.—The ratio of the light reflected from the planet at full phase to that of a self-luminous body of the same size and position which radiates as much light from each unit of surface as it receives from the sun under normal illumination was found to be 0.093; the albedo, 0.067.

The measurements of the radiation from the planet Mercury cover the period from June 17, 1923, to September 14, 1925. Some preliminary reports[1] of this work have already been given, but the

* *Contributions from the Mount Wilson Observatory, Carnegie Institution of Washington*, No. 533.

[1] *Pub. A.S.P.*, **35**, 194, 1923; *Pub. A.A.S., 30th Meeting, Mt. Wilson*, **5**, 76–77, 1923, *and 33d Meeting, Washington*, **5**, 271, 1924; *Pop. Astr.*, **31**, 657, 1923, and **33**, 299, 1925.

material could not be satisfactorily reduced until a system of radiometric magnitudes for the comparison stars had been established. Moreover, a study of the radiation from the moon should logically precede the discussion. The reduction of the stellar[2, 3] and lunar[4, 5] measurements has now been completed. The data from the former investigation and the methods developed in the latter are used in the reduction of the measurements of the radiation from Mercury.

METHODS OF OBSERVING

The methods of obtaining the deflections have already been described.[2] Save on four occasions the same thermocouple was used throughout the investigation. In all cases a rock-salt window was provided for the thermocouple cell. A water-cell of 1 cm thickness, a microscope cover-glass 1/8 mm thick, and, in the latter half of the work, a fluorite screen 4 mm thick were used as absorption screens.

All measurements were made in full daylight when the planet was near the meridian. The minimum elongation at which observations were made was about 11°, fixed by the condition that the 100-inch mirror must be screened from sunlight by the shutter of the dome. The observable phase angles were between 32° and 126°. The maximum angular diameter at which Mercury was observed, 9".34, is equivalent to 0.584 mm at the Newtonian focus of the 100-inch telescope. As the diameters of the receivers on the thermocouples were 0.62 and 0.80 mm, respectively, the entire image of the planet was effective in the measurements.

The measurements generally included six deflections each on the free radiation from the planet and on that transmitted by the water cell, the cover-glass, and the fluorite screen. This program was supplemented by six deflections on the free radiation and on that transmitted by the water-cell for one or two nearby comparison stars. The largest zenith distance at which observations were made on the planet occurred near the winter solstice and had a secant of 2.09. Experience gained in the measurement of the radiation from the comparison stars leads us to believe that, except for the prevailing

[2] *Mt. W. Contr.*, No. 369; *Ap. J.*, **68**, 279, 1928.
[3] *Mt. W. Contr.*, No. 478; *Ap. J.*, **78**, 320, 1933.
[4] *Mt. W. Contr.*, No. 392; *Ap. J.*, **71**, 102, 1930.
[5] *Mt. W. Contr.*, No. 504; *Ap. J.*, **81**, 17, 1935.

inferior seeing, the daytime sky so near the sun has no marked effect on the measurement of the radiation from the planet. Poor seeing and the small size of the image prevented any successful attempt to measure the radiation from its dark side.

The sensitivity employed in the electrical circuit varied greatly with the phase angle i, radius vector r, and distance ρ of the planet. When the radiometric magnitude of the planet was fainter than -2, the regular stellar arrangement was used; but when brighter than this limit, a 2-second galvanometer (sensitivity one-sixth the usual value) was used at one-fifth scale distance, with occasionally some resistance and shunt in the circuit. It was then, however, often necessary to observe the comparison stars with the higher sensitivity in order to obtain sufficient deflection. The ratio of the sensitivity on the star to that on the planet could be calculated from the changes in the electrical circuit and the scale distances but was also always determined independently by observations on the star or planet itself.

REDUCTION OF THE MEASUREMENTS

Transmission coefficients.—The transmissions of the screens and the atmosphere have already been given in detail.[4] The transmission of the fluorite screen was decreased in all wave-lengths by striae. A test of this screen was made on ten stars on different nights. The resulting transmission was 0.78 (absorption 0.27 mag.). Of this amount, 0.19 mag. has been applied as a correction to the observations with this screen on Mercury to reduce them to the transmission-curve already given; the curve itself includes the remaining 0.08 mag. due to reflection.

In comparing measurements on the radiation from the entire surface of a planet made on different occasions, it is necessary to reduce them to the zenith, to unit distance from the observer, and to mean distance from the sun. Reduction to zero phase angle would also be desirable, but the uncertainties as to procedure are too great. Finally, they can be reduced to no atmosphere.

Reduction to the zenith.—No observations on Mercury for atmospheric extinction are available, since they would have required a prolonged exposure of the 100-inch mirror to the daytime sky

with undesirable changes in its figure which would have affected the night program. The investigation of lunar radiation[5] showed that in the equation for extinction,

$$\Delta m_{rB} = a \sec Z \,, \qquad (1)$$

the coefficient a was 0.15 mag. The value of a in the similar equation for the reflected light from the moon was 0.11 mag. The more extensive investigation of stellar radiation gave 0.16 mag. Since a enters into the corrections only as a second-order term, it is assumed here that its values for planetary heat, for reflected light from the planet, and for radiation from the comparison stars are identical and equal to 0.16 mag.

Radiometric magnitude of the planet.—The radiometric magnitude of the whole radiation from the planet is given by

$$m_{rP} = m_r + D(205 \times 10^{-6} - S_s) + 2.5 \log b - 2.5 \log F - 0.16(\sec Z - \sec z) \,, \quad (2)$$

where m_r is the radiometric magnitude of the comparison star; D, the number of days since silvering; S_s, the coefficient of absorption due to silver tarnish for the comparison star, which depends on its spectral class; b, the deflection on the star; F, the free deflection on the planet; Z and z, the zenith distances of the planet and star, respectively.

The correction for tarnished silver in the telescope has already been described.[2] The absorption is nearly zero for planetary heat, but the positive correction arises from the condition that the scale of radiometric magnitude crosses that of visual magnitude at spectral type Ao. A small part of F is due to reflected light from the planet, the color of which is like that of a K-type star, and a small correction for silver tarnish should be applied to that part; but since the reflected light did not exceed 0.20 F, the correction did not exceed 0.003 mag. and was therefore neglected.

Radiometric magnitude of the reflected light.—The heavy line in Figure 1 shows the spectral energy-curve of a black body at 600° K, the approximate temperature of Mercury. The light line shows this curve after transmission by our atmosphere;[4] the dotted line, the same after transmission by a microscope cover-glass; and the arrow

at λ 1.45 μ, the infra-red limit of transmission by a water-cell. In the case of Mercury the water-cell is therefore superior to the cover-glass as a means of separating the reflected light from the planetary heat.

To use the water-cell deflections as a measure of reflected light, the water-cell absorption of the light must be determined. To do this we first plot the water-cell absorptions, *WC*, of the stars against

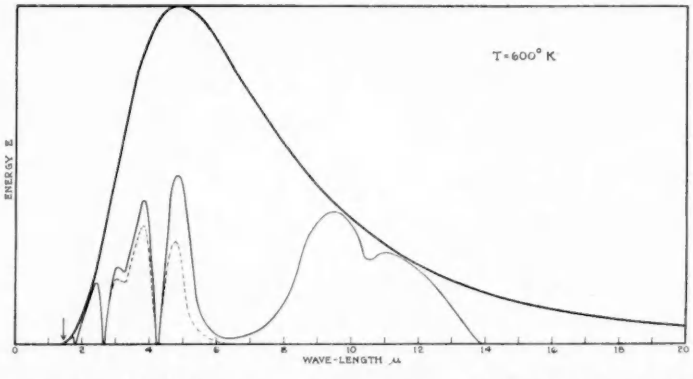

FIG. 1.—Heavy line indicates spectral energy-curve of a black body at 600° K; light line, the same after passage through our atmosphere (from Smithsonian observations without adjustments); dotted line, the same after passage through microscope cover-glass. The arrow points to the infra-red limit of transmission of a water-cell 1 cm thick.

visual *minus* water-cell magnitudes, $m_v - m_{WC}$, which might be called the water-cell index, *WCI*. Then, if we determine *WCI* for the light from Mercury, we can read its water-cell absorption from the plot.

The visual magnitudes of Mercury on the Harvard system were computed by the formula of G. Müller:[6,7]

$$m_v = -0.99 + 0.0284\,(i-50^\circ) + 0.000102\,(i-50^\circ)^2 + 5\log\rho + 5\log\frac{r}{r_0}. \quad (3)$$

The first term as given by Müller, based on the Potsdam scale of stellar magnitude, is −0.90. The average scale difference, Harvard *minus* Potsdam, for the thirteen comparison stars used by Müller is −0.09 mag. Hence for the Harvard scale this term becomes −0.99.

[6] *Pub. Ap. Obs. Potsdam*, **8**, 308, 1893.

[7] Müller, *Photometrie der Gestirne* (1897), p. 353.

The last two terms reduce the magnitude to the distance and radius vector at the time of observation. Their individual values, with reversed signs, appear in the fourth and fifth columns of Table II.

The mean value of *WCI* observed for Mercury on twenty-six days was +0.13 mag. with a probable error of ±0.03. The water-cell absorption of both giant and dwarf stars having this value of *WCI* is 0.66 mag. The water-cell absorption of the reflected light from Mercury may therefore be taken to be 0.66 mag., the equivalent of that of a star of spectral type gG8.

Before computing the radiometric magnitude of the reflected light from the planet, m_{rR}, we must apply a date correction j, which is based on the mean difference in water-cell absorption for stars observed during the night preceding or following the observations of Mercury and the average of their absorptions already published.[2] This difference is due to slow changes in transparency of the water-cell. The factor for the silver correction in the second term of equation (2) corresponding to a water-cell absorption of 0.66 mag. is $94D\times 10^{-6}$. We have, then, an equation derived from equation (2) which gives the water-cell magnitude:

$$m_{WC}=m_{rP}+2.5\log F-2.5\log WC-111D\times 10^{-6}+j\,. \qquad (4)$$

The value of the fourth term changed gradually from −0.05 mag. for the first observation to −0.14 mag. for the last, and j varied between −0.18 and +0.08 mag.

The whole reflected light from the planet is given by

$$m_{rR}=m_{WC}-0.66\,, \qquad (5)$$

while the radiometric magnitude of the whole planetary heat (all wave-lengths) which reaches us through our atmosphere, m_{rB}, is given by

$$m_{rB}=-2.5\log\left(2.512^{-m_{rP}}-2.512^{-m_{rR}}\right)\,. \qquad (6)$$

We may also write equations similar to (4) for the radiometric magnitudes of the whole radiation transmitted by the cover-glass, m_{Cg}, and the fluorite screen, m_{Fl}:

$$m_{Cg}=m_{rP}+2.5\log F-2.5\log Cg-30D\times 10^{-6}\,, \qquad (7)$$

$$m_{Fl}=m_{rP}+2.5\log F-2.5\log Fl-0.19\,. \qquad (8)$$

In equation (7) the value of the constant in the fourth term is derived from the mean of 205×10^{-6} for planetary heat and 145×10^{-6} for a G8-type star, since the cover-glass transmits approximately equal parts of planetary heat and reflected light. In computing m_{Cg}, a second approximation was made for equation (7), wherein this term was prorated between the actual values of the planetary heat and the reflected light for each observation. The last term of equation (8) is the correction for loss by striae in the fluorite screen.

The radiometric magnitude of the planetary heat transmitted by the cover-glass, m_{rCg}, is given by an equation similar to (6):

$$m_{rCg}=-2.5\log\left(2.512^{-m_{Cg}}-2.512^{-(m_{rR}+0.11)}\right), \qquad (9)$$

where the constant +0.11 in the exponent of the last term corrects the light reflected by the planet for reflection from and absorption by the cover-glass screen. The radiometric magnitude of the planetary heat transmitted by the fluorite screen, m_{rFl}, is given by

$$m_{rFl}=-2.5\log\left(2.512^{-m_{Fl}}-2.512^{-(m_{rR}+0.08)}\right), \qquad (10)$$

the correction for reflection by the fluorite screen being +0.08 mag.

Table I gives the observational data and their reduction according to equations (1) to (10). The dates are given in G.M.T., since most of them were prior to 1925. The value of sec Z for the planet is followed by the observed deflections on the free radiation and on that transmitted by the water-cell, the cover-glass, and the fluorite screen. Then follow the calculated radiometric magnitudes of the whole radiation from the planet as the telescope receives it, m_{rP}, and that transmitted by the water-cell, m_{WC}, by the cover-glass, m_{Cg}, and by the fluorite screen, m_{Fl}. The last three columns give the radiometric magnitudes of the light reflected from the planet, m_{rR}, the planetary heat transmitted by the cover-glass, m_{rCg}, and the whole planetary heat m_{rB} as observed inside our atmosphere.

RADIATION FROM THE PLANET AS RELATED TO PHASE

The phase angle, i, of the planet was computed from

$$\cos i=\frac{r^2+\rho^2-R^2}{2r\rho}, \qquad (11)$$

TABLE I

Observations and Reduction

Date G.M.T.	Sec Z	Free	WC	Cg	Fl	m_{rP}	m_{WC}	m_{Cg}	m_{Fl}	m_{rR}	m_{rCg}	m_{rB}
1923		mm	mm	mm	mm							
June 17.30	1.07	107.3	7.3	27.3	.....	−1.89	+1.02	−0.42	.....	+0.36	+0.21	−1.74
21.27	1.04	134.6	9.3	33.0	.....	2.24	+0.44	−0.72	.....	−0.22	+0.20	2.06
Aug. 12.46	1.24	122.7	9.3	40.7	.....	2.81	+0.02	−1.62	.....	−0.64	−1.13	2.65
Oct. 11.28	1.19	103.5	6.7	34.7	.....	3.04	−0.08	−1.87	.....	−0.74	−1.45	2.90
14.27	1.20	153.3	9.3	55.6	.....	3.53	−0.56	−2.45	.....	−1.22	−2.07	3.39
Dec. 14.40	2.05	116.5	7.9	36.1	.....	3.46	−0.59	−2.20	.....	−1.25	−1.69	3.31
1924												
Feb. 11.29	1.78	177.9	5.9	42.6	.....	3.20	+0.38	−1.67	.....	−0.28	−1.35	3.12
Mar. 6.32	1.46	117.7	7.8	37.2	.....	3.34	−0.47	−2.11	.....	−1.14	−1.61	3.19
Apr. 19.45	1.12	66.5	3.8	18.0	.....	2.37	+0.66	−0.98	.....	0.00	−0.48	2.24
20.44	1.09	57.5	3.6	15.5	.....	2.07	+0.84	−0.68	.....	+0.18	−0.10	1.92
June 7.28	1.06	109.6	5.8	28.4	56.4	2.90	+0.16	−1.46	−2.37	−0.50	−0.95	2.78
8.29	1.07	110.7	6.2	29.5	55.8	2.85	+0.13	−1.44	2.30	−0.53	−0.90	2.71
9.21	1.09	121.5	7.5	33.9	62.9	2.82	−0.07	−1.46	2.30	−0.73	−0.79	2.65
10.22	1.05	137.8	7.6	37.8	74.0	2.98	−0.11	−1.60	2.50	−0.77	−1.00	2.83
17.27	1.03	73.9	4.0	23.6	41.2	3.60	−0.58	−2.38	3.16	−1.24	−1.96	3.47
July 24.35	1.08	148.6	11.0	48.1	88.3	3.21	−0.45	−2.01	2.84	−1.11	−1.47	3.04
Aug. 28.45	1.35	37.8	2.7	8.0	19.6	1.60	+1.02	+0.06	1.07	+0.36	+1.29	1.41
Sept. 23.30	1.14	37.8	2.4	11.6	20.3	2.80	−0.01	−1.55	2.32	−0.67	−0.99	2.64
24.29	1.13	46.4	2.7	14.9	28.3	3.15	−0.25	−1.95	2.81	−0.91	−1.48	3.00
Nov. 20.42	2.11	123.0	9.6	38.3	72.4	3.22	−0.58	−1.98	2.88	−1.24	−1.32	3.03
21.42	2.09	122.4	9.2	35.9	68.5	3.25	−0.57	−1.94	2.80	−1.23	−1.25	3.07
Dec. 19.42	1.84	143.6	10.8	46.0	81.4	1.94	+0.71	−0.74	1.51	+0.04	−0.10	1.75
1925												
May 26.28	1.08	131.8	8.4	38.8	69.0	2.99	−0.26	−1.69	2.47	−0.92	−1.05	2.82
July 27.45	1.12	105.4	7.3	26.4	55.0	2.37	+0.36	−0.90	2.00	−0.30	−0.11	2.20
28.42	1.11	28.0	2.4	6.9	15.8	2.30	+0.13	−0.80	1.87	−0.53	+0.49	2.06
Sept. 14.32	1.10	120.1	7.9	43.8	69.8	−3.76	−0.96	−2.71	−3.36	−1.62	−2.26	−3.60

TABLE II

REDUCTIONS—*Continued*

DATE	i	r	REDUCTION TO UNIT ρ	REDUCTION TO MEAN r	REDUCTION TO 1 SQ. SEC.	m_{Tr}	T K			Δm_{rB}	m_{bB}	$E_B \times 10^{12}$	$E_R \times 10^{12}$
							m_{Tr}	m_{rB}	m_{rCg}				
1923			mag.	mag.	mag.							cal cm^{-2} min^{-1}	
June 17....	120°.0 W	0.431	+0.68	−0.23	3.04	1.95	470°	390°	422°	1.02	−2.30	144	12
21....	109.4 W	.412	+ .48	− .14	3.11	2.26	431	410	420	1.05	2.77	218	23
Aug. 12....	52.4 E	.433	− .43	− .24	3.20	1.52	544	456	491	0.99	4.30	908	84
Oct. 11....	101.8 W	.308	+ .26	+ .50	3.12	1.45	546	495	513	0.99	3.13	309	25
14....	85.3 W	.311	+ .06	+ .48	3.26	1.32	578	539	548	0.99	3.85	600	48
Dec. 14....	40.4 E	.411	− .50	− .13	3.22	1.62	525	527	524	0.99	4.93	1622	143
1924													
Feb. 11....	65.0 W	.456	− .19	− .36	3.31	1.77	498	493	497	1.00	4.66	1265	54
Mar. 6....	32.2 W	.435	− .62	− .25	3.14	1.58	534	522	525	0.99	5.06	1829	159
Apr. 19....	113.8 E	.366	+ .49	+ .12	3.04	1.76	493	434	459	1.00	2.64	197	14
20....	117.4 E	.372	+ .55	+ .09	2.99	1.82	468	419	442	1.02	2.30	144	12
June 7....	95.2 W	.411	+ .25	− .13	3.26	1.83	486	462	472	1.01	3.67	508	36
8....	92.7 W	.406	+ .20	− .10	3.26	1.81	487	456	469	1.01	3.62	485	47
9....	90.5 W	.401	+ .16	− .08	3.26	1.86	480	449	464	1.01	3.58	468	46
10....	87.9 W	.395	+ .11	− .05	3.26	1.83	485	467	474	1.01	3.77	557	48
17....	68.6 W	.356	− .19	+ .19	3.26	1.51	541	544	542	0.99	4.47	1062	79
July 24....	54.1 E	.411	− .40	− .14	3.21	1.57	533	497	511	0.99	4.56	1154	114
Aug. 28....	120.4 E	.438	+ .73	− .27	3.07	2.70	390	367	371	1.09	2.04	113	12
Sept. 23....	109.5 W	.311	+ .34	+ .47	3.01	1.65	497	481	491	1.00	2.83	235	22
24....	103.9 W	.310	+ .27	+ .48	3.08	1.52	529	513	518	0.99	3.24	342	29
Nov. 20....	33.3 E	.451	− .62	− .33	3.15	1.71	511	503	506	1.00	4.98	1699	192
21....	34.8 E	.448	− .61	− .32	3.16	1.82	495	506	501	1.00	4.99	1714	184
Dec. 19....	125.9 E	.314	+ .58	+ .46	2.73	1.65	485	429	453	1.01	1.73	85	9
1925													
May 26....	80.1 W	.406	.00	− .10	3.31	1.77	494	461	475	1.00	3.93	646	65
July 27....	92.7 E	.464	+ .28	− .39	3.29	2.09	451	410	428	1.03	3.35	378	37
28....	94.5 E	.465	+ .31	− .40	3.29	2.55	395	400	399	1.09	3.24	342	45
Sept. 14....	76.6 E	0.308	−0.09	+0.50	3.51	1.34	580	526	543	0.99	−4.19	821	78

where r is the radius vector of the planet, R that of the earth, and ρ the distance between them. The values of i, followed by the direction of the elongation, and of r, in astronomical units, are given in Table II. The fourth and fifth columns of this table give the reduction to unit distance from the earth and to mean distance from the sun, both expressed in magnitudes. These corrections, with reversed signs, are the values of the last two terms of equation (3), respectively, and are the same for both reflected light and planetary heat.

Atmospheric absorption.—Since Δm_r is a function of T, it is necessary to know the temperature of the radiating surface before the observations can be corrected for atmospheric absorption. The temperature corresponding to the average radiation over the surface of a planet, which we shall call the mean temperature, T_m, may be obtained from Stefan's law by

$$\log T_m = 2.713 - 0.1\,(m_r - \Delta m_r) - 0.25 \log [d^2(1+\cos i)]\,, \qquad (12)$$

where d is the diameter of the planet in seconds of arc and m_r a radiometric magnitude of that part of the planetary heat observed. Either m_{rB} or m_{rCg} may be used in equation (12) with the corresponding Δm_r. As a first approximation both Δm_{rB} and Δm_{rCg} may be computed for various temperatures from black-body curves and the atmospheric absorption coefficients. Curves can then be drawn showing the relation between the mean temperature and the radiometric magnitude of planetary heat per square second of arc of the radiating surface. Since both Δm_{rB} and Δm_{rCg} are functions of T, their difference is also a function of T, and we may write

$$m_{rCg} - m_{rB} = m_{Tr} = \Delta m_{rCg} - \Delta m_{rB}\,.$$

The first member of this equation is observed; the last, computed as a function of T. From this function a value of T_m may be obtained which is independent of the area of the radiating surface or the value of the observed deflection in energy units.

Since the temperature of the radiating surface is not uniform but decreases toward the boundary of the image from a maximum at the subsolar point, the atmospheric absorption corresponding to the mean temperature is not the mean atmospheric absorption, and

the first approximations of T_m obtained with that assumption need correction. These corrections depend on the phase angle i and on the temperature of the subsolar point, the latter a function of the radius vector, r. The mean atmospheric absorptions were computed for various values of r and i on the assumption of complete absorption of the solar radiation by a smooth sphere and complete re-radiation according to the cosine law. Isotherms on the disk of the planet are ellipses of the form

$$I = I_0(\cos i\sqrt{1-x^2-y^2}+x \sin i) .$$

TABLE III

	i	T_m	m_{rB}		m_{rCg}		m_{Tr}	
			δm	δT_m	δm	δT_m	δm	δT_m
$T=550°$ K	0°	497°	0.00	0°	+0.09	− 7°	+0.09	−15°
$r=0.476$	30	489	.00	0	+ .14	− 8	+ .14	−18
	60	472	+ .01	− 1	+ .20	− 9	+ .19	−23
	90	444	+ .01	− 1	+ .28	−12	+ .27	−26
	120	404	+0.02	− 2	+0.43	−14	+0.41	−25
$T=600°$ K	0	542	−0.01	+ 1	+0.07	− 5	+0.08	−13
$r=0.400$	30	532	.00	0	+ .11	− 9	+ .11	−17
	60	514	.00	0	+ .16	−11	+ .16	−24
	90	485	+ .01	− 1	+ .22	−13	+ .21	−27
	120	441	+0.02	− 2	+0.31	−14	+0.29	−26
$T=700°$ K	0	633	−0.01	+ 2	+0.03	− 2	+0.04	−11
$r=0.294$	30	621	− .02	+ 3	+ .04	− 4	+ .06	−13
	60	600	− .03	+ 4	+ .05	− 5	+ .08	−20
	90	565	− .06	+ 7	+ .11	−10	+ .17	−36
	120	514	−0.10	+12	+0.24	−15	+0.34	−49

The areas between isotherms differing by one-tenth I_0 were computed and multiplied by the atmospheric transmissions corresponding to the temperature of each area. The radiation from each zone transmitted by the atmosphere was summed; and this total divided by the corresponding total, without applying the atmospheric transmissions, gave the correct mean atmospheric transmission. Table III shows the corrections δT_m in degrees K to be applied to the first approximation of T_m. The corrections δm required by the first approximations for Δm_r and m_{Tr} are also given in Table III but have not been used in the present reduction. These differential correc-

tions are probably not appreciably affected by the assumption that Mercury has a smooth, black surface. The chief uncertainty in Δm_r arises from the uncertainty in the atmospheric transmissions themselves.

In a previous paper[4] it was shown that, for the moon, Δm_r, computed from the atmospheric transmissions determined by the Smithsonian Institution, must be decreased by the amount $\Delta m'_r = 0.18$ mag. in order to make the lunar temperature computed by its radiation and by the solar constant agree after accounting for the losses. A table of $\Delta m'_r$ as a function of T or of Δm_r was given in that paper.

In the case of the moon, only the transmission of the atmosphere between 8 and 14 μ was affected in the measurements, but for Mercury, the transmission in the region 1.3–6.6 μ becomes nearly as important (Fig. 1). The probable corrections in the latter region were estimated as follows, on the assumption that the reasons for using unit emissivity apply to Mercury as well as to the moon.

At full phase the mean temperature is nearest that of the subsolar point, varies but little with small changes in the phase angle, and is less affected by roughness of the surface. The four observations nearest zero phase angle were therefore selected, and the atmospheric transmission between 1.3 and 6.6 μ adjusted until the temperatures determined from m_{Tr}, m_{rB}, and m_{rC_g} agreed as nearly as possible. To bring about this agreement, the transmission had to be increased by 40 per cent. The mean temperatures so determined were 516°, 514°, and 514° K, respectively. Without this adjustment the transmissions previously given resulted in temperatures of 560°, 524°, and 537° K, respectively.

The temperatures thus determined for each observation from Table IV and equation (12), corrected by Table III, are given in the eighth, ninth, and tenth columns of Table II. For the larger phase angles they do not agree as well as for the four observations with the smallest phases, probably because on a rough surface the shadows near the terminator decrease the effective area radiating toward the earth. In fact, if the last term of equation (12), which takes into account the area of the illuminated surface, is increased by $0.1 \log [0.5 (1+\cos i)]$, the temperatures determined from m_{rB} and

m_{rCg} both agree in the mean at all observed phases with those determined from m_{Tr}.

Table IV gives the values of Δm_{rB}, Δm_{rCg} and m_{Tr} obtained from the atmospheric transmissions described above. It will be noted that over the temperature range 400°–600° K measured on Mercury Δm_{rB} is nearly constant and equal to 1 mag. For temperatures lower than 400° K, Δm_{rB} in Table IV differs from Δm_r, previously given, chiefly in the addition of the correction $\Delta m'_r$.[4]

TABLE IV

Temp.	Δm_{rB}	Δm_{rCg}	m_{Tr}
100° K	5.86	.....	.....
200	1.84	.....	.....
300	1.19	5.8	4.6
400	1.08	3.94	2.86
500	1.00	2.93	1.93
600	0.99	2.36	1.37
700	1.08	2.13	1.05

PLANETARY HEAT AND REFLECTED LIGHT

The magnitude of the planetary heat outside the atmosphere reduced to unit ρ and mean r is given by

$$m_{bB} = m_r - \Delta m_r - 5 \log \rho - 5 \log \frac{r}{r_0} . \qquad (13)$$

The radiation E_B in cal cm^{-2} min^{-1} received outside the atmosphere is[2]

$$E_B = 17.3 \times 10^{-12} \times 2.512^{-m_{bB}} . \qquad (14)$$

The values of m_{bB} and E_B obtained from m_{rB} and Δm_{rB} are also listed in Table II. The energy in the reflected solar radiation, E_R, in the last column, is obtained from equations (13) and (14) with the substitution of $m_{rR} - 0.41$ for $m_r - \Delta m_r$, 0.41 mag. being the atmospheric absorption for a star of type gG8, the light of which is the same in quality as that reflected from the planet.

MERCURY AND THE MOON COMPARED WITH A BLACK BODY

Figure 2 shows a plot of E_B and E_R from Table II against phase angle. The full line drawn through the observations of reflected

light E_R is that for similar measurements on the moon, while the broken line is computed for the visual light as given by equation (3), both adjusted to fit the observations on Mercury. A scale of radiometric magnitudes outside the atmosphere reduced to unit ρ and mean r is given on the right. This plot is comparable with that of

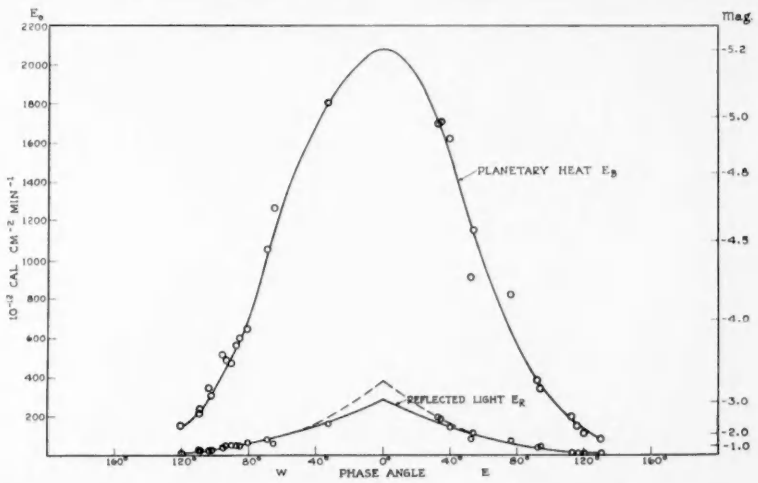

FIG. 2.—Planetary heat and reflected light from Mercury in relation to phase, as would be observed outside our atmosphere. Broken line, the extrapolated visual curve given by Müller.

the moon previously given.[5] Figure 3 shows the mean curve of E_B and E_R for Mercury (the heavy lines) compared with that for the moon (the light lines) and for a smooth, black body (the broken curve). The formula for the latter may be derived as follows:

If the planet has a smooth, black, non-conducting surface, any small area will receive radiation of intensity R_S from the sun and reradiate it toward the earth with intensity R_I, proportional to the cosines of the zenith distances of the sun S and earth E, respectively, as seen from this small area on the planet. The resulting expression

$$R_I = R_S \cos S \cos E$$

has the same form as Lambert's equation for reflected light from a small area on a planet. The integration of this equation over the

apparent disk of the planet has been given by Müller,[8] from which it follows that

$$R=R_0\frac{(\pi-i)\cos i+\sin i}{\pi}, \tag{15}$$

where $R_0=\frac{2}{3}\pi R_S$ is the radiation from the whole disk at zero phase angle and, further, that the mean intensity per unit area of the illuminated disk is

$$R_m=\frac{4R_S}{3(1+\cos i)}\cdot\frac{(\pi-i)\cos i+\sin i}{\pi}. \tag{16}$$

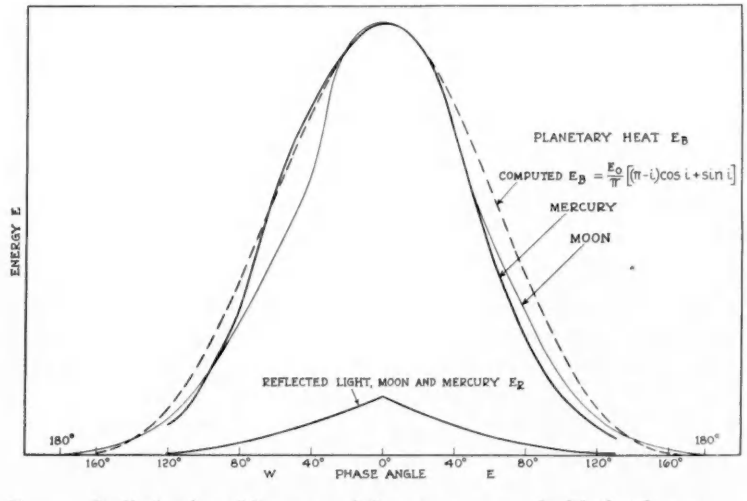

FIG. 3.—Radiation from Mercury and the moon compared with that from a smooth, slowly rotating, non-conducting black sphere.

In a similar comparison for lunar radiation given in a previous paper,[5] the expression for the mean intensity of radiation over the apparent surface (16) was unfortunately used instead of equation (15). This error greatly modifies the conclusions drawn there in regard to this relationship. Figure 4, which replaces Figure 5 in the former paper, shows the corrected curve.

From Figure 3 we see that the phase-intensity curve for Mercury fits the theoretical curve obtained from equation (15) somewhat closer than that for the moon. This may signify that Mercury is

[8] *Ibid.*, p. 56.

somewhat less rough than the moon, but the evidence is not very strong. Figure 2 shows that the visual light for Mercury, computed from equation (3) adjusted to fit the radiometric scale, agrees very closely with the thermocouple observations and quite closely with the similar observations on the moon, except near full moon. How-

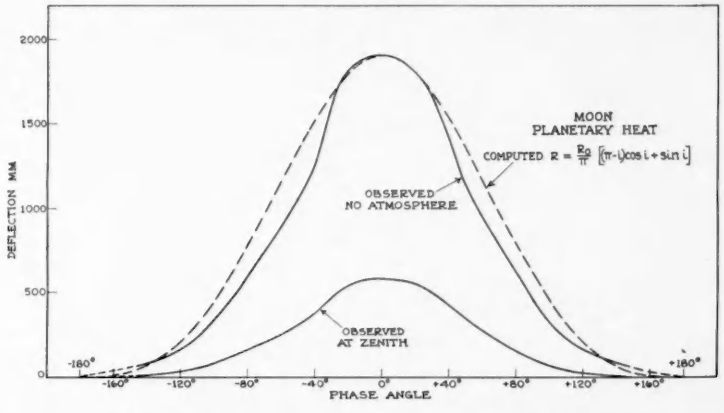

FIG. 4.—Planetary heat from the moon compared with that from a smooth slowly rotating non-conducting black sphere. This figure replaces Fig. 5 in *Mt. W. Contr.* No. 504; *Ap. J.*, **81**, 1935.

ever, since the visual observations on which equation (3) rests do not include phase angles less than 50°, the deviation of the visual from the radiometric curve depends on extrapolation.

TEMPERATURE OF MERCURY

The temperature of the subsolar point on Mercury, like that on the moon, can be computed from the measured planetary heat or from the solar radiation absorbed after allowing for the losses. We cannot, however, as in the case of the moon, measure the radiation from a small area at the subsolar point; nor have we data on the radiation from the dark side or the rate of cooling during an eclipse. Nothing is known of the spherical distribution of planetary heat or reflected light from the subsolar point. We may, however, apply what was observed on the moon to the planet Mercury, since the internal evidence here shows that their physical conditions are probably much the same.

Temperature from the planetary heat.—The distribution of radiation over the disk of the full moon was found to be

$$E = a \cos^{\frac{2}{3}} \theta , \tag{17}$$

where a is a constant and θ the angular distance from the subsolar point. In a previous paper[4] the exponent of cos θ was erroneously inverted, but the integration over the surface was properly given in the following paper,[5] in which the average energy was found to be three-fourths the value at the subsolar point.

Figure 2 shows that the value of the planetary heat received from the whole disk of Mercury at mean distance from the sun, unit distance from the earth, and at zero phase angle is

$$E_0 = 2080 \times 10^{-12} \text{ cal cm}^{-2} \text{ min}^{-1} .$$

If the whole disk radiated at the same rate as the subsolar point, and the distribution over the disk is the same as for the moon, the total radiation received at one astronomical unit would be

$$E_s = \tfrac{4}{3} \times 2080 \times 10^{-12} = 2770 \times 10^{-12} \text{ cal cm}^{-2} \text{ min}^{-1} .$$

Applying the inverse-square law, we find that the radiation from the subsolar point on the surface of Mercury is

$$e_m = 2770 \times 10^{-12} \times 3.815 \times 10^{9} = 10.56 \text{ cal cm}^{-2} \text{ min}^{-1} ,$$

which corresponds to the temperature

$$T = 600^\circ \text{ K} .$$

Temperature from the solar constant.—With the solar constant taken as 1.95 cal cm^{-2} min^{-1}, the energy received at the subsolar point on Mercury from the sun at mean distance is

$$e'_0 = 13.02 \text{ cal cm}^{-2} \text{ min}^{-1} .$$

The reflected light at zero phase angle taken from Figure 2 is

$$E_R = 291 \times 10^{-12} \text{ cal cm}^{-2} \text{ min}^{-1} ,$$

which at the surface of the planet becomes

$$e'_K = 291 \times 10^{-12} \times 3.81 \times 10^9 = 1.11 \text{ cal cm}^{-2} \text{ min}^{-1} .$$

Hence the net energy absorbed by the planet for conversion into planetary heat is

$$e_0 = 13.02 - 1.11 = 11.91 \text{ cal cm}^{-2} \text{ min}^{-1} ,$$

and the corresponding temperature is

$$T = 617^\circ \text{ K} .$$

The discrepancy of 17° C in the temperature obtained by the two methods may be due in part to unknown losses by conduction in the planet or to a peculiar distribution of the radiation about the subsolar point. It was found in the study of the moon that the reflected energy was 0.24 cal cm^{-2} min^{-1}, which was 0.124 of the incident solar radiation, as against 0.085 for Mercury. On the other hand, Jost's observation[9] on the visual light of Mercury at 7° phase angle during the eclipse of May 28, 1900, was −2.8 mag., about a magnitude brighter than that given by equation (3). Hence there is some reason to think that Mercury may be brighter at zero phase angle than the lunar curve indicates. If we use the broken line in Figure 2, we get

$$e_0 = 13.02 - 1.45 = 11.57 \text{ cal cm}^{-2} \text{ min}^{-1} , \qquad T = 612^\circ \text{ K} .$$

If we adopt 610° K, which is nearly the mean of the values resulting from two direct methods, for the temperature of the subsolar point on Mercury at mean distance from the sun, the temperature at perihelion will be 685° and at aphelion 555° K.

RADIOMETRIC ALBEDO

The albedo of a planet is the ratio of the light reflected by the whole illuminated hemisphere to that received by it, and is given by

$$A = pq ,$$

[9] *Heidelberg Mitt.*, **1**, 5, 1901.

where p is the ratio of the brightness of the planet at full phase to that of a self-luminous body of the same size and position which radiates as much light from each surface unit as it receives from the sun under normal illumination. The factor p may be obtained from the equation

$$\log p = 0.4\,[m_r\,(\text{sun}) - m_r''\,(\text{Mercury})] + \log \pi - 2 \log \sin 1'' .$$

It has already been shown that m_r (sun) is -27.18 (or -27.63 outside the atmosphere). From Figure 2 we see that the radiometric magnitude of the reflected light at unit ρ and mean r is -3.06, which becomes -1.00 at unit r. The area of Mercury at unit distance is 35.0 square seconds. The reduction to 1 square second is 3.86 mag., whence m_r'' is $+2.86$ mag., and $p = 0.093$. The value of q depends on the law of reflection,[10] and for Mercury is given as 0.72, whence $A = 0.067$. The value of A for the moon was 0.093.

CARNEGIE INSTITUTION OF WASHINGTON
MOUNT WILSON OBSERVATORY
October 1935

[10] H. N. Russell, *Ap. J.*, **43**, 190, 1916.

A SCALE OF WAVE-LENGTHS IN THE INFRA-RED SOLAR SPECTRUM*

HAROLD D. BABCOCK, CHARLOTTE E. MOORE,[1] AND WENDELL P. HOGE

ABSTRACT

Interferometer measurements made in 1927 have in some cases been slightly improved in relative value without systematic change of scale. Similar *new* observations extend the scale to λ 10603. Standards of reference have been chosen from the A band of atmospheric oxygen as previously determined from neon standards.

With the *concave grating alone* provisional standards have been measured as far as λ 12103 in terms of adopted solar standards in the visual region by the method of overlapping orders.

Methods of reduction are described, and *tables* for finding the correction due to observer's motion relative to the sun are given.

Results, in Table VI, include 249 lines, of which 142 are telluric. The *accuracy* of the wave-lengths in Table VI, when tested indirectly by means of a much larger collection of data based on these standards, is found to be decidedly higher than that of most laboratory data in the infra-red, and even well beyond λ 10000 our wave-lengths appear to be reliable to about 1 part in a million.

Since the publication of *A Study of the Infra-Red Solar Spectrum with the Interferometer*[2] the difficulties that hamper photographic observations in this region of the spectrum have been much reduced. Nevertheless, no further investigations of the kind described in that paper appear to have been made, and the provisional scale of solar wave-lengths to λ 8980 is still without confirmation or extension by other observers. As improved photographic plates have become available, our measurements, however, have been carried to greater wave-lengths, and the need of reliable standards beyond λ 10000 has therefore increased.

This paper presents some results selected from the earlier publication, now slightly improved in relative value by later grating measurements, but without systematic change from the scale of 1927, together with new observations with the interferometer terminating at λ 10603, and, further, a list of tentative standards

* *Contributions from the Mount Wilson Observatory, Carnegie Institution of Washington*, No. 534.

[1] University Observatory, Princeton.

[2] Babcock, *Mt. W. Contr.*, No. 328; *Ap. J.*, 65, 140, 1927.

obtained with the grating alone in the region λλ 10600–12103. These data, collected in the course of a more detailed investigation now several years in progress, are set forth in advance of the publication of the larger paper in order to call attention to the need of collaboration by other observers in the task of establishing the scale of solar wave-lengths in the infra-red.

NEW INTERFEROMETER MEASUREMENTS

The new measurements with the Fabry-Perot interferometer cover the interval λλ 8824–10603, the method being the same as that used for shorter wave-lengths, involving integrated sunlight and reference standards (Table I) chosen from the A band of atmospheric

TABLE I

ATMOSPHERIC OXYGEN LINES USED AS STANDARDS FOR INTERFEROMETER MEASUREMENTS

λ	Int.	λ	Int.
7665.944	10	7689.177	4
7670.600	9	7690.217	4
7671.670	9	7695.836	2
7676.563	7	7696.868	2
7677.618	7	7702.736	1
7682.756	5	7703.754	1
7683.800	5		

oxygen. Although these lines of oxygen have not been internationally adopted as standards, our experience strongly supports the arguments already advanced in favor of their use. The wave-lengths of the lines in Table I, derived from a considerable amount of unpublished data on the telluric bands of oxygen in the solar spectrum, are essentially the same as those published in 1927. Two weaker lines and three stronger ones have now been added to the list. The intensities stated in Table I are provisional and are given only to indicate the well-known decrement from doublet to doublet. In this part of the P-branches the members of each doublet appear identical, although nearer the origin this is not the case. Naturally, the intensities of all these lines differ notably from plate to plate, being dependent on the solar altitude during the exposure.

The interferometer spectrograms were made with the same gold

films on silica plates as were used in 1927, and similar precautions for the avoidance of error were observed. The etalons were 7.5, 10, and 15 mm in thickness. The former auxiliary spectrograph was moved several years ago into another building near by, where additional space permitted important changes in construction. In consequence a greater range of the infra-red region is now accessible, and the same grating can be used in either of two types of mounting. This novel plan has the advantage of economy of gratings and of space, which for our purpose outweighs some less desirable features. The auxiliary dispersion was about 4.5 A per millimeter.

TABLE II

THICKNESS OF ETALON FROM EACH STANDARD ON ONE SPECTROGRAM

λ	Observed Order of Interference	Product = Double Thickness in mm
7665.944	19229.701	14.741381
7670.600	19218.014	70
7671.670	19215.356	87
7676.563	19203.099	80
7677.618	19200.454	75
7682.756	19187.624	83
7683.800	19185.009	77
7689.177	19171.590	75
7690.217	19168.997	75
7695.836	19154.996	71
7696.868	19152.448	14.741386
Mean	.....	14.741378 ± 0.000002 M.E.

The Fabry-Perot interferometer is a powerful and highly satisfactory instrument especially well adapted to our present requirements. Even with exposures of more than two hours (the usual exposure has been about one hour), the results have been free of systematic deviations from the mean. Further, within wide limits the intensity of a line has no influence on its measured position. For example, the thickness of an etalon derived from the standards in Table I in the regular course of our work is the same for both strong and weak lines (Table II). This evidence is conclusive, since the relative wave-lengths of the standards in Table I are independent of their intensities, having been derived from accordant measurements

of both grating and interferometer spectrograms on which any possible intensity effect would have influenced the results quite differently, and on which the absolute intensities of all the lines varied widely. Furthermore, the well-known structure of the oxygen bands provides tests which indicate that these wave-lengths are highly reliable. The agreement shown in Table II is therefore significant.

The old and the new series of interferometer observations include some lines in common between λ 8824 and λ 8980, and for these the agreement is satisfactory.

Our method of measurement and reduction of the interferometer spectrograms is essentially the same as that in regular use for both emission and absorption spectra whenever large numbers of lines are observed simultaneously. In view of some apparent misunderstanding about the origin of this method, we remark that it was devised by Babcock and first published in papers[3] of which he was a joint author but which appear to have been overlooked by several later writers. For example, Childs,[4] to whom the method has been ascribed,[5] omitted from the text of his paper any reference to the work that had been done at the Mount Wilson Observatory, although he did give, without comment, in a short bibliography, a reference to a letter in *Nature*[6] which briefly discussed the subject. Much of Childs's paper is obviously a compilation of information drawn from many sources; but, although distinctly valuable, these parts of it have evidently been mistaken by others for the product of original research.

The first account of the method[3] showed that economy of labor and increase of accuracy result from its application. Either in its first form or slightly modified to adapt it to different auxiliary spectrographs it has supplanted the earlier procedure in which the focal length of a lens or mirror had to be determined and the magnification of the auxiliary spectrograph measured for every spectrum line.

[3] St. John and Babcock, *Mt. W. Contr.*, Nos. 137, 202; *Ap. J.*, **46**, 145, 1917; **53**, 260, 1921.

[4] *Journal of Scientific Instruments*, **3**, 97–103 and 129–135, 1926.

[5] Burns, Meggers, and Kiess, *Bureau of Stds. Jour. Research*, **1**, 303, 1928; M. E. Warga, *Pub. Allegheny Obs.*, **6**, 151, 1928.

[6] Babcock, *Nature*, **114**, 276, 1924.

An examination of the results given by different etalons revealed no need for a so-called phase-change correction. While admitting that a considerably larger number of observations might show the existence of this effect, we believe its magnitude, for our apparatus, is too small to require attention here. If present, it affects our results systematically. Independent observations would be a valuable check on our work.

CONCAVE-GRATING MEASUREMENTS

For establishing the scale of wave-lengths in the region beyond λ 10603, we have used the method of overlapping spectra from different orders of a concave grating. By a simple arrangement of mirrors, our 21-foot concave grating may be used in either the Rowland or the stigmatic mounting without disturbing the grating itself. The latter form is particularly useful as an auxiliary for the interferometer and also as an independent instrument for direct photographs of spectra under conditions requiring economy of light, and is the arrangement used for obtaining standards in the solar spectrum beyond λ 10600. A comparison spectrum was photographed on each side of the infra-red by the use of a special occulting device and a change of color filters; but neither of these operations involved contact with, or disturbance of, any part of the spectrograph, and, since the comparison spectrum was that of the sun itself, the illumination of the grating remained unchanged. Thus some of the insidious sources of systematic error were avoided.

The occulting mechanism was set up independently of the spectrograph at a point on the optical axis several meters in front of the slit, where it was easily operated without touching the main apparatus. It was operated in parallel light; and, as no image of the sun was formed on the slit, integrated sunlight was used throughout, just as for our interferometer measurements. Except for the addition of the occulter and the removal of the interferometer, the projection system was the same as when the interferometer was in use.

Since the comparison-spectrum exposure could not be made simultaneously with that on the infra-red, the second-order spectrum was exposed at the beginning and the end and at equally spaced intervals during the main exposure. Any possible systematic

displacement of the infra-red spectrum relative to the comparison spectrum on the different plates is too small to be revealed by such measurements as we have yet been able to make.

A limitation in the use of overlapping higher orders of spectra lies in the practical impossibility of employing the best width of slit for both the orders used. In our case a slit properly adjusted for the infra-red is too wide for the comparison spectrum. Since errors would certainly be introduced if the slit-width were changed each time a part of the comparison was put on, we have used throughout the correct adjustment for the infra-red.

For spectrographs that utilize nearly all their theoretical resolving power a reliable general rule is to make the slit-width equal to λ/ψ, where λ is the wave-length at the center of the plate and ψ the angle, measured in radians in the plane of dispersion, subtended at the slit by the ruled surface of the grating. This rule is based on the work of Schuster,[7] slightly refined by some unpublished results by J. A. Anderson, and has the added authority of extended observational verification. For the Rowland mounting of the concave grating, ψ is always equal to the width of the ruled surface divided by its radius of curvature; hence the slit-width is simply a constant times the wave-length.

For the stigmatic mounting, ψ is the width of the ruled surface times the cosine of the angle of incidence divided by the focal length of the collimator. The angle of incidence corresponding to any wave-length is readily found from the fundamental equation for grating spectra. In our case the slit-width ranges between 29 λ and 45 λ for extreme positions of the camera in the stigmatic mounting, while for the same grating used in the Rowland arrangement it is always 58 λ.

The slit-width determined by this rule gives about 80 per cent of the resolving power that would be afforded by an infinitely narrow slit, yet is not so narrow as to waste an excessive amount of the incident light. For the case of an emission line it gives 77 per cent of the intensity that would be available with an indefinitely wide slit.

It thus appears that our comparison spectra were photographed with a slit having twice the optimum width. In consequence the

[7] *Ap. J.*, **21**, 197, 1905.

resolving power was lower than it would normally be in the second order—45 per cent, instead of 80 per cent, of the maximum; but, as the second order gives approximately twice the resolving power of the first, the net result is a slightly larger resolving power than for the infra-red spectrum.

An extremely useful filter for removing undesirable light from the spectrograph is the "heat transmitting" glass No. 254 made by the Corning Glass Works. A filter absorbing all radiation of wave-length less than λ 10000 and transmitting without absorption beyond that point would be a valuable addition to our equipment.

The observations beyond λ 10000 were made almost entirely on Eastman Xenocyanine plates. Emulsions of different characteristics were used, among them some kindly sent to us by Dr. C. E. K. Mees, director of the Research Laboratory of the Eastman Kodak Company, while yet in the experimental stage. It is a pleasure to acknowledge our indebtedness to Dr. Mees for his continued interest and helpfulness. A minor difficulty arose through the low sensitivity of Xenocyanine plates to the green comparison spectrum. A heat-absorbing filter opaque to $\lambda > 10000$ would have been useful.

For reduction purposes a relation of the form

$$\lambda = A + Bs + Cs^2$$

was assumed, where s is the reading of the screw of the measuring machine corresponding to the wave-length λ, and A, B, C are constants, which were determined by a least-squares reduction of the data for the standard lines. For a typical plate the resultant equation is

$$\lambda = 5389.486 + 2.23026s - 0.0000152s^2 .$$

The standards used for this plate and the corresponding differences between them and the observed values are given in Table III.

To bridge the gap λλ 10603–10743 that still exists between our standardized lines obtained with the interferometer and lines determined with the grating alone, we have included in Table VI six lines whose wave-lengths have been thus far measured only by interpolation. These lines naturally have somewhat lower weight than

the others. The relative wave-lengths of a few other lines beyond λ 10707 have been slightly adjusted by interpolation, but the scale

TABLE III

RESIDUALS FROM A LEAST-SQUARES REDUCTION*

Standard λ	Standard—Observed	Standard λ	Standard—Observed
5389.486	0.000	5473.910	−0.005
5409.799	+ .008	5512.989	+ .002
5432.955	− .008	5534.848	.000
5445.053	+ .001	5590.126	+ .008
5462.970	0.000	5624.558	−0.007

* Mean error of an observation ±0.003 A.

of the plates as determined from the second-order comparison has been maintained.

CORRECTION FOR VELOCITY

Corrections for the motion of the apparatus relative to the sun have been applied to the observed wave-lengths when appreciable, a procedure which has increased the accordance of the results derived from different spectrograms. In the infra-red this correction may be a considerable amount; and, as some observers seem to have overlooked its importance, the details necessary for its calculation are given here.

The velocity of a point on the earth's surface relative to the sun is the resultant of two components, V_d, due to the rotation of the earth about its axis, and V_a, due to the orbital motion of the earth, a small effect due to the moon being neglected. The displacement, $\Delta\lambda$, of a spectral line, λ, corresponding to the resultant of V_d and V_a is $\Delta\lambda = \lambda(V_d + V_a)/c$, where c is the velocity of light in air, assumed to be 2.997×10^5 km/sec.

From elementary considerations we have, in kilometers per second,

$$V_d = \frac{2\pi R}{86{,}164} \sin t \cos \delta \cos \phi ,$$

where t is the sun's hour angle, δ its declination, ϕ the observer's latitude, and R the equatorial radius of earth, 6378.39 km.

Table IV gives values of V_d/c for the arguments t and δ for a station on the equator ($\phi = 0$). For any other station the tabular value

TABLE IV

CORRECTION TO WAVE-LENGTH FOR OBSERVER'S DIURNAL VELOCITY RELATIVE TO THE SUN*

HOUR ANGLE t	DECLINATION					
	±0°	±8°	±12°	±16°	±20°	±23°27′
	Mar. 21 Sept. 24 Sept. 24 Mar. 21	Apr. 11 Sept. 3 Oct. 15 Mar. 1	Apr. 22 Aug. 22 Oct. 26 Feb. 18	May 5 Aug. 9 Nov. 7 Feb. 5	May 21 July 24 Nov. 22 Jan. 21	June 22 June 22 Dec. 23 Dec. 23
0^h00^m	0	0	0	0	0	0
15	10	10	10	10	10	9
30	20	20	20	19	19	19
45	30	30	30	29	28	28
1 00	40	40	39	39	38	37
15	50	49	49	48	47	46
30	59	59	58	57	56	54
45	68	68	67	66	64	63
2 00	77	77	76	74	73	71
15	86	85	84	83	81	79
30	94	93	92	91	88	86
45	102	101	100	98	96	94
3 00	109	108	107	105	103	100
15	116	115	114	112	109	107
30	123	121	120	118	115	113
45	129	127	126	124	121	118
4 00	134	133	131	129	126	123
15	139	137	136	133	130	127
30	143	141	140	137	134	131
45	147	145	143	141	137	134
5 00	149	148	146	144	140	137
15	152	150	148	146	143	139
30	153	152	150	147	144	141
45	154	153	151	148	145	142
6 00	155	153	151	149	145	142

* The tabular numbers are values of $10^8 V_d/c$. To obtain the correction for any line, multiply the tabular number for the declination and hour angle corresponding to mid-exposure by the wave-length of the line, in angstroms, and by the cosine of the latitude and divide the product by 10^8. The resulting correction, in angstroms, is opposite in sign to t, i.e., negative after noon, positive before noon. See note to Table V.

is to be multiplied by cos ϕ. The approximate dates corresponding to tabulated declinations permit the use of Table IV in practically

all cases without recourse to the *Ephemeris*, since the hour angle of the sun at mid-exposure can be ascertained with more than sufficient accuracy from approximate values of the equation of time, the observer's longitude, and the standard time. It is convenient to make for one's observing station a brief table, combining for chosen dates the reduction from local time to standard time with the equation of time, the small variations in the latter quantity from year to year being disregarded.

A simple way of obtaining V_a is to take from the *Ephemeris* the tabulated variation in the logarithm of the earth's radius vector, subtract 1 from the corresponding number, multiply the difference by the astronomical unit in kilometers (149,500,000), and divide by the number of seconds in the tabular interval.

Analytically, we have

$$V_a = \frac{2\pi ae}{T\sqrt{1-e^2}} \sin\theta ,$$

where a and e are the semimajor axis and eccentricity of the earth's orbit, T the sidereal year in mean solar seconds, and, for the epoch 1940,

$$\theta = 281^\circ 54'.5 - \text{sun's longitude} .$$

Table V gives the values of V_a/c computed by these formulae for every 5° of the sun's longitude, with $e = 0.01674$ and $T = 31{,}558{,}000$ sec. As the change in the longitude of perihelion is slow, this table for 1940 is amply accurate for use at present and for some years to come. Trial shows that the errors arising from the use of the mean dates assigned to the values of the sun's longitude in place of the longitudes themselves are negligible; hence, with the aid of Tables IV and V both V_d and V_a can be found without access to a solar ephemeris.

The tables show that for stations at the equator and in latitude 50° a solar line at λ 10000 measured in terms of terrestrial standards in early morning near the beginning of October will be observed too small by 0.032 A and 0.026 A, respectively. In late afternoon near

TABLE V

CORRECTION TO WAVE-LENGTH FOR EARTH'S ORBITAL MOTION: EPOCH 1940*

Sun's Longitude	Approx. Date	$10^8 V_a/c$	Approx. Date	Sun's Longitude
0°	Mar. 21	−163	Sept. 24	180°
5	26	165	29	185
10	31	166	Oct. 4	190
15	Apr. 5	166	9	195
20	11	165	14	200
25	16	162	19	205
30	21	158	24	210
35	26	153	29	215
40	May 1	147	Nov. 3	220
45	6	139	8	225
50	11	131	13	230
55	17	121	18	235
60	22	111	23	240
65	27	100	28	245
70	June 1	88	Dec. 3	250
75	6	75	8	255
80	12	62	13	260
85	17	48	18	265
90	22	34	23	270
95	27	20	27	275
100	July 3	− 6	Jan. 1	280
105	8	+ 9	6	285
110	13	23	11	290
115	18	38	16	295
120	24	52	21	300
125	29	65	26	305
130	Aug. 3	78	31	310
135	8	91	Feb. 5	315
140	14	103	9	320
145	19	114	14	325
150	24	124	19	330
155	29	133	24	335
160	Sept. 3	141	Mar. 1	340
165	8	148	6	345
170	14	154	11	350
175	19	+159	16	355

* Multiply the tabular number from third column corresponding to the sun's longitude, or to the date, by the wave-length, in angstroms, of the line whose displacement is sought and divide by 10^8. The result, in angstroms, has the tabular sign except for longitudes and dates on the right; for these the tabular sign is to be reversed. Components from Tables IV and V are most conveniently combined before multiplying by λ.

the beginning of April the observed wave-length will be too great by the same amounts.

Solar wave-lengths measured in terms of atmospheric oxygen standards were corrected in accordance with the above formulae. Solar lines measured in terms of solar standards require no correction. For atmospheric lines measured in terms of solar standards the calculated correction is applied with sign reversed. When both solar and atmospheric standards are used in the reduction, attention to the detailed application of corrections is particularly necessary.

RESULTS

The proposed standard lines given in Table VI have been selected from a considerably larger number, many of which are as well determined as those listed. Our choice has been made with respect to the apparent reliability of the result, the spacing of the lines, their intensities, their freedom from close companions, and in some degree their origin, whether solar or terrestrial. As complete data are still lacking for the classification of the lines as to origin, we have temporarily assumed that all the lines in Table VI of wave-length greater than λ 11000, with the exception of two, are due to water vapor in the earth's atmosphere. Beyond λ 11423 the wave-lengths were obtained from a single spectrogram, and the second decimal place has considerable uncertainty. The measurements were made in air at temperatures near 20° C and pressures of about 74.5 cm of mercury. Corrections to reduce them to 15° C and 76 cm seem hardly worth evaluating and applying.

To avoid an accumulation of errors, reductions of all the spectrograms have been carried to the third decimal place. Interferometer data between λ 9900 and λ 10604 were rounded off to read 0 or 5 in the third place, while results from the grating alone are stated to the nearest 0.01 A. We omit a statement of the indicated accuracy of each line in Table VI because the real reliability of such data is well known to be less than that computed from the consistency of the measurements. We remark, however, that these wave-lengths are decidedly more accurate than most laboratory observations now available in the infra-red region.

TABLE VI

A SCALE OF WAVE-LENGTHS IN THE INFRA-RED SOLAR SPECTRUM*

λ	Element	Int.	λ	Element	Int.
7050.853	Atm.	2	7690.217	Atm. *O*	4
7068.423	*Fe*	2	7695.836	Atm. *O*	2
7090.390	*Fe*	3	7696.868	Atm. *O*	2
7122.206	*Ni*	5	7702.736	Atm. *O*	1
7130.925	*Fe*	4	7703.754	Atm. *O*	1
7148.150	*Ca*	5	7714.309	*Ni*	7
7178.422	Atm.	2	7727.616	*Ni*	8
7202.208	*Ca*	2	7742.722	*Fe*	9
7227.493	Atm.	8	7780.567	*Fe*	9
7236.136	Atm.	4	7797.587	*Ni*	6
7260.730	Atm.	2	7807.915	*Fe*	5
7275.398	Atm.	9	7832.207	*Fe*	9
7287.378	Atm.	6	7849.984	⊙	5
7303.197	Atm.	5	7887.117	Atm.	3
7315.516	Atm.	3	7893.511	Atm.	4
7335.335	Atm.	3	7920.664	Atm.	7
7369.206	Atm.	2	7937.149	*Fe*	9
7383.721	Atm.	3	7945.857	*Fe*	9
7393.609	*Ni*	4	7971.520	Atm.	4
7405.790	*Si*	4	7994.488	*Fe*	2
7422.286	*Ni*	4	8012.940	Atm.	4
7445.758	*Fe*	7	8046.056	*Fe*	8
7462.342	*Cr*	5	8075.158	*Fe*	2
7491.652	*Fe*	3	8107.841	Atm.	4
7511.031	*Fe*	8	8125.444	Atm.	3
7531.153	*Fe*	4	8146.214	Atm.	5
7555.607	*Ni*	6	8165.338	Atm.	3
7574.046	*Ni*	3	8186.371	Atm.	8
7583.796	*Fe*	5	8194.836	*Na*	6
7619.212	*Ni*	3	8212.132	Atm.	5
7657.605	*Mg*	4	8218.112	Atm.	10
7665.944	Atm. *O*	10	8239.925	Atm.	4
7670.600	Atm. *O*	9	8252.727	Atm.	6
7671.670	Atm. *O*	9	8272.041	Atm.	8
7676.563	Atm. *O*	7	8279.600	Atm.	9
7677.618	Atm. *O*	7	8300.407	Atm.	10
7680.267	*Si*	4	8327.060	*Fe*	6
7682.756	Atm. *O*	5	8333.584	Atm.	5
7683.800	Atm. *O*	5	8357.041	Atm.	6
7689.177	Atm. *O*	4	8367.332	Atm.	6

* Differences between the data here given and those in *Trans. I.A.U.*, **5**, 1935, Report of Commission 14, result from additional observations. Most of the few lines formerly listed beyond λ 12000 are now considered to be either spurious or unsuitable for use as standards. Improved spectrograms are being measured as far as λ 13500, but the results are not yet ready for publication.

TABLE VI—*Continued*

λ	Element	Int.	λ	Element	Int.
8373.711	Atm.	5	9275.072	Atm.	2
8387.782	*Fe*	9	9289.855	Atm.	2
8397.152	Atm.	2	9301.910	Atm.	5
8412.356	*Ti*	3	9311.735	Atm.	6
8435.655	*Ti*	3	9330.456	Atm.	5
8468.418	*Fe*	7	9348.382	Atm.	2
8514.081	*Fe*	6	9363.332	Atm.	3
8526.674	*Fe*	3	9374.278	Atm.	2
8556.795	*Si*	7	9406.903	Atm.	9
8582.271	*Fe*	5	9444.410	Atm.	5
8611.813	*Fe*	6	9463.993	Atm.	3
8648.472	*Si*	9	9476.753	Atm.	4
8674.756	*Fe*	6	9491.526	Atm.	2
8688.642	*Fe*	10	9504.435	Atm.	3
8717.833	⊙	7	9512.630	Atm.	5
8728.024	—*Si*	7	9533.411	Atm.	4
8736.040	*Mg*	12	9575.680	Atm.	2
8752.025	*Si*	10	9587.125	Atm.	5
8773.907	*Al*	4	9598.871	Atm.	7
8804.637	*Fe*	3	9614.048	Atm.	4
8824.236	*Fe*	9	9624.496	Atm.	3
8866.943	*Fe*	8	9643.105	Atm.	3
8879.318	Atm.	3	9659.729	Atm.	3
8912.101	⊙	7	9686.386	Atm.	3
8930.269	Atm.	4	9700.140	Atm.	2
8958.401	Atm.	4	9708.922	Atm.	4
8963.492	Atm.	4	9724.576	Atm.	4
8986.600	Atm.	5	9730.636	Atm.	4
8993.042	Atm.	0	9749.322	Atm.	12
9018.090	Atm.	3	9765.497	Atm.	4
9031.395	Atm.	4	9779.408	Atm.	4
9047.411	Atm.	2	9799.475	Atm.	5
9052.972	Atm.	7	9813.461	Atm.	3
9074.308	Atm.	7	9821.754	Atm.	3
9085.453	Atm.	3	9831.961	Atm.?	4
9092.481	Atm.	5	9861.746	*Fe*	1
9105.401	Atm.	7	9889.052	*Fe*	5
9115.644	Atm.	3	9898.972	*Ni*, Atm.	5
9132.442	Atm.	3	9944.220	*Fe*	3
9160.904	Atm.	4	9986.490	⊙	3
9178.535	Atm.	3	9997.665	⊙	2
9192.568	Atm.	5	10036.670	Sr^+	5
9205.586	Atm.	3	10065.070	*Fe*	8
9225.007	Atm.	6	10077.665	⊙	3
9251.100	Atm.	6	10087.140	⊙	3

TABLE VI—*Continued*

λ	Element	Int.	λ	Element	Int.
10092.745	⊙	3	11004.12	Atm.	4
10118.995	⊙	3	11020.87	Atm.	3
10123.895	⊙	8	11036.92	Atm.	3
10145.580	*Fe*	10	11054.74	Atm.	4
10172.095	⊙	2	11074.61	Atm.	7
10193.245	*Ni*	4	11098.96	Atm.	4
10216.335	*Fe*	9	11123.30	Atm.	5
10218.415	*Fe*	3	11143.34	Atm.	6
10272.950	⊙	1	11157.30	Atm.	15
10288.950	*Si*	6	11175.63	Atm.	2
10327.360	Sr^+	7	11213.91	Atm.	4
10340.900	*Fe*	3	11227.53	Atm.	9
10343.840	*Ca*	8	11268.16	Atm.	6
10371.285	*Si*	9	11310.76	Atm.	3
10395.795	*Fe*	4	11316.77	Atm.	3
10455.450	*S*	7	11371.98	Fe^+–	3N
10459.430	*S*	7	11394.76	Atm.	2
10469.680	*Fe*	7	11423.29	Atm.	15
10585.165	*Si*	12	11427.91	Atm.	10
10603.440	*Si*	10	11460.15	Atm.	20
10627.63	*Si*	8	11477.37	Atm.	10
10660.98	*Si*	10	11501.74	Atm.	10
10683.11	*C*	9	11530.62	Atm.	12
10685.35	*C*	8	11565.63	Atm.	15
10689.73	*Si*	8	11580.76	Atm.	10
10707.32	*C*	8	11613.87	Atm.	20
10743.47	⊙	6	11638.27	Atm., *Fe*	20
10772.86	⊙	4	11661.81	Atm.	10
10784.58	*Si*	3	11691.94	Atm.	20
10799.58	⊙	10	11720.45	Atm.	20
10834.01	⊙	5	11750.03	Atm.	8
10857.31	⊙	6	11774.41	Atm.	15
10863.50	*Fe, Ca*	3	11780.84	Atm.	20
10874.92	⊙	2	11795.86	Atm.	8
10892.24	⊙	5	11810.14	Atm.	8
10903.70	⊙	5	11899.54	Atm.	10
10930.86	⊙	5	11915.37	Atm.	4
10946.32	⊙	10	12103.47	Atm.	8
10965.45	*Mg?*	5			
10984.42	*Si*	3			

This conclusion is reached through a study of our larger body of solar observations, which are based on the standards of Table VI, and is supported, in respect to the relative values of our wave-lengths, by comparisons of differences in wave-number for selected pairs of lines. For example, two solar lines of Sr^+ beyond λ 10000 give a difference of 801.46 cm^{-1}, representing the separation of two energy-levels in the atom. From laboratory data involving three other pairs, in the violet and ultra-violet, Fowler[8] finds 801.45 cm^{-1} for the spacing of the same two energy-levels. Two infra-red pairs of *Si* lines show, from our measurements, a mean $\Delta\nu = 77.124$ cm^{-1}, while the corresponding solar pair near λ 5700 give 77.118 cm^{-1}. Three other *Si* pairs lying between λ 10371 and λ 10979 have $\Delta\nu$ equal respectively to 194.770, 194.791, and 194.801 cm^{-1}; and two corresponding pairs in the solar spectrum near λ 5700 have $\Delta\nu$ equal to 194.770 and 194.802 cm^{-1}.

Among the lines most difficult to measure in the whole solar spectrum are those of the intense triplet of $Ca^+(3^2D - 4^2P^o)$. Our separation for the pair λλ 8498–8662 is 222.882 cm^{-1}. This value may be compared with the refined observations on H and K from laboratory sources, where the lines may be made very narrow and where the agreement between many observers is close. The mean of our own unpublished work with the interferometer is $\Delta\nu = 222.908$ cm^{-1}. If we assume that all the error is in λ 8662, our solar wave-length for this line would be 0.02 A too great.

In laboratory data for the infra-red we seldom find agreement as close as that just shown. It would hardly be fair, however, to present such data for the lines just discussed, since *Si* in particular is characterized by very diffuse lines in those laboratory sources from which the wave-lengths are available. Enough has been said, however, to show that even well beyond λ 10000 our relative values are probably reliable to 1 part in a million, while most laboratory data are subject to errors of several times this amount.

With respect to systematic errors in our scale of wave-lengths, we find confirmation for the foregoing general statement in two interesting tests. Here, again, it is necessary to draw upon our more extended solar data, since the special lines included in Table VI are

[8] *Report on Series in Line Spectra*, London, 1922.

too few to serve our purpose. From known term values for the spectra of certain elements, chiefly *Fe*, scores of lines have been predicted and identified in the infra-red solar spectrum. Since the effects of chance agreement between predicted positions of the lines and their measured solar wave-lengths are minimized by the large number of lines involved and by the fact that such identifications depend upon multiplet structure as noted below, these identifications indicate that systematic errors in the solar data do not exceed a few hundredths of an angstrom.

Russell, Babcock, and Miss Moore[9] have called attention to new series lines of *Mg* in the sun. These data also serve as a check upon the homogeneity of our scale of wave-lengths throughout the region λλ 6895–10813. For example, the difference in wave-number between homologous lines in the singlet and triplet series, amounting to about 1554 cm^{-1}, may be used as a measuring stick for testing the scale of wave-lengths. Applied eight times, with some overlapping, it covers the region mentioned; and the probable error of an individual value of this interval is found to be only ± 0.04 cm^{-1}. Dividing the error equally between the two lines involved in a single difference, we find the probable error of a single wave-number to be $\pm 0.04/\sqrt{2}$. Even when tested by these lines of *Mg*, which are extremely difficult to measure, our scale of wave-lengths therefore appears to be homogeneous within about 1 part in 330,000.

Measurements for the improvement of Table VI, which will also extend our determinations of wave-length beyond λ 13500, are now in progress at Mount Wilson. Independent investigations at other observatories are much to be desired, however, as a control on our work, and, in fact, are required by the policy of the International Astronomical Union as a prerequisite to the formal adoption of standards.

From the preceding remarks it will be apparent that the identifications in the second column of Table VI have been made by amplifying Rowland's method of coincidences to include the results of multiplet analysis of the various spectra. The work is still in progress, and details will be discussed in our succeeding paper.

The intensities in the final column, although on an approximately

[9] *Phys. Rev.*, **46**, 826, 1934.

uniform scale, are only provisional, and we expect some of them to be changed in the final publication. The values given are included because they are of some assistance in finding the lines, but they are not intended for other use. We remark that, in this paper, both the intensities and the identifications are secondary in importance to the wave-lengths.

We are indebted to several members of the Observatory Staff for assistance in obtaining grating spectrograms on Mount Wilson, and to Professor John C. Duncan, director of the Whitin Observatory at Wellesley College, for efficient help with both the interferometer and the grating spectrographs in Pasadena.

CARNEGIE INSTITUTION OF WASHINGTON
MOUNT WILSON OBSERVATORY
November 1935

NEW ELEMENTS FOR THE SPECTROSCOPIC BINARY BOSS 6142*

ROSCOE F. SANFORD

ABSTRACT

Elements.—A new set of orbital elements is derived for the primary of the spectroscopic binary Boss 6142, based upon data for the earliest Mount Wilson (1911–12) velocities, the recent Mount Wilson and Victoria velocities (1924–34), and the numerous Ottawa observations (1915–16). The only significant change is a decrease in the period from 13^d435 to 13^d4187. All available data give 144 km/sec as the semiamplitude of velocity variation for the secondary star, as compared with Young's tentative value of 167 km/sec. The secondary's spectrum tends to make the measured velocities too close to the γ-value when the stronger lines of the primary coalesce with the weaker lines of the secondary.

The derived minimum masses of primary and secondary are 13.5 ⊙ and 11.0 ⊙, respectively; the minimum distances from the center of mass, 21,572,000 and 26,438,000 km.

Detached lines.—Young's mean value for the velocity from the detached lines of calcium is −24.4 km/sec; that from recent Victoria and Mount Wilson spectrograms, −18.0 km/sec; and Merrill's mean velocity from the detached sodium lines, −19.5 km/sec. The agreement of the recent calcium and sodium velocities may indicate a systematic difference between the measures made at Ottawa and at Victoria and Mount Wilson.

Dr. R. K. Young[1] has published elements for the spectroscopic binary Boss 6142,[2] based on radial velocities from 1911 to 1916, inclusive.

Spectrograms taken at Mount Wilson, primarily to obtain the radial velocities from the detached lines of sodium and calcium, yielded, as by-products, stellar radial velocities that indicate an error in the period which has put them out of step with Young's elements by at least one-half a period in the elapsed interval. Young had derived a rough value of the period from the Ottawa observations of 1915–16, which he then attempted to evaluate more exactly with the aid of four velocities obtained at Mount Wilson in 1911–12. Unfortunately, he used incorrect Julian dates for three of them, which led to an erroneous period.

* *Contributions from the Mount Wilson Observatory, Carnegie Institution of Washington*, No. 535.

[1] *Pub. Dom. Obs. Ottawa*, **3**, 373, 1919.

[2] HD 224151, BD +56°3115, Bradley 3184; α 23^h 50^m5, δ +56°53′ (1900), Bo, vis. mag. 6.0.

TABLE I

RADIAL VELOCITIES FOR BOSS 6142

Plate No.	Julian Day	Phase	Stellar Vel.		Detached-Line Vel.	
			Prim.	Sec.	*Ca*	*Na*
			Early Mount Wilson			
			km/sec	km/sec	km/sec	km/sec
γ 888	2419342.758	4d017	− 53	.....	.....	.....
987	9408.662	2.828	− 11	.....	.....	.....
1003	9411.633	5.799	−133	.....	.....	.....
1701	9676.811	2.603	− 23	.....	.....	.....
			Victoria			
9672	2423800.572	6.823	−126	.....	−20	.....
15703	5148.903	13.284	+116	−144	.....	.....
15720	5153.858	4.820	− 93	.....	.....	.....
15772	5184.853	8.978	− 90	.....	−23	.....
21680	7351.889	2.184	− 4	.....	−23	.....
21762	7381.803	5.261	−100	.....	− 7	.....
21783	7403.740	0.361	+102	.....	.....	.....
21797	7410.685	7.306	−112	+124	.....	.....
			Recent Mount Wilson			
G 214	2425582.665	4.229	− 57	.....	.....	[−18]
γ 17806	6262.726	13.355	+126	−180	−16	.....
γ 17868	6287.878	11.670	+ 52	.....	.....	.....
C 5673	6342.670	12.787	+100	−152	−20	.....
G 620	6994.789	7.389	−145	.....	.....	−20
G 970	7440.599	10.382	− 33	.....	.....	−17
V 490	7462.656	5.602	−114	+103	−18	.....
γ 20157	7465.659	8.605	−126	.....	−17	.....
G 1058	7650.965	6.049	−150	.....	.....	−20
1063	7677.855	6.102	−124	.....	.....	−18
1064	7677.938	6.185	−130	.....	.....	−21
1069	7678.906	7.153	−112	.....	.....	−16
1070	7678.971	7.176	−118	.....	.....	−18
1078	7710.783	12.192	+ 65	.....	.....	[−26]
1082	7711.731	13.140	+105	−173	.....	−23
1083	7711.856	13.265	+132	−151	.....	−19
1087	7712.737	0.727	+ 88	−162	.....	−20
V 650	7738.720	13.292	+102	.....	−18	.....

It seemed worth while to determine a period which would harmonize all available radial velocities, now extending from 1911 to 1934, inclusive, and to ascertain whether the change in period would produce any significant change in the other elements.

Table I contains the data for the four early Mount Wilson spectrograms; for eight spectrograms kindly lent by Professor W. E. Harper, of the Dominion Astrophysical Observatory, Victoria, B.C., and measured by the writer; and for the recent Mount Wilson spectro-

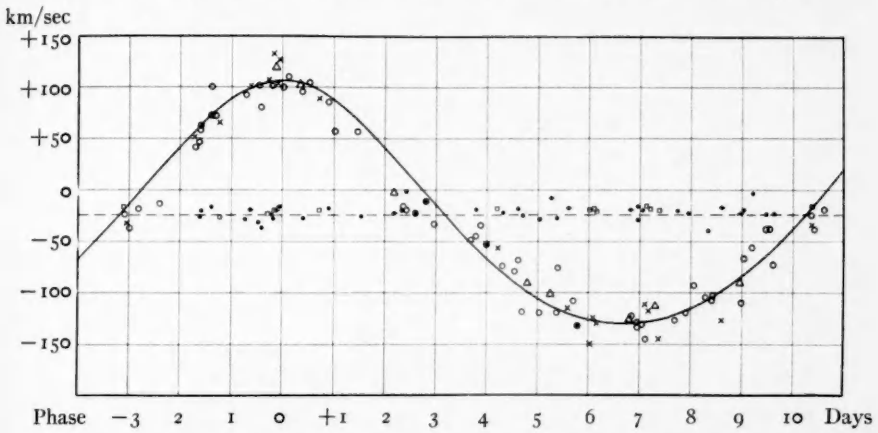

FIG. 1.—Radial velocity-curve for Boss 6142. Large dots and crosses represent old and recent Mount Wilson velocities; triangles, those from Victoria; circles, the Ottawa values by Young. The broken horizontal line indicates the systemic velocity. Barred dots show the detached *Ca*-line velocities recently determined at Mount Wilson, and dots Young's values from these lines. Merrill's velocities from the detached lines of sodium appear as encircled dots.

grams. The Ottawa observations have not been repeated here. The Victoria spectrograms and those from the Mount Wilson γ, C, and V series have comparable dispersions (about 35 A/mm at $H\gamma$). I am indebted to Dr. P. W. Merrill for permission to use the stellar velocities derived by him and Miss Cora G. Burwell from his plane-grating spectrograms (prefix G, dispersion of approximately 34 A/mm) for quite another purpose. The care with which these measures have been made is attested by the fact that, although the velocities are based largely on the one rather poor helium line, D_3, their deviations from the velocity-curve are no larger than those to be found among the other velocities.

An examination of the primary's velocities showed at once that Young's period is too long. All observations from 1911 to 1934 were found to be most consistently grouped about a single epoch when his period of $13^d.435$ was shortened to $13^d.4187$ (Fig. 1). Since more than six hundred orbital revolutions are involved, the error in the adopted period is probably less than $0^d.0001$.

The elements which seem to represent this assemblage of velocities best were derived by means of a set of standard velocity-curves and are given in Table II, together with Young's values. The velocity-curve in Figure 1 is based on the new elements for the primary.

TABLE II

ELEMENTS OF BOSS 6142

Elements	Sanford	Young
P	13.4187	13.435 days
T	J.D. 2420801.379	2420800.634 G.M.T.
ω	0°	339°.56
e	0.1	0.105
K_1	117.5	115.5 km/sec
K_2	144	[167]* km/sec
$m_1 \sin^3 i$	13.5	[18.5]$\odot$
$m_2 \sin^3 i$	11.0	[12.7]$\odot$
$a_1 \sin i$	21,572,000	21,200,000 km
$a_2 \sin i$	26,438,000	[30,700,000] km
m_1/m_2	1.23	[1.45]
γ	−24.3	−26.7 km/sec

* Bracketed values involve Young's determination of K_2, which he calls "only roughly approximate."

The observations fit the velocity-curve as well as could be expected in view of the poor quality of the stellar lines (class Bo) upon which the velocities rest. The differences in the two sets of elements for the primary, with the exception of the period, are insignificant. The considerable change in ω is unimportant for an orbit of such small eccentricity, based on velocities of a low order of accuracy.

The radial velocity for the secondary star, which had been measured by Young on nine plates, was determined on two Victoria and six Mount Wilson spectrograms. The secondary's lines are considerably weaker than the primary's and give less accurate radial velocities, but indicate approximately the same spectral class. Young's nine values and the eight published in Table I have been used to de-

rive a value of K_2 (secondary's semiamplitude of velocity variation), all its other elements being inferred from the primary's. $K_2 = 144$ km/sec, although 23 km/sec less than Young's value, seems to give the best adjustment. This difference is partly due to the smaller amplitude indicated by the new observations and partly to the fact that the systemic velocity of the primary has in my determination been assumed to be that of the secondary; whereas, if Young's K_2 is made to give the best fit for his observations, the γ-velocity for the secondary will turn out to be about 10 km/sec greater algebraically than that given by the primary. The procedure here adopted seemed preferable, and $K_2 = 144$ km/sec was therefore adopted. The values of $m \sin^3 i$ and $a \sin i$ in Table II are, of course, equal to the minimum possible values of the masses and the mean distances for the component stars.

The velocities from the detached lines of calcium (when measurable) are given in Table I and plotted in Figure 1 as barred dots, while Young's twenty-nine values appear as small dots. From the latter Young derived -24.4 km/sec as the weighted mean. The straight mean of the nine values in Table I is -18.0 km/sec, or -19.4 km/sec if the one outstanding low value is not included. From measures of the detached sodium lines D1,2 on the twelve spectrograms (G series) listed in Table I, Merrill[3] finds a mean value -19.5 km/sec. The mean radial velocity for calcium derived from the measures in Table I and Merrill's value for sodium are therefore in substantial agreement, but are 5 or 6 km/sec greater algebraically than Young's value. This discrepancy may indicate the existence of a systematic difference, at least in the determination of the calcium-line velocities. The elements, however, represent equally well the stellar velocities for the primary as obtained, on the one hand, at Ottawa and, on the other, at Victoria and Mount Wilson. Merrill's individual sodium-line velocities are given in the last column of Table I and plotted in Figure 1 as squares.

CARNEGIE INSTITUTION OF WASHINGTON
MOUNT WILSON OBSERVATORY
November 1935

[3] See *Mt. W. Contr.*, No. 536 (in press).

STATIONARY LINES IN THE SPECTRUM OF THE BINARY STAR BOSS 6142*

PAUL W. MERRILL

ABSTRACT

The spectroscopic binary Boss 6142 has a velocity range of 235 km/sec in a period of 13.4 days, but the detached lines D1,2, and λλ 5780, 6284 (and probably λ 5797) remain stationary.

Four interstellar lines have been known for years, viz., H and K of ionized calcium, D1 and D2 of neutral sodium. Recent observations at Mount Wilson have disclosed four additional detached lines whose approximate wave-lengths are 5780.4, 5796.9, 6283.9, and 6613.9 A;[1] and another one, a vague feature near λ 4427, is suspected. The chemical identification of these lines has not yet been made. It would be natural to test their behavior in a spectroscopic binary whose stellar lines undergo periodic oscillations, but a suitable object could not be found at once. Most binaries whose orbital elements have been computed are apparently too near to show the new detached lines clearly. Moreover, since the new lines are not sufficiently sharp for the most precise measurement, a binary with a considerable range in velocity is required. In this respect Boss 6142 (HD 224151, BD +56°3115), which shows the new lines fairly well, is quite satisfactory and was chosen for observation.

The orbit of this star, announced as a binary by W. S. Adams[2] in 1912, was computed in 1916 by R. K. Young[3] and recently revised by R. F. Sanford.[4] The period is 13.4 days, the velocity range 235 km/sec. Other data are R.A. $23^h50^m.5$, Dec. +56°53′, 1900; vis. mag. 6.0; type Bo.

Photographs of the visual portion of the spectrum made at Mount Wilson with the Cassegrain grating spectrograph are listed

* *Contributions from the Mount Wilson Observatory, Carnegie Institution of Washington*, No. 536.

[1] *Pub. A.S.P.*, **46**, 206, 1934. [2] *Mt. W. Contr.*, No. 59; *Ap. J.*, **35**, 163, 1912.

[3] *Pub. Dominion Obs.*, **3**, 373, 1919.

[4] *Mt. W. Contr.*, No. 535; *Ap. J.*, **83**, 121, 1936.

in Table I. The first one was with the 10-inch camera, dispersion 65 A/mm; the others, with the 18-inch camera, 34 A/mm. The spectra are widened and, with the exception of 970 and 1078, of good quality. All but one are on the III C or III F emulsion supplied by the Eastman Kodak Company.

The displacements and wave-lengths in Table I are the means of measurements by Miss Burwell and the writer. The stellar velocities depend chiefly on D3 of helium, a line of moderate intensity, not very well defined. Fairly large residuals from the orbit calculated by

TABLE I

MEASUREMENTS IN THE SPECTRUM OF BOSS 6142

G.M.T.	Plate	Star		D1,2	λ 5780	λ 5797	λ 6278	λ 6284
		Obs. km/sec	Comp. km/sec	km/sec	I.A.	I.A.	I.A.	I.A.
1928 Dec. 1.66	G 214*	− 57	− 77	(−18)	.....	.....	(6277.7)	(6283.5)
1932 Oct. 13.79	620	−145	−127	20	.....	.....	7.4	3.9
1934 Jan. 2.60	970†	− 33	− 17	17	.....	.....	.....	.....
July 31.96	1058	−150	−126	20	5780.6	.....	.....	3.6
Aug. 27.85	1063	−124	−127	18	0.3	5796.6	7.6	3.9
27.94	1064	−130	−128	21	0.4	7.2	7.8	4.2
28.91	1069	−112	−129	16	0.8	6.7	7.6	4.7
28.97	1070	−118	−129	18	0.6	7.2	7.9	3.9
Sept. 29.78	1078†	+ 65	+ 78	(26)	(0.5)	.....	.....	(4.4)
30.73	1082	+105	+104	23	0.6	.....	7.5	3.7
30.86	1083	+132	+105	19	0.8	.....	7.6	3.9
Oct. 1.74	1087	+ 88	+ 97	−20	0.5	6.9	7.9	4.2
Mean	.....	.....	.....	−19.5	0.58	6.9	7.67	4.02
High velocity	.....	+108	+102	−20.7	0.63	(6.9)	7.65	3.93
Low velocity	.....	−130	−128	−18.9	0.54	6.9	7.67	4.05
Other stars	.....	.....	.....	.....	5780.44	5796.88	6277.70	6283.91

* 10-inch camera.

† Underexposed.

Sanford[4] must therefore be expected. The sodium lines D1,2, on the other hand, are strong and sharp and their measured displacements accordant. The mean velocity agrees well with that obtained by Sanford from detached H and K. The other lines are rather weak and difficult to measure. The feature λ 6278 is the head of the terrestrial *a* band of molecular oxygen. Its appearance is somewhat similar to that of the neighboring detached line λ 6284. Since the true wave-lengths of λλ 5780, 5797, 6284, are not independently known, the values given are the measured wave-lengths, reduced on the assumption that their displacements are equivalent to those of the D1,2 lines.

At the foot of the table, following the mean values from all the

plates, are given the means for plates with high[5] and low[6] stellar values, respectively. The stellar displacements differ by 238 km/sec (calculated value 230), or 4.8 A (4.6) at λ 6000, while the displacements of the detached lines differ by 0.12 A or less. In the last line are preliminary wave-lengths from a dozen or more other stars.

The general conclusion is that D1, D2, λ 5780, λ 6284 certainly, and λ 5797 probably, do not follow the oscillations of the stellar lines but remain stationary within the errors of determination. These lines therefore are detached and probably interstellar.

The color excess of Boss 6142 measured by Joel Stebbins and C. M. Huffer[7] is +0.16. It is possible that the intensities of the new detached lines have a stronger correlation with space reddening than that shown by the available measurements of detached H and K.

CARNEGIE INSTITUTION OF WASHINGTON
MOUNT WILSON OBSERVATORY
November 1935

[5] Nos. 1082, 1083, 1087.

[6] Nos. 620, 1058, 1063, 1064, 1069, 1070.

[7] *Pub. Washburn Obs.*, **15**, 217, 1934.

TABLES FOR INTENSITIES OF LINES IN MULTIPLETS*

HENRY NORRIS RUSSELL[1]

ABSTRACT

Tables are given showing the common logarithms of the ratio of the theoretical intensities of the strongest line of a multiplet to each other line, and to the sum for the whole multiplet, according to the quantum formulae for unperturbed *LS* coupling. Multiplicities from 2 to 11 are included, and term types as far as I (except for multiplicities 10 and 11). The numerical values for multiplicities 9, 10, and 11 are also given; and certain noteworthy regularities in multiplets of the same type but different multiplicity are discussed.

The formulae for the relative intensities of lines in normal multiplets, derived from the quantum theory, have been extensively used in the calibration of astrophysical spectra—though they are known to be inaccurate for the more complicated spectra, where perturbations are large. The writer's original tabulation[2] contains several errors (apology for which is due, even at this interval), and the careful work of White and Eliason[3] shows a few small inaccuracies. Moreover, terms of multiplicity 9 and 10 have recently been identified in the rare earths, and those of multiplicity 11 are anticipated.

Intensities for these multiplicities have therefore been calculated and those for the lower multiplicities recomputed. The equations defining the intensities may be written in the form:

Ordinary multiplets (SP, PD, etc.):

$$x=\frac{(r+k-n+1)(r+k-n)(k-n+1)(k-n)}{r+k-2n+1} \tag{1}$$

$$y=\frac{2(r+k-2n)(r+k-n)n(k-n)(r-n)}{(r+k-2n+1)(r+k-2n-1)} \tag{2}$$

$$z=\frac{(r-n)(r-n-1)n(n+1)}{r+k-2n-1} \tag{3}$$

* *Contributions from the Mount Wilson Observatory, Carnegie Institution of Washington*, No. 537.

[1] Research Associate, Mount Wilson Observatory.

[2] *Proc. Nat. Acad.*, **11**, 322, 1925 (*Mt. W. Comm.*, No. 93).

[3] *Phys. Rev.*, **44**, 753, 1933.

Symmetrical multiplets (PP, DP, etc.):

$$x=\frac{(r+k-2n+1)\{(r+k)(k-2n+1)+2n(n-1)\}^2}{(r+k-2n+2)(r+k-2n)} \tag{4}$$

$$y=\frac{2(r+k-n)n(k-n)(r-n)}{r+k-2n} \tag{5}$$

In both cases

$$s=rk(k^2-1)\ .$$

Here x denotes the intensity of a line in the principal diagonal of the multiplet, y that of one of the first satellites, and z of one of the second satellites, while s is the sum of the intensities of all the lines of the multiplet. Also, r is the multiplicity, k has the values 2, 3, 4, 5, ... , for the combinations SP, PP, PD, DD, ... , and n is the number of the line in the diagonal to which it belongs. The leading line of the multiplet is always x_1.

It is customary to present the computed intensities in standard multiplet form. This permits the verification of the sum rule. But in astrophysical work the logarithm of the number of "active atoms" is usually derived, whether from a calibration of estimated intensities or from measured widths and a "curve of growth." The present tables give the common logarithm of the ratio of the intensity of the strongest line of the multiplet to a given line, and of the sum for the whole multiplet to the strongest line (thus making all the entries positive). Multiplets of the same type (SP, PP, ...), rather than of the same multiplicity, are grouped together, partly to save space, partly to exhibit some remarkable regularities which will be discussed below. Data for the various multiplicities are given in parallel columns. Those for the decets and undecets are not carried to those types which are very unlikely to be observable. For each multiplet the diagonal lines x are given first, with the satellites y and z below. Blanks in the table denote that the line does not exist, owing to limitations of multiplicity; dots, that its theoretical intensity is zero.

TABLE I

COMPUTED INTENSITIES OF MULTIPLETS

Multiplicity	2	3	4	5	6	7	8	9	10	11
	SP									
$J+n$	$1\frac{1}{2}$	2	$2\frac{1}{2}$	3	$3\frac{1}{2}$	4	$4\frac{1}{2}$	5	$5\frac{1}{2}$	6
s	0.176	0.255	0.301	0.331	0.352	0.368	0.380	0.390	0.398	0.405
x_1	0.000	0.000	0.000	0.000	0.000	0.000	0.000	0.000	0.000	0.000
y_1	0.301	0.222	0.176	0.146	0.125	0.109	0.097	0.087	0.079	0.072
z_1		0.699	0.477	0.368	0.301	0.255	0.222	0.196	0.176	0.160
	PP									
$J+n$	$2\frac{1}{2}$	3	$3\frac{1}{2}$	4	$4\frac{1}{2}$	5	$5\frac{1}{2}$	6	$6\frac{1}{2}$	7
s	0.255	0.380	0.456	0.507	0.544	0.572	0.594	0.612	0.626	0.639
x_1	0.000	0.000	0.000	0.000	0.000	0.000	0.000	0.000	0.000	0.000
x_2	0.398	0.699	0.896	1.049	1.176	1.285	1.382	1.467	1.545	1.617
x_3			1.100	0.794	0.632	0.528	0.455	0.400	0.358	0.324
y_1	0.699	0.477	0.368	0.301	0.255	0.222	0.196	0.176	0.160	0.146
y_2		0.574	0.401	0.317	0.264	0.227	0.200	0.179	0.162	0.148
	PD									
$J+n$	$2\frac{1}{2}$	3	$3\frac{1}{2}$	4	$4\frac{1}{2}$	5	$5\frac{1}{2}$	6	$6\frac{1}{2}$	7
s	0.222	0.331	0.398	0.444	0.477	0.503	0.523	0.539	0.553	0.564
x_1	0.000	0.000	0.000	0.000	0.000	0.000	0.000	0.000	0.000	0.000
x_2	0.252	0.271	0.280	0.285	0.289	0.291	0.293	0.294	0.295	0.296
x_3		0.623	0.681	0.712	0.729	0.741	0.748	0.754	0.758	0.761
y_1	0.954	0.748	0.648	0.586	0.544	0.513	0.490	0.471	0.456	0.442
y_2		0.748	0.574	0.489	0.437	0.400	0.373	0.352	0.336	0.322
y_3			0.681	0.602	0.553	0.519	0.493	0.473	0.457	0.444
z_1		1.924	1.602	1.431	1.322	1.245	1.189	1.144	1.109	1.079
z_2			1.380	1.079	0.921	0.820	0.748	0.695	0.653	0.620
z_3				0.954	0.699	0.564	0.477	0.415	0.368	0.331

TABLE I—*Continued*

Multiplicity	2	3	4	5	6	7	8	9	10	11
	DD									
$J+n$	$3\frac{1}{2}$	4	$4\frac{1}{2}$	5	$5\frac{1}{2}$	6	$6\frac{1}{2}$	7	$7\frac{1}{2}$	8
s	0.252	0.382	0.465	0.523	0.566	0.600	0.626	0.648	0.667	0.682
x_1	0.000	0.000	0.000	0.000	0.000	0.000	0.000	0.000	0.000	0.000
x_2	0.192	0.253	0.297	0.331	0.358	0.379	0.397	0.413	0.426	0.437
x_3		0.442	0.632	0.778	0.899	1.002	1.094	1.176	1.251	1.318
x_4			0.836	1.477	2.263	.....	2.520	2.017	1.752	1.581
x_5				.....	1.263	0.944	0.772	0.658	0.576	0.514
y_1	1.146	0.903	0.778	0.699	0.644	0.602	0.570	0.544	0.523	0.505
y_2		0.919	0.690	0.574	0.501	0.450	0.411	0.382	0.358	0.338
y_3			0.836	0.632	0.531	0.467	0.423	0.389	0.363	0.342
y_4				0.875	0.719	0.643	0.596	0.561	0.535	0.514
	DF									
$J+n$	$3\frac{1}{2}$	4	$4\frac{1}{2}$	5	$5\frac{1}{2}$	6	$6\frac{1}{2}$	7	$7\frac{1}{2}$	8
s	0.243	0.368	0.447	0.503	0.544	0.576	0.602	0.623	0.641	0.656
x_1	0.000	0.000	0.000	0.000	0.000	0.000	0.000	0.000	0.000	0.000
x_2	0.155	0.160	0.164	0.166	0.168	0.169	0.170	0.171	0.172	0.173
x_3		0.331	0.349	0.360	0.368	0.374	0.378	0.381	0.383	0.385
x_4			0.553	0.594	0.620	0.637	0.649	0.658	0.664	0.669
x_5				0.895	0.984	1.035	1.067	1.089	1.105	1.117
y_1	1.301	1.063	0.942	0.865	0.812	0.772	0.740	0.715	0.695	0.678
y_2		1.063	0.835	0.719	0.646	0.595	0.557	0.528	0.504	0.485
y_3			0.951	0.740	0.636	0.570	0.524	0.489	0.463	0.441
y_4				0.895	0.722	0.637	0.583	0.545	0.516	0.493
y_5					0.887	0.813	0.766	0.732	0.707	0.686
z_1		2.608	2.243	2.041	1.909	1.813	1.740	1.683	1.637	1.599
z_2			2.097	1.740	1.544	1.415	1.322	1.252	1.196	1.151
z_3				1.740	1.398	1.211	1.088	1.000	0.933	0.880
z_4					1.431	1.114	0.942	0.829	0.748	0.686
z_5						1.114	0.845	0.699	0.602	0.532

TABLE I—*Continued*

Multiplicity	2	3	4	5	6	7	8	9	10	11
	FF									
$J+n$	$4\frac{1}{2}$	5	$5\frac{1}{2}$	6	$6\frac{1}{2}$	7	$7\frac{1}{2}$	8	$8\frac{1}{2}$	9
s	0.259	0.396	0.485	0.548	0.597	0.634	0.665	0.690	0.712	0.730
x_1	0.000	0.000	0.000	0.000	0.000	0.000	0.000	0.000	0.000	0.000
x_2	0.130	0.157	0.177	0.194	0.207	0.219	0.228	0.237	0.244	0.250
x_3		0.278	0.346	0.400	0.445	0.482	0.514	0.541	0.565	0.587
x_4			0.457	0.598	0.714	0.813	0.900	0.979	1.050	1.115
x_5				0.695	0.990	1.260	1.531	1.820	2.155	2.583
x_6					1.078	1.959	.....	2.268	1.775	1.516
x_7						.....	1.384	1.058	0.878	0.759
y_1	1.431	1.176	1.041	0.954	0.892	0.845	0.808	0.778	0.753	0.732
y_2		1.182	0.932	0.802	0.718	0.658	0.613	0.577	0.549	0.525
y_3			1.059	0.820	0.696	0.617	0.561	0.518	0.485	0.458
y_4				0.996	0.772	0.658	0.586	0.535	0.497	0.467
y_5					0.981	0.783	0.685	0.624	0.581	0.548
y_6						1.056	0.907	0.836	0.791	0.759
	FG									
$J+n$	$4\frac{1}{2}$	5	$5\frac{1}{2}$	6	$6\frac{1}{2}$	7	$7\frac{1}{2}$	8	$8\frac{1}{2}$	9
s	0.255	0.390	0.477	0.539	0.586	0.623	0.653	0.678	0.699	0.717
x_1	0.000	0.000	0.000	0.000	0.000	0.000	0.000	0.000	0.000	0.000
x_2	0.113	0.115	0.117	0.118	0.119	0.120	0.121	0.121	0.122	0.122
x_3		0.233	0.241	0.247	0.251	0.254	0.257	0.258	0.260	0.261
x_4			0.368	0.385	0.397	0.406	0.412	0.418	0.422	0.425
x_5				0.528	0.560	0.582	0.598	0.609	0.618	0.626
x_6					0.736	0.794	0.832	0.858	0.877	0.892
x_7						1.067	1.174	1.238	1.281	1.311
y_1	1.544	1.291	1.158	1.073	1.011	0.965	0.929	0.899	0.875	0.855
y_2		1.291	1.042	0.912	0.829	0.769	0.724	0.689	0.660	0.636
y_3			1.162	0.920	0.795	0.715	0.658	0.615	0.581	0.554
y_4				1.084	0.854	0.737	0.662	0.609	0.570	0.538
y_5					1.037	0.827	0.723	0.656	0.610	0.574
y_6						1.016	0.845	0.761	0.708	0.670
y_7							1.028	0.957	0.913	0.881
z_1		3.091	2.703	2.482	2.334	2.225	2.142	2.076	2.021	1.976
z_2			2.593	2.209	1.991	1.845	1.738	1.656	1.591	1.538
z_3				2.260	1.882	1.669	1.526	1.422	1.342	1.279
z_4					1.991	1.623	1.417	1.280	1.180	1.103
z_5						1.748	1.396	1.200	1.070	0.976
z_6							1.505	1.179	1.000	0.881
z_7								1.230	0.954	0.802

TABLE I—*Continued*

Multiplicity	2	3	4	5	6	7	8	9	10	11
	GG									
$J+n$	$5\frac{1}{2}$	6	$6\frac{1}{2}$	7	$7\frac{1}{2}$	8	$8\frac{1}{2}$	9		
s	0.265	0.408	0.502	0.569	0.621	0.662	0.696	0.724		
x_1	0.000	0.000	0.000	0.000	0.000	0.000	0.000	0.000		
x_2	0.099	0.114	0.127	0.136	0.144	0.152	0.158	0.164		
x_3		0.207	0.242	0.271	0.295	0.316	0.335	0.351		
x_4			0.326	0.391	0.446	0.493	0.534	0.569		
x_5				0.464	0.576	0.672	0.757	0.833		
x_6					0.634	0.827	1.001	1.164		
x_7						0.864	1.231	1.611		
x_8							1.241	2.310		
x_9								.....		
y_1	1.643	1.380	1.239	1.146	1.079	1.028	0.987	0.954		
y_2		1.383	1.123	0.984	0.893	0.827	0.777	0.738		
y_3			1.247	0.991	0.856	0.768	0.705	0.656		
y_4				1.163	0.915	0.785	0.701	0.641		
y_5					1.111	0.874	0.751	0.673		
y_6						1.086	0.865	0.753		
y_7							1.095	0.900		
y_8								1.185		
	GH									
$J+n$	$5\frac{1}{2}$	6	$6\frac{1}{2}$	7	$7\frac{1}{2}$	8	$8\frac{1}{2}$	9		
s	0.263	0.405	0.497	0.564	0.615	0.656	0.689	0.717		
x_1	0.000	0.000	0.000	0.000	0.000	0.000	0.000	0.000		
x_2	0.089	0.090	0.091	0.092	0.093	0.093	0.094	0.094		
x_3		0.182	0.186	0.189	0.192	0.194	0.195	0.196		
x_4			0.281	0.290	0.296	0.301	0.305	0.309		
x_5				0.390	0.406	0.418	0.427	0.434		
x_6					0.515	0.541	0.560	0.575		
x_7						0.666	0.709	0.739		
x_8							0.867	0.936		
x_9								1.192		
y_1	1.732	1.471	1.330	1.238	1.172	1.121	1.082	1.048		
y_2		1.471	1.211	1.072	0.981	0.916	0.866	0.827		
y_3			1.332	1.076	0.940	0.851	0.787	0.739		
y_4				1.244	0.993	0.861	0.776	0.715		
y_5					1.184	0.942	0.816	0.735		
y_6						1.143	0.914	0.797		
y_7							1.119	0.911		
y_8								1.112		
z_1		3.466	3.063	2.829	2.670	2.553	2.461	2.388		
z_2			2.976	2.574	2.343	2.185	2.068	1.978		
z_3				2.653	2.255	2.026	1.871	1.756		
z_4					2.402	2.009	1.784	1.631		
z_5						2.185	1.799	1.580		
z_6							1.984	1.610		
z_7								1.786		

TABLE I—*Continued*

Multiplicity	2	3	4	5	6	7	8	9	10	11
	HH									
$J+n$	$6\frac{1}{2}$	7	$7\frac{1}{2}$	8	$8\frac{1}{2}$	9	$9\frac{1}{2}$	10		
s	0.270	0.417	0.514	0.585	0.640	0.684	0.720	0.750		
x_1	0.000	0.000	0.000	0.000	0.000	0.000	0.000	0.000		
x_2	0.081	0.090	0.098	0.104	0.110	0.115	0.120	0.124		
x_3		0.165	0.187	0.205	0.221	0.235	0.247	0.258		
x_4			0.256	0.294	0.327	0.355	0.380	0.402		
x_5				0.356	0.416	0.469	0.515	0.556		
x_6					0.468	0.561	0.644	0.717		
x_7						0.600	0.744	0.874		
x_8							0.765	0.996		
x_9								0.990		
y_1	1.813	1.544	1.398	1.301	1.231	1.176	1.133	1.097		
y_2		1.545	1.278	1.134	1.038	0.968	0.915	0.872		
y_3			1.402	1.138	0.995	0.901	0.833	0.781		
y_4				1.310	1.050	0.910	0.819	0.752		
y_5					1.246	0.992	0.856	0.768		
y_6						1.202	0.956	0.826		
y_7							1.175	0.940		
y_8								1.166		
	HI									
$J+n$	$6\frac{1}{2}$	7	$7\frac{1}{2}$	8	$8\frac{1}{2}$	9	$9\frac{1}{2}$	10		
s	0.269	0.415	0.512	0.583	0.637	0.680	0.716	0.746		
x_1	0.000	0.000	0.000	0.000	0.000	0.000	0.000	0.000		
x_2	0.074	0.074	0.075	0.076	0.076	0.076	0.077	0.077		
x_3		0.149	0.152	0.154	0.155	0.157	0.158	0.159		
x_4			0.229	0.234	0.238	0.241	0.244	0.246		
x_5				0.313	0.322	0.329	0.335	0.339		
x_6					0.405	0.419	0.430	0.439		
x_7						0.507	0.530	0.547		
x_8							0.626	0.660		
x_9								0.773		
y_1	1.887	1.619	1.473	1.377	1.306	1.252	1.209	1.174		
y_2		1.619	1.352	1.207	1.112	1.042	0.989	0.946		
y_3			1.474	1.209	1.066	0.972	0.904	0.851		
y_4				1.380	1.118	0.978	0.885	0.819		
y_5					1.313	1.056	0.919	0.829		
y_6						1.264	1.013	0.881		
y_7							1.229	0.987		
y_8								1.204		
z_1		3.774	3.360	3.117	2.950	2.825	2.728	2.649		
z_2			3.287	2.874	2.632	2.466	2.342	2.246		
z_3				2.971	2.560	2.320	2.155	2.033		
z_4					2.728	2.320	2.083	1.920		
z_5						2.524	2.121	1.887		
z_6							2.342	1.945		
z_7								2.172		

To use the table, proceed as follows:

Write the ordinary notation for the line.

a) If the term types (S, P, D, ...) are the same, it belongs to a symmetrical multiplet. If the difference ΔJ of the inner-quantum numbers (subscripts) is zero, it belongs to the diagonal x; if it is ± 1, to y. To find n, subtract the *greater* of the J's from the quantity $J+n$ given at the head of the column for the appropriate multiplicity and type.

b) If the term types differ by one step (e.g., DF), the line is in an ordinary multiplet and belongs to the group x, y, z, according as the change in J from the term of lower type (in this case D) to the other is $+1$, 0, or -1. To find n, subtract J for the term of *lower* type from tabular $J+n$.

c) If the term types differ by more than one step, e.g., $^5P-{}^5F$, or the multiplicities are not the same, the elementary theory is not applicable.

As examples we may have

$$a)\quad {}^7F_3-{}^7F_4^0\,, \qquad \Delta J=1\,, \qquad J+n=7\,.$$

Enter the table with y_3 and obtain 0.617.

$$b)\quad {}^6D_{3\frac{1}{2}}^{3\frac{1}{2}}-{}^6P_{2\frac{1}{2}}\,, \qquad \Delta J=+1\,, \qquad J+n=4\tfrac{1}{2}\,; \qquad x_2=0.289\,.$$

Here $s=0.477$, so that the intensity of this line is 0.514 that of the strongest line and 0.171 that of the whole multiplet. In this way the intensity of any spectral line relative to the strongest line of the multiplet, or to the sum of the whole, can be obtained without writing out the multiplet arrangement.

In the more important cases the tables permit of extension to supermultiplets, resulting from transitions between related groups of lines of the same multiplicity. For example, suppose that the multiplet in example (*b*) represents a transition between a member of a triad of terms $^6P^0$ $^6D^0$ $^6F^0$ and a pentad ^6S ^6P ^6D ^6F ^6G formed by the addition of a p- and a d-electron, respectively, to the same parent term ^5D of the next stage of ionization. Kronig's results are equivalent to the following rules: The relative total intensities of the multiplets of such a group are the same as those of the lines in an individual multiplet with term types the same as those of the jumping

electron (in this case P and D), with multiplicity 1, 3, 5, 7, according as the limit is an S, P, D, F, ... term, and with inner quantum numbers 0, 1, 2, 3, ... , for terms of types S, P, D, F, ... In this particular case, the corresponding term is $^5P_2-{}^5D_1$. We then use the table for ^{5}PD with z_2 and find 1.079; also S = 0.444. Hence the total intensity of this multiplet is 0.083 that of the strongest multiplet of the group ($^6F^0-{}^6G$) and 0.030 times the combined intensity of the nine sextet multiplets in the supermultiplet.

In preparing the tables, the numerical calculations were made by direct arithmetic (which is as quick as anything else in this case) and carried far enough to assure accuracy of one part in a thousand for the weakest line. The sums by rows and columns, when arranged in multiplet form, then afford a first test for errors. Four-place logarithms of the ratios of the intensities of individual lines to the intensity of the strongest line, x_1, were then taken, and the results rounded to three places. The vertical and horizontal differences, with the tabulation here employed, then give a searching test for any residual errors. As a further control the logarithms were independently read from a twenty-inch slide rule. It is believed that no errors exceeding one unit of the last place have escaped detection.

The following small errors were found in White and Eliason's Tables:[4]
These have been checked by duplicate computation.

As the numerical values of the intensities for multiplicities 9, 10, 11 have not previously been published, they are given in Table II, the intensity of the strongest line being taken as 100. The form is similar to that of Table I.

The conspicuous regularities exhibited in the tables deserve discussion. For ordinary multiplets we find from (1)

$$x_1 = (r+k)k(k-1)\,,$$

$$\frac{x_n}{x_1} = \frac{(k-n+1)(k-n)}{k(k-1)}\left\{1+\frac{n(n-1)}{(r+k)(r+k-2n+1)}\right\}.$$

[4] Note that in these tables n is counted upward along the diagonal lines.

^{7}HI, y_4 should be 10.5 instead of 10.0.
^{8}GH, x_3 should be 63.8 instead of 63.3.
^{8}DF, y_3 should be 29.9 instead of 30.2.

TABLE II

INTENSITIES IN MULTIPLETS

(Strongest Line = 100)

9	10	11
SP		
100.0	100.0	100.0
81.8	83.3	84.6
63.6	66.7	69.2
PP		
100.0	100.0	100.0
3.4	2.9	2.4
39.8	43.9	47.5
66.7	69.2	71.4
66.3	68.9	71.2
PD		
100.0	100.0	100.0
50.8	50.6	50.5
17.6	17.4	17.3
33.8	35.1	36.1
44.4	46.2	47.7
33.6	34.9	36.0
7.2	7.8	8.3
20.2	22.2	24.0
38.4	42.9	46.7
DD		
100.0	100.0	100.0
38.7	37.6	36.6
6.7	5.6	4.8
1.0	1.8	2.6
22.0	26.5	30.6
28.6	30.0	31.2
41.5	43.9	46.0
40.8	43.4	45.5
27.5	29.2	30.6

9	10	11
DF		
100.0	100.0	100.0
67.4	67.3	67.2
41.6	41.4	41.2
22.0	21.7	21.4
8.1	7.8	7.6
19.2	20.2	21.0
29.7	31.3	32.8
32.4	34.5	36.2
28.5	30.5	32.1
18.5	19.7	20.6
2.1	2.3	2.5
5.6	6.3	7.1
10.0	11.7	13.2
14.8	17.8	20.6
20.0	25.0	29.4
FF		
100.0	100.0	100.0
58.0	57.0	56.2
28.8	27.2	25.9
10.5	8.9	7.7
1.5	0.7	0.3
0.5	1.7	3.1
8.7	13.2	17.4
16.7	17.6	18.5
26.5	28.3	29.9
30.3	32.7	34.8
29.2	31.9	34.2
23.8	26.3	28.3
14.6	16.2	17.4

9	10	11
FG		
100.0	100.0	100.0
75.6	75.5	75.5
55.1	54.9	54.8
38.2	37.8	37.6
24.6	24.1	23.7
13.9	13.3	12.8
5.8	5.2	4.9
12.6	13.3	14.0
20.5	21.9	23.1
24.3	26.2	27.9
24.6	26.9	28.9
22.1	24.5	26.6
17.3	19.6	21.4
11.0	12.2	13.2
0.8	1.0	1.1
2.2	2.6	2.9
3.8	4.5	5.3
5.2	6.6	7.9
6.3	8.5	10.6
6.6	10.0	13.2
5.9	11.1	15.8

9			
GG	GH	HH	HI
100.0	100.0	100.0	100.0
68.7	80.5	75.2	83.8
44.6	63.6	55.3	69.4
27.0	49.1	39.6	56.8
14.7	36.8	27.8	45.8
6.9	26.6	19.3	36.4
2.4	18.2	13.4	28.4
0.5	11.6	10.1	21.9
0.0	6.4	10.2	16.9
11.1	8.9	8.0	6.7
18.3	14.9	13.4	11.3
22.1	18.2	16.5	14.1
22.9	19.3	17.7	15.2
21.3	18.4	17.0	14.8
17.6	16.0	14.9	13.1
12.6	12.3	11.5	10.3
6.5	7.7	6.8	6.3
	0.4		0.2
	1.0		0.6
	1.8		0.9
	2.3		1.2
	2.6		1.3
	2.5		1.1
	1.6		0.7

Hence, for a fixed multiplet type, when k is constant and r increases, x_n/x_1 rapidly approaches a limiting value (which is characteristic of the Zeeman pattern with this number of components). Also, $s/x_1 = r(k+1)/(r+k)$ and approaches a limit, but more slowly. When $r>k$, and the full number of components, $k-1$, characteristic of the term type is developed, we have, by (3), for the last z-term

$$z_{k-1} = (r-k)k(k-1)\,,$$

$$\frac{z_n}{z_{k-1}} = \frac{n(n+1)}{k(k-1)}\left\{1+\frac{(n-k)(n-k+1)}{(r-k)(r+k-2n+1)}\right\}.$$

The ratios of the intensities of these lines to the last and strongest also rapidly approach a limit. For the first satellites we find

$$\frac{y_1}{x_1} = \frac{2}{k}\frac{(r+k-2)(r-1)}{(r+k-3)(r+k)}\,,$$

$$\frac{y_n}{y_1} = \frac{n(k-n)}{k-1}\left\{1+\frac{(n+1)(n-k+1)r^2+\cdots\cdot}{r^4+\cdots\cdot}\right\}.$$

The former ratio approximates its limit slowly; the latter, as fast as the others. The intensity ratio for two y-lines equidistant from the ends is unity to the order $1/r^3$. These relations hold when the full number of components for the multiplet type is developed. When $k>r$, this is not the case; and the faintness of the satellites arises from the fact that only a part of the sequence characteristic of the term type is present.

For symmetrical multiplets the equations are more complex, but the nature of the results is the same, except that for the fainter lines of the main diagonal the terms of order $1/r^2$ contribute an important part of the whole intensity.

The writer is much indebted to Dr. Dunham and to Miss Carlson for assistance with the computations and checking the numerical tables.

CARNEGIE INSTITUTION OF WASHINGTON
MOUNT WILSON OBSERVATORY
December 1935

THE SPECTRUM OF ARCTURUS

SIDNEY G. HACKER

ABSTRACT

This paper summarizes with critical comments the atomic and molecular spectra identified in Arcturus (α Boötis; Draper class Ko) in the region λλ 4119–6743. The spectrograms were taken with the 15-foot auto-collimating spectrograph at the coudé focus of the 100-inch Mount Wilson reflector. They consist of (1) a set of low dispersion plates (exposure: 0^h42^m) mapping the region λλ 4119–6743 with a dispersion increasing from 2.30 A/mm at λ 4120 to 13.10 A/mm at λ 6600 and (2) a set of high-dispersion plates (exposure: 6^h16^m) mapping the two regions λλ 4245–4520 and λλ 4525–4975 with a dispersion of 0.97 A/mm at λ 4200 and 2.17 A/mm at λ 4900. The plates were measured on a Hilger comparator and reduced by the Hartmann formula in the usual way. Visual estimates of the intensities on an arbitrary scale were made at the time of measurement.

On the high-dispersion plates 307 unblended lines gave a weighted mean of -5.36 ± 0.03 km/sec for the radial velocity. On the low-dispersion plates 702 lines gave -6.63 ± 0.22 km/sec, and the weighted mean for the 1099 lines is -6.17 ± 0.20 km/sec.

The following twenty-eight elements have been identified on these plates as present in Arcturus: *H, Na, Mg, Al, Si, Ca, Sc, Sc⁺, Ti, Ti⁺, V, V⁺, Cr, Cr⁺, Mn, Mn⁺, Fe, Fe⁺, Co, Ni, Cu, Zn, Sr, Sr⁺, Y⁺, Zr, Zr⁺, Cb, Ru, Ba⁺, La⁺, Ce⁺, Nd⁺, Sa⁺, Eu⁺, Gd⁺.*

From the available evidence the following seem to be absent: *Si⁺, Y, Mo, La, Yb, Lu⁺, Hf⁺, W, Tl.*

The following may be present or absent (the available evidence is insufficient for definiteness): *Li, Mg⁺, Ni⁺, Ga, Ge, Mo⁺, In, Ba, Pr⁺, Tb⁺, Dy⁺, Ho⁺, Yb⁺.*

The following ten are not available on these plates: *K, Ca⁺, Co⁺, Rb, Rh, Pd, Ag, Cd, Er⁺, Pb. Ca⁺* has very strong lines beyond the violet limit of the plates.

Five molecular spectra have been found to be present on these plates: *CH, CN, C_2 SiF, BO.* There may possibly be a trace of *AlO* and *TiO;* but the evidence, which is discussed, is found to be far from definite. *CaH, MgH,* and *ZrO* are absent.

Of the 350 or so unblended lines otherwise unidentified, about 100 coincide, within the errors of measurement, with lines noted as band lines in the sun-spot spectrum. More than 200 unidentified solar lines seem to be present in Arcturus; and those which are strengthened in the spot spectrum relative to the disk are, in general, stronger in Arcturus.

Throughout the stellar spectrum the relative intensities of the arc lines are strikingly similar to those in the sun-spot spectrum, but the enhanced lines are stronger.

Altogether, about 3000 lines have been identified. Approximately 30 unblended lines of moderate strength remain unidentified.

Arcturus (α Boötis), α $14^h11^m.1$, δ $+19°42'$ (1900), is classed as spectral type Ko in the *Draper Catalogue.* It is, moreover, a giant star with a surface temperature of 4300° K, according to the thermocouple measurements of Pettit and Nicholson.[1] The spectroscopic method of Adams and Russell[2] gives 3850° K. The trigonometric parallax of Arcturus is given by Schlesinger[3] as $0''.080 \pm 0.005$. Pease[4]

[1] *Ap. J.*, **68**, 279, 1928.

[2] *Ibid.*, p. 9, 1928. [3] *General Catalogue of Stellar Parallaxes* (New Haven, 1924).

[4] *Pub. A.S.P.*, **33**, 171, 1921.

has measured its diameter with the interferometer attached to the 100-inch Mount Wilson reflector as 0".020. The star's radius is therefore 27 times that of the sun. Its mass is about 9 times that of the sun.[5] The surface gravity of Arcturus is therefore of the order 1/80 of the gravity at the surface of the sun.

The spectrum of Arcturus was first observed by G. B. Donati[6] in 1862. In the following year L. M. Rutherfurd[7] remarked that nearly every line observed in Arcturus had its counterpart in the solar spectrum. Secchi,[8] in 1869, made the significant observation that the spectrum of Arcturus resembled more closely the sun-spot spectrum than it did the spectrum of the solar disk.

The present investigation was undertaken, at the suggestion of Professor H. N. Russell, as a subject for a doctoral thesis. Through the co-operation of the Princeton and Mount Wilson observatories the writer has had access to a complete set of photographs of the spectrum of Arcturus. The spectrograms were taken with the 15-foot auto-collimating spectrograph at the coudé focus of the 100-inch Mount Wilson reflector. These cover the region from λ 4119 to λ 6743 in three sections, with other plates filling the gaps between. These "low-dispersion plates" have a dispersion increasing from 2.30 A/mm at λ 4120 to 13.10 A/mm at λ 6600. In addition, two high-dispersion plates cover the regions λλ 4245–4520 and λλ 4525–4975 (0.97 A/mm at λ 4300 and 2.17 A/mm at λ 4900).

The present paper summarizes with critical comments the atomic and molecular spectra identified on these plates. A list of individual wave-lengths, intensities, and identifications has been published by the Princeton University Observatory.[9] The writer is now engaged in a calibration of the intensities, similar to that made by Russell, Adams, and Moore for the solar spectrum.

All the plates have an iron-arc comparison spectrum. The measurements were made on a Hilger comparator and were reduced by the Hartmann formula in the usual way. The probable error of a

[5] Russell, Dugan, and Stewart, *Astronomy*, **2**, 875, 1927.

[6] *Intorno alle strie degli spettri stellari. Nuovo Cimento*, **15**, 292; *Annali del Museo Fiorentino*, 1862.

[7] *Amer. J. Sci. and Arts* (2), **35**, 407, 1863.

[8] *C.R.*, **68**, 950, 1869.

[9] *Contributions*, No. 16, 1935.

measured wave-length for good lines on the low-dispersion plates increases from ±0.01 A in the violet to ±0.03 A in the red.

On the high-dispersion plates 397 well-defined, unblended lines gave a weighted mean radial velocity of −5.36±0.03 km/sec. On the low dispersion plates 702 lines gave −6.63±0.22 km/sec. The mean for the 1099 lines is −6.17±0.20 km/sec. The mean of thirteen determinations by various observatories with the systematic corrections and weights assigned by J. H. Moore[10] gives a radial velocity of −5.19±0.06 km/sec.

The intensities of the lines were estimated visually on an arbitrary scale at the time of measurement, the faintest line just visible being called intensity 0. Lines of intensity 0 to 3 may be described as weak lines; 4 to 7, of medium strength; 7 to 11, strong; and greater than 11, very strong. A comparison of independent intensity estimates, made at different times, of a thousand lines of moderate strength shows that the accidental error of an estimate is about one unit of the scale.

A preliminary comparison with the solar and spot spectra furnished tentative identifications of the stellar lines. For this purpose the *Revised Rowland Table*[11] and Miss C. E. Moore's published table of the *Atomic Lines in the Sun-Spot Spectrum*[12] were used. In addition, Miss Moore made available for this purpose her original unpublished sun-spot ledger, which was of very great value.

The wave-lengths and intensities were then examined by multiplets, element for element, using Miss Moore's *Multiplet Table of Astrophysical Interest*[13] and the theoretical intensities.[14] When the latter were not available (singlets, intersystem combinations, unclassified lines), King's laboratory intensities[15] and temperature classifications were used as a guide. In other cases a comparison

[10] *Pub. Lick Obs.*, **18**, 113, 1932.

[11] *Pub. Carnegie Inst. of Washington*, No. 396; *Papers of the Mount Wilson Obs.*, **3**, 1928.

[12] Princeton, 1933.

[13] Princeton, 1933.

[14] H. N. Russell, *Proc. Nat. Acad.*, **11**, 314, 1925; Sommerfeld and Hönl, *Sitz. Preuss. Akad. Wiss.*, **9**, 141, 1925.

[15] A. S. King, various papers in *Astrophysical Journal* since about 1915.

with other lines in the same region, of similar excitation potential and laboratory intensity, furnished a rough but good criterion.

The violet limit of stellar spectrograms—in this case λ 4119—is a handicap to the completeness of their study. The ultimate lines of many of the elements occur to the violet of λ 4100, e.g., the (H) and (K) lines of Ca^+ at λ 3968 and λ 3933, known to be the strongest lines in Ko spectra.

In the following discussion the word "blend" is used to signify an unresolved group to which the element under consideration contributes an important fraction of the intensity. Lines completely overshadowed by other lines are called "masked." The estimated intensity of a line is given in parentheses immediately after its wavelength. In some cases where the multiplet is mentioned explicitly, the approximate excitation potential (E.P.) is quoted. Where significant, the character of the line is indicated by one or more of the following letters accompanying the intensity estimate: *d*, double; *w*, wide; *h*, hazy; *r*, red wing; *v*, violet wing. Capital letters indicate that the particular characteristic is very marked. The adjective "stellar" refers only to Arcturus.

ELEMENTS PRESENT IN THE SPECTRUM OF ARCTURUS

H.—*Hα* is one of the strongest lines in this spectrum. It is sharp, is apparently all "core," shows no perceptible wings, and has an intensity of about 50. *Hβ* is less clean-cut and is of about the same intensity. *Hγ*, with an intensity of about 40, is wide and has wings. The impression of the absence of wings, as in *Hα*, is a visual one; but microphotometric tracings of stellar spectra commonly reveal in such cases a central core of great intensity superposed on wide, much less intense contours of actual wings.

Li.—The ultimate lines, λ 6707.77 and λ 6707.94, were not seen when measuring. Later they were purposely looked for on a longer exposed corresponding plate of the same region and dispersion. There is a very slight indication that they may be present. The fading, continuous background is very weak in this region; and in order to be definitely seen here, any line would have to be strong.

Na.—The D lines are among the strongest, having intensities of 25 and 40. The pair λ 5682 and λ 5688, $3^2P^o-4^2D$, have an inten-

sity of 10 each. All other lines are weaker, the pair λ 6154 (0) and λ 6160 (1), $3^2P^o-5^2S$, surprisingly so. λ 4978 (7) is blended with a faint *Fe* line, and λ 4664 (6) with a strong *Cr* line.

Mg.—The triplet in the green, $3^3P^o-4^3S$, is very heavy; λ 5183 (30) is substantially unblended; λ 5172 (25) is unblended; and λ 5167 (18) is blended with a strong *Fe* line. λ 4571 has an intensity of 25.

The diffuse series of singlets is strong; the sharp series is weaker, as indicated in the accompanying table.

λ	Multiplet	Intensity
5528	$3^1P^o-4^1D$	10
4703	$3^1P^o-5^1D$	15
4351	$3^1P^o-6^1D$	35, badly blended (strong *Fe*$^+$, very strong *Cr*)
4167	$3^1P^o-7^1D$	20
5711	$3^1P^o-5^1S$	5
4730	$3^1P^o-6^1S$	5
4354	$3^1P^o-7^1S$	—, badly blended in wing of strong *Sc*$^+$
4380	$3^1P^o-p^2\,^3P$	3d?

The increase in intensity for the later series members is noticeable, but less conspicuous, in the sun.

The lines in the $4^3S-{}^3P^o$ groups have excitation potentials of more than 5 volts and are absent; they are faint and their absence is not surprising.

Mg$^+$.—The strong line λ 4481.14 (E.P. 8.8) may correspond to a line measured at λ 4481.14, intensity 0, a possible blend with *Gd*$^+$. The companion, λ 4481.34, is masked by a strong *Ti* line at λ 4481.28, intensity 6. The pair at λ 4427 are masked in the star.

Al.—The ultimate lines λ 3944 and λ 3961 are inaccessible. The pair, λ 6696 (2) and λ 6698 (0*w*), $4^2S-5^2P^o$ (E.P. 3.1), are present, the former blended possibly with an unidentified solar line, the latter unblended. The intensities are in good agreement with those in the spot. The next group of this series is absent.

Si.—The ultimate lines λ 3905 and λ 4102 are out of reach. The line λ 6155 (E.P. 5.6) is present, unblended, and is of intensity 0.

The leading member of the $4s^3P^o - 5p^3D$ group, λ 5797 (7*W*), is badly blended. The second member, λ 5793 (2), is unblended. The third line, λ 5772 (4*w*), is disturbed by a faint line of *V*. All the lines mentioned above have an excitation potential of about 5 volts. Their presence suggests that *Si* is fairly abundant.

Si+.—The only available pair of strong lines, λ 6347 and λ 6371, $4^2S - 4^2P^o$, are absent. This is not surprising in view of their high excitation potential of 8 volts.

K.—The lines of the principal series occur in the regions λ 4040 and λ 7600 and are beyond the limits of the plates.

Ca.—The ultimate line λ 4226, intensity 100, is the strongest in the entire observed portion of the spectrum. Ten multiplets arising from the 4^3P^o level (E.P. 1.9) and the 3^2D level (E.P. 2.5) are present, the lines arising from the former being conspicuously stronger. The singlet lines of *Ca* are all present, most of them unblended, and are all of medium strength or slightly greater. The correlation with the spot intensities is marked for all the lines of the element.

About 70 lines have been identified, including blends to which *Ca* is a sensible contributor.

Ca+.—The ultimate lines (H) and (K) are beyond the violet end of the plate. It is well known that they reach their maximum intensity in stars of class Ko and are the strongest lines in Ko spectra.

The strong triplet near λ 8500 is also inaccessible. The penultimate lines of the sharp and diffuse series are in the ultra-violet, and there are only a few faint lines of high excitation potential in the observed region. These have not been detected.

Sc.—The stronger members of the multiplets arising from the ground state a^2D are all present or masked. In the $a^2D - z^2F^o$ group, λ 4791 (0) and λ 4753 (2) are unblended, and λ 4779 (7) is blended with a faint *Fe* line. In the $a^2D - z^2D^o$ group, λ 6210 (4) and λ 6305 (7) are unblended; λ 6239 is in a very wide band of intensity 1 but is doubtless present. The presence of the $a^2D - z^2P^o$ group is doubtful.

The intersystem combinations $a^2D - z^4D^o$ at λ 6239 and λ 6258 are masked. The strongest lines arising from the level a^4F (E.P. 1.4) are present, λ 5671 having an intensity of 7. The strong laboratory line λ 5520, $a^2F - z^2G^o$ (E.P. 1.9), is absent.

The correlation between the intensities in the stellar and spot spectra is conspicuous.

Sc+.—Two multiplets whose lines arise from the a^3F level (E.P. 0.6) and two from the a^3P level (E.P. 1.5) are present. Four lines of the $a^3P - z^3P^o$ group are substantially unblended and have intensities of about 5. The lines of the $a^3F - z^3D^o$ multiplet are very strong: λ 4314 (20), λ 4320 (15), and λ 4305 (12) are substantially unblended; λ 4294 (12) is due principally to *Sc*+; and λ 4325 (40*W*) is blended with *Ti* and faint *Fe*. Four lines belonging to singlet combinations are present and unblended, the strongest, λ 4246, having an intensity of 30*W*. Here again the stellar and spot intensities are in good agreement.

Ti.—About 500 lines are identified as entirely or predominantly due to *Ti*. A total of 78 complete multiplets and 50 lines of the singlet system have been identified. Eight lines, predicted from the structure of the laboratory spectrum and observed in the spot spectrum, are present and are unblended in the stellar spectrum.

The ultimate lines and the six great multiplets of excitation potential 0.8 are by far the strongest *Ti* lines in Arcturus, and the intensities decrease progressively for lines having higher excitation potentials.

Most lines of spot intensity −2 are either present, and unblended, or can be identified as contributing to blends.

The spectrum of *Ti* is better developed in Arcturus than in present laboratory sources. It accounts for some of the strongest lines in the star. The correlation of stellar and spot intensities is marked throughout.

Ti+.—All lines found in the spot spectrum, and a few other faint ones, occur in the spectrum of Arcturus.

Two satellite lines of the $b^4P - z^4D^o$ group, λ 4423.22 and λ 4427.90, which have not been observed in the laboratory, are present as sensible contributors to blends. There are about 100 stellar lines to which *Ti*+ is a sensible or predominant contributor. They are not so conspicuous as those of the neutral atom. All the ultimate lines of *Ti*+ are, however, beyond the violet limit of the plates.

V.—About 100 lines of *V* are substantially unblended, and about

80 more are sensible contributors to blends. Seven lines of the great multiplet near λ 4400, $a^6D - y^6F^o$ (E.P. 0.3), are unblended. For each of them the estimated stellar intensity is very nearly twice the spot intensity, and this appears to be true for the satellite lines as well.

Lines of *V* are much more prominent than in the sun, but many faint lines observed in the laboratory do not appear.

V+.—Four stellar lines have been attributed entirely to V^+, the strongest having an intensity of 4. Among the blended stellar lines there are about 10 to which V^+ is a sensible contributor. The ultimate lines are in the ultra-violet, and the low-level lines in the region available on these plates are seriously affected by blends. Lines for which V^+ is chiefly responsible are not prominent, and in general are weaker than those of neutral vanadium even when multiplets having the same excitation potential are compared.

Cr.—Fifty-two multiplets of *Cr* have been identified, about 110 stellar lines being unblended and 90 blended. The three lines of the ultimate triplet, $a^7S - z^7P^o$, are very heavy and each is 0.4 A wide: λ 4254 (50); λ 4274 (70), with *Ti* an important contributor; λ 4289 (50), substantially unblended. The corresponding triplet near λ 5200, $a^5S - z^5P^o$, is strong; and the $a^5D - z^5P^o$ multiplet (E.P. 1.0) near λ 5300 shows a number of strong unblended lines. To the red of this the *Cr* lines are very weak, except for the pair of low-level lines at λ 6330 (5) and λ 6362 (3)—a fact explained by the high excitation potential of almost all the other groups.

The unclassified lines of *Cr* account for 34 unblended stellar lines and 26 blends.

Cr+.—Six multiplets, in which the lower excitation potential ranges from 3.09 to 4.06, are definitely present. There are 18 unblended lines, all very weak, and 7 blends.

Mn.—The ultimate lines of *Mn* are out of range. On these plates *Mn* accounts for 33 unblended lines, 24 of which have an intensity of 4. *Mn* contributes to 21 blended lines. The three lines λλ 4754 (15), 4783 (15), and 4823 (10) of the $z^8P^o - e^8S$ multiplet (E.P. 2.3) were all estimated at the same intensity, 12, on the low-dispersion plates. The intensities in parentheses are the intensities assigned when measuring the high-dispersion plate. The disk and spot intensities of these lines are in the inverse order compared with the theo-

retical intensities (3:4:5), whereas King's laboratory intensities are the same for the three lines.

The resonance group, $a^6S - z^8P^o$, is the next strongest multiplet, λ 5432 being of intensity 7, and the line measured as double by Rowland at λ 5394.64 and λ 5394.72 being blended at λ 5394.69 into one line of intensity 9. This apparent duplicity may possibly be due to fine structure.

The three lines of the $z^6P^o - e^6S$ multiplet (E.P. 3.1) are present and unblended, all having an intensity of 6. The three main multiplets arising from the a^4D level (E.P. 2.9) are present and prominent; the lines of the $a^6D - y^6P^o$ multiplet (E.P. 2.2) are prominent. Two lines of the group near λ 5400, $z^4P^o - e^4S$ (E.P. 3.8), are present and unblended, having intensities of 3 and 2, respectively.

Mn$^+$.—Six unclassified lines of *Mn*$^+$ are apparently present but are very faint. At λ 4253 and λ 4348 there are stellar lines of intensities 8*H* and 7, respectively. The coincidence in wave-length with *Mn*$^+$ lines is very good. However, the multiplet relations of this element are incompletely known.

Fe.—Neutral iron accounts for more lines in the spectrum of Arcturus than any other element. There are about 600 lines unblended or substantially unblended and 100 others to which *Fe* is the principal contributor. Practically all *Fe* arc lines which have been observed in the laboratory are accounted for in Arcturus. A large number are, of course, involved in serious blends. Fourteen predicted lines, present in the solar spectrum with Rowland intensities of −1 to −3, have been identified in the star.

There are more than 20 multiplets present whose lines are substantially unblended and very strong. The intensities decrease with increasing excitation potential, but few of the lines of high excitation potential can be called weak. For example, the entire $z^5D^o - e^5F$ multiplet (E.P. 3.2) is present; the faintest second satellite line, λ 4574, apparently unblended, has an intensity of 3.

The strongest multiplet in the observed portion of the spectrum is the $a^3F - z^3G^o$ group near λ 4200 (E.P. 1.5); these six lines range in intensity from 60 to 15, are very wide, and have conspicuous wings. λ 4383 (60) and λ 4404 (50) are approximately 0.47 A and 0.56 A wide, respectively. The width of the latter may be increased

by blends. λ 4415 is also very wide and has been assigned intensity 50.

The solar *Fe* lines show, in general, but little change of intensity between the disk and the spot. The intensities in Arcturus correlate equally well with both. There are, however, at least 15 low-level multiplets whose lines are greatly strengthened in the spot. They are uniformly the strongest *Fe* lines in Arcturus.

Fe$^+$.—There are 27 unblended lines of *Fe*$^+$ and about 13 blends. Seven complete multiplets are present.

The lines of *Fe*$^+$ are conspicuously weakened in the spot spectrum but are of moderate strength in Arcturus. Lines absent from the spot are, in general, absent from the star.

The lines of neutral iron in the same region of the spectrum and having about the same excitation potential are conspicuously stronger in the star than those of *Fe*$^+$.

Co.—There are 45 unblended lines due to *Co* and about 30 more to which this element is an important contributor. The relative behavior of lines of different excitation potential is normal.

Co$^+$.—All the lines of *Co*$^+$ are beyond the violet limit of these plates.

Ni.—There are 135 unblended or substantially unblended lines in the spectrum of Arcturus which are due to *Ni* and about 50 blends to which *Ni* is the principal contributor. The correlation of the stellar intensities with those of the spot spectrum is marked. Those lines predicted from the structure of the laboratory spectrum which are present in the spot spectrum are practically all present in Arcturus; likewise, predicted lines absent from the spot are absent from Arcturus.

Lines of low excitation potential (1 volt or less) are noticeably stronger in the stellar spectrum than those for which the excitation potential is 4 volts or more. Many strong lines having an excitation potential of about 3.5 volts are, however, present.

All the prominent singlets of *Ni* known in the laboratory and in the solar spectrum are present and strong in the star. Five multiplets are of outstanding beauty in the spectrum of Arcturus; practically all the lines are present, substantially unblended, and have at least moderate intensities. These are $a^1D - z^5D^o$, E.P. 0.4; $z^5G^o - e^5F$,

E.P. 3.5; $z^5F^o - e^5F$, E.P. 3.7; $b^1D - y^3F^o$, E.P. 1.7; and $a^3P - y^3D^o$, E.P. 1.9.

Ni+.—Only three faint lines of *Ni*+ lie in the region available on these plates (E.P. 4.0). Of these, λ 4244 (1) may be present and unblended; the others, if present, are blended or masked.

Cu.—The ultimate lines are inaccessible. The lines of the $a^2D - 4^2P^o$ multiplet, E.P. 1.4 to 1.6, are present: λ 5105 (10) is unblended; λ 5700 (7) is blended with a strong *Sc* line; λ 5782 (10) is blended with a weak *Fe* line.

The $4^2P^o - 4^2D$ group (E.P. 3.8) is present, the three lines all being blends to which *Cu* is a large contributor: λλ 5153 (6), 5218 (5), 5220 (3).

Zn.—In the $4^3P^o - 5^3S$ multiplet (E.P. 4.0), λ 4722 and λ 4810 both have intensity 3, and the former is rather hazy. Both lines have a Rowland intensity of 3 in the solar spectrum and 1 in the spot, and it is interesting to find them so strong in the star. The third line, λ 4680, has intensity 1 and is somewhat wide and hazy; but *Zn* is probably only a partial contributor to it.

Ga.—One low-level line of *Ga* is accessible on the plates. This line, λ 4172, is greatly strengthened in the spot; but in Arcturus it is unfortunately masked by a line of intensity 20, due mostly to *Fe*.

Ge.—The line λ 4685 (E.P. 2.0), which is absent from the spot spectrum, may possibly contribute to an otherwise unidentified line of intensity 2 in Arcturus. The other accessible line of *Ge*, λ 4226 (E.P. 2.0), is completely masked by *Ca*.

Rb.—The ultimate lines of *Rb*, which are present in the spot spectrum, lie in the infra-red. No discussion of this element is possible, therefore, at present.

Sr.—The conspicuous ultimate line of *Sr*, λ 4607, $5^1S - 5^1P^o$, which has a Rowland intensity of 1 in the solar spectrum and 3 in the spot, has an intensity of 5 in Arcturus. The other multiplets are absent.

Sr+.—One of the ultimate lines, λ 4215, is available on the plates. It has an intensity 20*W* and may be slightly disturbed by a faint *Fe* line.

In the $5^2P^o - 6^2S$ group (E.P. 3.0), λ 4161 is unblended and has an intensity of 2, and *Sr*+ may contribute to a bad blend at λ 4305 (12).

Y.—The multiplets in the red arising from the low a^2D level are

absent. Most of the lines of the stronger multiplets in the violet arising from this same level are beyond the limits of the plates. The diagonal lines in the strongest multiplet $a^4F - z^4G^\circ$ are all blended or masked. This is also true for the multiplet $a^2D - y^2D^\circ$.

Although a few stellar lines agree in wave-length with other lines of *Y*, the agreement is doubtless accidental; and there is no existing evidence of the presence of neutral yttrium in Arcturus.

Y^+.—Lines arising from the low-level multiplets of Y^+ are present, and the lines having higher excitation potentials are noticeably fainter than the low-level lines. Y^+ is an important or a sole contributor to about 15 lines. Nine of these are unblended and range in stellar intensity from 15 to 1.

The strong line λ 4374 ($a^1D - z^1D^\circ$) has intensity 15 in the star and is principally due to Y^+. In the $a^3F - z^3F^\circ$ group the corner line, λ 5087, has been assigned intensity 3, and λ 5200 intensity 5; the latter may therefore be a blend, or both lines may be more nearly intensity 4. Some of the satellites are present.

Zr.—Neutral *Zr* is represented by a dozen faint unblended lines: four of intensity 0, two of intensity 1, five of intensity 2, and one of intensity 3. The multiplet $a^5F - y^5F^\circ$ (E.P. 0.6) near λ 4200 is doubtless present, but only λ 4241 (2) is unblended. The multiplet $a^5F - y^5G^\circ$ near λ 4800 is better represented. The corner line λ 4687 is unblended and is of intensity 3. λλ 4739, 4772, and 4805 are also unblended and are all of intensity 2.

The leading members of the $a^3F - z^3F^\circ$ multiplet near λ 6100 (E.P. 0.0) are absent, although their spot intensities are 3 on the Rowland scale.

Zr^+.—Zr^+ is represented by 10 unblended lines and 20 blends. Ten multiplets are present.

λ 4613 (spot intensity 1) is present and probably accounts for a line of about intensity 4. The other member of this multiplet $a^2G - z^2F^\circ$, λ 4461, is present in a blend.

λ 4574 has Rowland intensity −1N in both the spot and the disk. It is present in Arcturus and has an intensity of 0. The other member of the multiplet $6^2P - x^2D^\circ$ (E.P. 2.4), λ 4629, is absent in the spot and in the star, though it is present in the disk.

Cb.—Seven lines of the $a^6D - z^6F^o$ multiplet are available for discussion, but unfortunately the three strongest lines lie beyond the violet limit of these plates. Two of the seven lines are unblended in the star and in the disk, though they are absent in the spot. They are given in the accompanying table where the disk intensity is on Rowland's scale, and the laboratory intensity is King's. The similarity of behavior in the star and in the disk of λ 4139 relative to λ 4137 is interesting, and may favor the identification of *Cb* in Arcturus.

λ	Stellar Int.	Disk Int.	Lab. Int.
4137	1	−3	200
4139	4	−1	300

The deciding factor in the identification of *Cb* in Arcturus would doubtless be the line λ 4100, which is unblended in both the disk and the spot and has Rowland intensity 0 in both. The present evidence seems sufficiently convincing for us to say that *Cb* is present in Arcturus.

Mo.—The strong ultimate lines of the $a^7S - z^7P^o$ multiplet are inaccessible. The multiplet $a^5S - z^5P^o$ (E.P. 1.3) near λ 5500 and six available unclassified lines appear to be absent.

Mo$^+$.—The laboratory spectrum is incompletely analyzed, and the intensities in the multiplets are abnormal. Two lines of the $a^4D - z^4P^o$ multiplet (E.P. 2.8), λ 4184 and λ 4433, agree in wave-length with two unidentified stellar lines of intensities 1*h* and 0, respectively. Five other lines of this multiplet occur in blends; and in at least three cases the lines, if present, would be masked. Nothing definite can be said at present regarding the presence of *Mo*$^+$ in Arcturus.

Ru.—Eight lines of *Ru* are available on these plates. Two stellar lines, otherwise unidentified, are probably due to low-level lines of *Ru:* λ 4584 (1) and λ 5171 (5). The strong *Ru* line λ 4554, of stellar intensity 6, has an intensity of 1 in the spot spectrum; but it is blended with a faint *Fe* line in the star. λ 4144 is masked by *Fe.* λλ 4757, 4869, and 5636 were not seen on these plates.

Rh.—The ultimate lines are inaccessible. No discussion of this

element can, therefore, be made at present. The laboratory spectrum is incompletely analyzed.

Pd.—All the lines available for the possible discussion of *Pd* are beyond the violet limits of the plates.

Ag.—The leading lines of the principal series are near λ 3300, and therefore no discussion of this element is possible.

Cd.—The solar evidence for this element depends upon one line, λ 3261 ($5^1S-5^3P^o$), which is inaccessible in the star.

In.—One ultimate line, λ 4511 ($5^2P^o-6^2S$, E.P. 0.3), is accessible on these plates but is absent.

Ba.—The principal ultimate line of *Ba*, λ 5535.48 (1000*R* I in the laboratory), may possibly contribute to the production of the stellar line at λ 5535.46 (6), which is largely due to *Fe.* This *Ba* line is definitely absent from the spot spectrum.

Ba$^+$.—The nine lines of *Ba*$^+$ accessible on these plates are present, five unblended and two substantially so, namely:

λ	Int.	E.P.	Multiplet
4554	20	0.0	$6^2S-6^2P^o$
4934	20*	.....	.....
5853	7	0.6	$5^2D-6^2P^o$
6141	5*	.....	.....
6496	5	.....	.....
4524	1	2.5	$6^2P^o-7^2S$
4130	8	2.7	$6^2P^o-6^2D$
4166	4*W*	(CN contributing)	

* Substantially unblended.

λ 4899 is badly blended in a stellar line, intensity 8*W*, due principally to *Ti.*

La.—Six ultimate lines of *La* are accessible on these plates. They are all absent.

La$^+$.—Some 10 unblended lines are attributed to *La*$^+$, with intensities ranging from 0 to 11. This element is probably a sensible contributor to about 10 other lines. For the most part those lines which are absent from the spot are absent from the star, despite the the fact that the excitation potential seldom exceeds 1 volt. For ex-

ample, in the star, of the $a^3F - z^3D^o$ multiplet λ 4662 seems to be present, unblended, and of intensity 2, but λ 4860 is definitely absent.

Ce+.—A total of 45 lines of *Ce*+ having an arc intensity of 100 or greater on King's scale[16] lie in the region covered by the plates. All but 2 lines are present or are accounted for in Arcturus; 18 are blends to which *Ce*+ contributes; 10 are masked; and 15 are unblended. One line, of intensity 75V (King), apparently accounts for the stellar line at λ 5274.28 of intensity 0. Fainter *Ce*+ lines are absent. The maximum stellar intensity is 4 or 5, but most of the unblended lines have an intensity of 2. Their presence in the flash spectrum lends additional weight to the correctness of the identifications.

Pr+.—Seventeen strong lines of *Pr*+ having an arc intensity of 100 or greater on King's scale[16] are available. Seven of these are masked by strong stellar lines; eight others are, at best, blends. The two others are: λ 4333 (int.: King, 100 IV; star, 3*h*) and λ 4510 (int.: King, 100 III; star, 1). The evidence is insufficient for a decision.

Nd+.—About 40 lines of *Nd*+ of laboratory intensity 50 or greater on King's scale are accounted for in Arcturus. Of these, 11 are unblended, or substantially so, with intensities ranging from 2 to 10; 16 are blends; 12 are masked; and 2 lines, λ 5451 and λ 5485, of laboratory intensities 100 IV and 80 V, are absent.

Sa+.—Twenty-one strong *Sa*+ lines lie in the region measured, and are present in both disk and spot spectra. Of these, 12 are unblended in Arcturus, with intensities ranging from 1 to 6, and 9 of these have intensities between 1 and 3; λ 4318 and λ 4329 both have intensity 6*h;* 7 are blends; and 2 are masked. The data for this element are incomplete, but they suffice to establish its presence in the star. The identifications are further confirmed by the presence of the lines in the flash spectrum; doubtless they can be extended when the spectrum is studied more extensively in the laboratory.

Eu+.—The *raies ultimes*, λ 4129 and λ 4205 ($a^9S^o - z^9P$), are present. The former is unblended and has a stellar intensity of 15, and the latter is a large contributor to a line of intensity 15*d* but is blended with *V*+.

[16] *Ap. J.*, **68**, 194, 1928.

In the $a^7S^0-z^9P$ multiplet (E.P. 1.67) λ 4435.60 is present and, as in the flash spectrum, is in the violet wing of the stellar line measured at λ 4435.64 (25), attributed largely, but not entirely, to *Ca*. The second member of this group is a blend. The other accessible Eu^+ lines are comparatively faint and are probably absent from the stellar spectrum.

Gd^+.—This element accounts for two stellar lines λ 4191 (1) and λ 4342 (3*V*), to which King assigns[17] the intensities 200 IV and 300 IV, respectively. Two other lines in the star, λ 4130 (7*H*) and 4316 (4), agree in wave-length with lines of Gd^+ of intensities 300 V and 150 IV. Though otherwise unidentified, their intensities would seem to indicate that they are blends. Nine other lines are blends, and nine are masked.

Tb^+.—King lists[17] six lines of Tb^+ which have an intensity of 50 or greater. Three of these are masked, and one may be present in a hazy patch of intensity 1. One strong line given by King, λ 4278 of intensity 200 V, may be present in the star, blended with an unidentified solar line. Nothing definite can be said concerning the presence of Tb^+ in the spectrum of Arcturus.

Dy^+.—The presence of Dy^+ is doubtful. The three strongest lines[17] are masked or blended, and there is no satisfactory evidence for the presence of the fainter lines.

Ho^+.—The strongest lines[17] of this element are to the violet of λ 4046. There are only five, very weak, lines of Ho^+ available in the region of the spectrum covered by these plates. Four of these are masked. The strongest (lab. int. 6 V) differs by 0.04 A in wave-length from a stellar line of intensity 0. Consequently, there is no evidence of Ho^+ in Arcturus.

Er^+.—The two strongest Er^+ lines, λλ 3896 and 3906, are to the violet of the region measured.

Yb.—The strong ultimate line of *Yb*, λ 5556.49, the only line of a neutral rare-earth which is present in the sun, does not appear in Arcturus.

Yb^+.—The ultimate lines of Yb^+ are to the violet of the region covered by these plates. Two weaker lines are available: λ 5335

[17] *Ibid.*, **72**, 221, 1930.

(200 V, King) is absent, and λ 4786 (80 V, King) is masked. Nothing can, therefore, be said about the presence of this element.

Lu+.—The two leading lines of the $a^3D - z^3P^o$ multiplet (E.P. 1.5 to 1.7) lie in the region of these plates. One, λ 6221, is absent; and the other, λ 5476, is masked.

Hf+.—Four lines (E.P. 1.5 to 2.7) of *Hf*+ are available. They are all absent except λ 4336, which agrees well in wave-length with an unidentified stellar line of intensity 0. This agreement is probably accidental. The low-level lines are beyond the violet limits of the plates.

W.—Five of the seven lines, including the leading members, of the $a^5D - z^5P^o$ multiplet (E.P. 0.206 to 0.768) are absent from the stellar spectrum. The two lines of the $a^7S - z^5P^o$ group (E.P. 0.364) are masked. λ 4294 (E.P. 0.364), which has Rowland intensity $-1d$ in the spectra of both disk and spot, is the only other available line. An otherwise unidentified stellar line of intensity 5*H* agrees in wave-length, but there is no reason to conclude that this might even be a blend involving *W*.

Tl.—λ 5350 is available but absent; it is also absent from the solar and spot spectra.

Pb.—Unfortunately, the two great lines of *Pb* (both 1000*R* in the laboratory) are beyond the violet limits of these plates.

MOLECULAR SPECTRA IN ARCTURUS

There are, unfortunately, very few band spectra for which the published laboratory measures are adequate in either accuracy or completeness for a critical comparison with astronomical spectra of high dispersion. In some cases only the band heads have been measured; in others, although the individual lines have been measured with precision, only those wave-numbers which are important in the structural analysis have been published. For these reasons most of the wave-lengths available for the identification of individual molecular lines in Arcturus are derived from the solar spectrum. Many of the bands are formed largely of very close doublets or triplets which are unresolved in the star and appear as broad or hazy "bands."

CH.—About sixty lines of *CH* have been found in Arcturus. The

majority of these account for lines otherwise unidentified or only partly identified; many of them appear as unresolved, hazy patches. The intensity range is roughly 1 to 10. It is probable that a good many more lines could be added if more complete and accurate laboratory wave-lengths were available.

CN.—There are more than 30 lines, otherwise unidentified, due to *CN*. In addition, the presence of *CN* accounts for about 45 "bands" or widened lines on these plates. The range of intensity is about 1 to 10. The *CN* lines listed in the *Revised Rowland*[10] as present in the solar spectrum can be accounted for, line for line, in Arcturus.

C_2.—The three heads of the Swan bands of C_2 given by Richardson,[18] namely λλ 4737, 5165, and 5635, are available for discussion on these plates. The first, λ 4737, is absent. The second, λ 5165.22, is undoubtedly present and is represented by a very wide band of intensity 5 lying between two *Fe* lines, λ 5164.61 (5) and λ 5165.44 (7). The third head is at λ 5635.53 and may possibly be present in the wing of a stellar line of intensity *2w* at λ 5635.90, which is otherwise identified only as being partly due to *Fe* at λ 5635.83. Four unblended individual lines of C_2 are represented in the star, with intensities varying from 0 to 2. Individual lines of C_2 are also accounted for in three blends.

SiF.—The three band heads of the *a*-system of *SiF* listed by Richardson[18] as present in the spot spectrum are available on these plates.

1. λ 4368.22: There is a stellar line of intensity *5wd* at λ 4368.34, with a pronounced violet wing. This line is only partly accounted for by *Cr* and *Ni*.

2. λ 4400.50: There is a strong Sc^+ line of intensity 12 at λ 4400.40 and a strong *V* line of intensity 15 at λ 4400.58. A hazy patch lies between these two lines, and is perhaps due principally to the wings of the Sc^+ and *V* lines.

3. λ 4430.23: There is a strong *Fe* line of intensity 6 at λ 4430.18 and a strong *Ti* line also of intensity 6 at λ 4430.36. The region between these two lines is very hazy and is of intensity 2.

Individual lines of the (0, 0) band (the λ 4368 system) of *SiF*, as listed by Richardson, can nearly all be accounted for. Fifteen of

[18] *Ibid.*, **73**, 216, 1931.

these lines are unblended in the star and range in intensity from o to 3. A stellar line at λ 4370.17, of intensity 3*W* and 0.3 A wide, is a blend of at least four individual *SiF* lines, with weak *Ni* and *Cr*, probably masked.

Of the band heads, we can say that (1) λ 4368 is present in a blend to which *SiF* is an important contributor; (2) λ 4400 may be blended or masked, depending on the relative intensities of the wings of the bordering Sc^+ and *V* lines; (3) λ 4430 is present and is of intensity 2.

CaH.—Two of the three known band heads,[18] λ 6382 and λ 6389, are available on these plates; but both are absent from the stellar spectrum.

MgH.—The three band heads[18] of *MgH* at λλ 5621, 5210, and 4844 are absent.

SiH.—If the head[18] of the *SiH* band, λ 4143.89, which occurs in the spot spectrum, is present in Arcturus, it is doubtless concealed by the great *Fe* line at λ 4144.01 (30). Great "wings" stretch out for more than 2.0 A toward the red and for more than 1.0 A toward the violet from this *Fe* line.

AlO.—Richardson[18] lists three band heads of *AlO* at λλ 4647.96, 4842.26, and 5079.26. A stellar line of intensity o*h* agrees well in wave-length with the first. This may be identical with an unidentified solar (atomic) line (Rowland int.: disk 1, spot 1) at λ 4647.96.

The second head, λ 4842, is absent from Arcturus.

There is a stellar line of intensity 9, possibly double, 0.1 A to the violet of the position of the third head λ 5079.26. This line is a blend of two strong *Fe* lines at λ 5078.98 and λ 5079.23. The latter would mask the *AlO* head.

This evidence is not decisive as to the presence of *AlO* in Arcturus, although it is probably present in the spot spectrum.

BO.—The heads of the α-group of *BO*, listed by Richardson,[18] λλ 4363.4, 4612.7, and 5040.1, are available for discussion here. λ 5040.1 is masked in Arcturus by a *Ti* line at λ 5040.00 of stellar intensity 11. λ 4612.7 is probably present in a wide, hazy patch at λ 4612.6 of intensity o*w* which is otherwise altogether unidentified. *BO* probably accounts for only part of this stellar line. λ 4363.4 is present as a stellar line at λ 4363.40, of intensity o, otherwise unidentified.

These band heads of *BO* are faint in the star. It is, therefore, no serious objection to the identification that the many individual lines between λ 4656 and λ 5245 identified by Nicholson and Perrakis[19] in the spot spectrum do not show up in the star. The spot lines are very faint, the two strongest having a Rowland intensity of 0.

TiO.—Richardson[18] lists three band heads of *TiO:* λλ 4954, 5166, and 7054. The third is not available on these plates. Jevons[20] lists a *TiO* band head at λ 6478, and Christy[21] has given a list of individual lines of *TiO.*

The head λ 6478 is absent from the stellar spectrum. The head λ 5166.86 is overwhelmingly masked by an enormous blend of *Mg* and *Fe* at λ 5167.37, of intensity 18*W*. The head λ 4954.55 could account for an unidentified stellar line of intensity 1 at λ 4954.55.

There are many coincidences of stellar lines with the individual lines listed by Christy. Undoubtedly, all such coincidences are accidental, for nearly all of these faint stellar lines are already easily identified otherwise, and many of the lines listed by Christy are absent.

The evidence here for *TiO*, as in the case of *AlO*, is insufficient for us to be able to say definitely whether or not this molecule is present in Arcturus. In the cases of both *AlO* and *TiO* there is the bare possibility of a trace of their presence in the star. If, for instance, the faint stellar line at λ 4954 is the band head of *TiO*, the absence of Christy's lines would not be surprising, since the band heads themselves are faint.

ZrO.—The three band heads of *ZrO*, λλ 6229, 6344, and 6473, given by Richardson[18] are all absent from these plates.

CONCLUSION

Among the 350 or so unblended lines otherwise unidentified, about 100 coincide, within the errors of measurement, with lines noted as band lines by Miss Moore in the spot spectrum, on account of the

[19] *Ibid.*, **68**, 327, 1928.

[20] *Band-Spectra of Diatomic Molecules* (London, 1932), p. 9. Jevons gives here a convenient table of "band-systems observed in celestial spectra," with a detailed list of references.

[21] *Phys. Rev.*, **33**, 701, 1929.

absence of Zeeman effect. Most of these also appear as faint unidentified lines in the spectrum of the disk.

A detailed study of the innumerable band lines present in the spot spectrum has not been made. When this has been done and when better laboratory measures of sundry band spectra have been made, it is probable that a large number of the fainter "unknown" lines in Arcturus may be identified.

Approximately 30 clear lines ranging in intensity for the most part from 4 to 10 remain entirely unidentified. These cannot be matched with lines in the solar or spot spectrum. This number does not include lines in "bands" and bad blends, which were measured but later rejected as apparently not real.

More than 200 unidentified solar lines agree, within the accuracy of measurement, with those in Arcturus. The lines which are strengthened in the spot spectrum are, in general, stronger in the stellar spectrum. About three-fourths of these lines lie in the limited region λ 4120 to λ 4900. This would suggest that they may also be due to bands.

Altogether, about 3000 lines have been identified in the spectrum of Arcturus.

ACKNOWLEDGMENTS

This work was undertaken as a thesis for the doctorate in astronomy at Princeton University at the suggestion of Professor Henry Norris Russell, director of the Princeton Observatory. Through his co-operation and the courtesy of Director W. S. Adams of the Mount Wilson Observatory the beautiful photographs of the spectrum of Arcturus were available for measurement.

Professor Russell has advised and directed the writer throughout the measurements, reductions, and identifications. He has made available the spectroscopic library of the Princeton Observatory and has given the writer the benefit of his wide spectroscopic experience. The writer is greatly indebted to him for discussions in regard to this paper and other problems of astronomy as well.

Miss Charlotte E. Moore has made available a wealth of unpublished and otherwise unavailable material. She has supervised the details of the work on the identifications. Without her invaluable

unpublished ledger of the sun-spot spectrum and her published "Multiplet Table" it would have been impossible to complete the thesis in the requisite time.

Finally, Professor Russell and Miss Moore have taken much of their valuable time to check and revise the details of this paper. The writer is most appreciative of all this help. He is also indebted to Professor R. S. Dugan and Professor J. Q. Stewart for their encouragement and kindness to him.

INDIANA UNIVERSITY
BLOOMINGTON, INDIANA
August 30, 1935

PHOTOMETRIC OBSERVATIONS OF SOME OF BARNARD'S DARK NEBULAE

OTTO STRUVE AND C. T. ELVEY

ABSTRACT

Observations of several dark nebulae show that their surface brightnesses differ by a few hundredths of a magnitude from that of the sky background. The computed Δm which should be added (because of scattering of general starlight in the dark nebula) to the observed sky brightness is about 0.15 mag. The discrepancy may be due to a lower albedo of the particles than was assumed in the computation, or to scattering in interstellar space. The existence of scattering of general starlight by interstellar clouds is demonstrated by a series of observations of B15, the core of which is appreciably darker than the rim, although the latter is about as opaque as the former.

I

Recent investigations of the surface brightness of the sky by Van Rhijn,[1] Dufay,[2] and others have shown that most of it comes from the combined light of unresolved faint stars, from the zodiacal light, and from atmospheric sources, such as the permanent aurora. Dufay concludes that there is at present no real evidence that any measurable amount of light comes to us from interstellar space. Indeed, it would seem from Table I that the best available data allow only 50 per cent of the total light of the night sky to atmospheric radiations and to unknown sources, such as interstellar scattering. Since the atmospheric radiations are known to be appreciable, we estimate that not much more than 10 per cent of the total light could be attributed to interstellar scattering.

TABLE I

COMPOSITION OF SKY BRIGHTNESS (AFTER DUFAY)

Unresolved starlight	Transmitted	0.20
	Scattered	.14
Zodiacal light	Transmitted	.11
	Scattered	.05
Atmospheric radiations and unknown sources		0.50

Other methods must be used to ascertain whether or not interstellar scattering produces an appreciable part of the sky brightness

[1] *Pub. Astr. Lab. Groningen*, **31**, 1921.

[2] Dufay, *Etude de la lumière du fond du ciel nocturne*, Paris, 1934.

at night. We know from the work of Hubble and of Hertzsprung that nebulous masses in the neighborhood of bright stars scatter enough light to produce luminous areas which are easily seen projected against the general illumination of the night sky. Scattering of general starlight has not heretofore been observed, and we have made an attempt to measure it in the case of several dark nebulae listed in Barnard's catalogue of these objects.

The dark nebulae appear on the photographs as vacancies among the stars. Some of them are practically opaque and should therefore be especially suitable for a study of interstellar scattering. Stars located in the vicinity of such dark nebulae produce bright halos, indicating that the material composing the nebulae acts as a fairly efficient scatterer. Hertzsprung's investigation for the Pleiades[3] and recent computations by Struve[4] prove that the efficiency of the nebular material in reflecting starlight is quite considerable, even though the opacity is not nearly complete. An unpublished investigation, by Keenan, of the nebula NGC 7023 shows that its efficiency is even greater than that of the nebulae in the Pleiades.

The present investigation was undertaken to answer the following questions: (1) What are the surface brightnesses of some of Barnard's dark nebulae? (2) Does interstellar scattering within the nebulae, and in the open regions, contribute measurably to the brightness of the night sky? (3) Are all dark nebulae alike with respect to their light-scattering properties?

Barnard has mentioned that some of the dark nebulae observed by him were appreciably blacker than the normal background of the sky between the stars, while other nebulae appeared distinctly luminous on a darker background. Because of Eberhard effect and other sources of error, no actual measures are possible on Barnard's original plates. However, there can be no doubt that the observations are real.[5]

Seeliger's[6] extensive investigations on the illumination of a cosmic

[3] *A.N.*, **195**, 449, 1913. [4] *The Telescope*, **2**, 124, 1935.

[5] See, for example, Plate 5, Part I, *Atlas of Selected Regions of the Milky Way*, by E. E. Barnard, Chicago, 1927.

[6] *Sitz-Ber. Bayerisch. Akad. Wiss.*, **31**, 265, 1901. The application of Seeliger's theory is justified for three reasons: (1) nearly all bright nebulae illuminated by stars of spectral classes B1 or later have continuous spectra; (2) the nebula in the Pleiades

dust cloud by a distant star have led to the following expression for the surface brightness[7] of an opaque dust cloud:

$$I = \frac{pI_0S^2}{r^2}\,\varphi(a)\,\frac{\cos i}{\cos i + \cos \epsilon}\,. \qquad (1)$$

Here I_0 is the surface brightness of the star, S is its radius, and r is the distance between the star and the cloud; p is the reflecting power of the particles composing the nebula (which is related to the albedo), i is the angle of incidence, ϵ is the angle between the line of sight and the normal to the surface of the cloud, and $\varphi(a)$ is the phase function.[8]

According to Seeliger, the opaque cloud reflects light as a solid smooth surface which obeys the law of diffuse reflection of Lommell-Seeliger and whose albedo depends upon the phase angle.

Schönberg[9] has applied this formula to the case of an opaque cloud illuminated by a star similar in size and surface brightness to the sun and located at a distance of 1000 astronomical units from the cloud. For a phase angle $a = 0$, the surface brightness expressed in terms of the equivalent number of first-magnitude stars per square degree is

$$I_{\max} = 6p\,.$$

If $p = \frac{1}{3}$, the surface brightness of the nebula, $I = 2$, is several times greater than the brightest measured part of the zodiacal light, which is 0.32.

The average surface brightness of the night sky produced by the stars[10] is about 5 mag. per square degree. The combined light of one

---

appears to reflect starlight non-selectively; (3) several bright nebulae show dark markings which have bright rims and therefore belong to the same general structure as do the other parts of the nubulae; these markings presumably appear dark because they are closer to the earth than the illuminating stars, and the bright rims are caused by a phase-angle effect which would be absent if the nebular light were caused by atomic processes.

[7] Schönberg, *Handbuch d. Astrophysik*, **2**, Part I, 163, 1929.

[8] If I_0 is expressed as the equivalent number of stars of magnitude 1 per square degree, then I is expressed in the same unit.

[9] Schönberg, *op. cit.*, p. 164.

[10] Bottlinger, *Zs. f. Ap.*, **4**, 373 (Table 2), 1932.

hemisphere is about -5.8. The apparent magnitude of the sun as seen from a distance of 1000 a.u. would be about -11, which is approximately equal to the apparent magnitude of the full moon. If all of the light coming from one hemisphere of the sky were concentrated at one point having $\alpha = 0$, then the surface brightness of the nebula should be one hundred times less than that computed by Schönberg, or sixteen times less than the brightest part of the zodiacal light. Since the latter is easily visible to the eye, no difficulty should be experienced in measuring surface brightnesses that are 3 mag. fainter. In fact, the total illumination from all stars of one hemisphere is greater than that of the planet Venus at its maximum. It is therefore not surprising that for a moderate albedo ($p = \frac{1}{3}$) the surface brightness of the nebula illuminated by general starlight should be within reach of modern photometric instruments.

If $\alpha = 0$,

$$\varphi(\alpha)\,\frac{\cos i}{\cos i + \cos \epsilon} = \tfrac{1}{2}\,;$$

and, retaining Schönberg's expression for the surface brightness,

$$I = \tfrac{1}{2} p I_0 \frac{S^2}{r^2} = \tfrac{1}{2}\,\frac{p}{\pi}\, I_0 \omega\,.$$

If one hemisphere is uniformly bright, $\omega = 2\pi$. Assuming that we can still put $\alpha = 0$, we obtain

$$I = p I_0\,. \tag{2}$$

There is, however, an error in our assumption that $\alpha = 0$ for all parts of the hemisphere. Consequently, we shall compute the surface brightness I of the nebula from Seeliger's exact formula. To evaluate the effect of the phase angle we replace $\pi S^2/r^2 = d\omega$. Let us assume that $\epsilon = 0$, $i = \alpha$. Then

$$\varphi(\alpha)\,\frac{\cos i}{\cos i + \cos \epsilon} = \frac{\varphi(\alpha)\cos \alpha}{1 + \cos \alpha}\,.$$

Furthermore,

$$d\omega = d\alpha \sin \alpha\, d\beta\,.$$

Integrating over one hemisphere, we find

$$I=\frac{p}{\pi} I_0 \, 2\pi \int_0^{\pi/2} \frac{\varphi(\alpha) \sin \alpha \cos \alpha}{1+\cos \alpha} \, d\alpha .$$

For $\varphi(\alpha)$ we shall first use Euler's law:

$$\varphi_1(\alpha)=\cos^2 \frac{\alpha}{2} .$$

Hence,

$$\int_0^{\pi/2} \frac{\cos^2 \frac{\alpha}{2} \sin \alpha \cos \alpha}{1+\cos \alpha} \, d\alpha=\tfrac{1}{4} .$$

Accordingly,

$$I=0.5 \, pI_0 . \tag{3}$$

This is one-half the amount given by (2). The use of Euler's law in $\varphi(\alpha)$ is theoretically not quite satisfactory, and we have used it here because of the simple form to which it reduces our integral. For comparison we have evaluated the integral, using for $\varphi(\alpha)$ the law of Lambert:

$$\varphi_2(\alpha)=\frac{\sin \alpha+(\pi-\alpha) \cos \alpha}{\pi} .$$

Using the substitution $x=\alpha/2$, we find

$$\int_0^{\pi/2} \frac{\varphi_2(\alpha) \sin \alpha \cos \alpha}{1+\cos \alpha} \, d\alpha \approx 0.2 .$$

Hence

$$I=0.4 \, pI_0 . \tag{4}$$

This differs but slightly from (3), and we shall assume in the following discussion that the surface brightness of the nebula is one-half that computed on page 165, or thirty-two times less than the bright-

est portion of the zodiacal light.[11] If the latter is equivalent[12] to 1300 stars of apparent magnitude 10, then the former should be equivalent to about 40 stars of the same apparent magnitude.

On a perfectly black background such a surface brightness could easily be photographed; but in reality the background of the sky is not black but has a surface brightness[13] of about 4 mag, most of which comes from atmospheric sources and from the zodiacal light. The additional brightness caused by the equivalent of 40 stars of magnitude 10 would give an increase in magnitude of 2.5 log $290/250 = 0.15$ mag. This is within the precision of the methods of photographic photometry.

II

After some preliminary photoelectric observations of dark nebulae by Elvey had shown that in order to obtain the required sensitivity of the cell the area of the sky projected upon the photometer had to be made too large to successfully avoid stars, we decided to adopt a photographic method. Ordinary exposures are subject to serious errors because of Eberhard effect produced by the closely packed star images in the Milky Way clouds. We therefore constructed a Fabry photometer for use in the focus of the Yerkes 40-inch refractor. The optical arrangement is shown in Figure 1. The apertures in the focal diaphragm, D, have diameters of 1.7 mm = 18″.0 and 11.92 mm = 126″.4. The former is used to photograph stars of the North Polar Sequence for purposes of standardization, while the latter is used for the surface brightnesses of the sky.

If E is the light intensity of a star and B is the surface brightness of the area under investigation, then the method consists in finding such a star that

$$E + B\omega' = B\omega ,$$

[11] Had we used simple elementary considerations based upon the assumption that the reflecting nebula is a plane surface for which Lambert's law of reflection holds, we should have found $I = 2AI_0$, where A is the albedo of the surface. The assumption, frequently made in similar computations, that the luminosity of the source is spread over a sphere of unit radius, corresponds to the case where the elements of the nebula reflect the incident light equally in *all* directions (or over a solid angle of 4π). This is not consistent with Seeliger's theory.

[12] Bottlinger's tables in *Zs. f. Ap.*, **4**, 382, 1932, are expressed in these units.

[13] *Pub. Astr. Lab. Groningen*, **31**, 1921.

where ω' is the solid angle subtended by the smaller diaphragm, as seen from the center of the 40-inch lens, and ω is the solid angle subtended by the larger diaphragm. In our instrument $\omega' = 254$ square seconds of arc and $\omega = 12{,}550$ square seconds of arc.

The $f:1$ lens O′ is focused at the 40-inch objective, forming an image of uniform density in its focal plane P. The appearance of the images is the same for star and sky. Well-exposed images of stars of photographic magnitude 12 taken with the narrow diaphragm, or of the sky taken with the wider diaphragm, were obtained in five minutes on Eastman Hyper-Press plates.

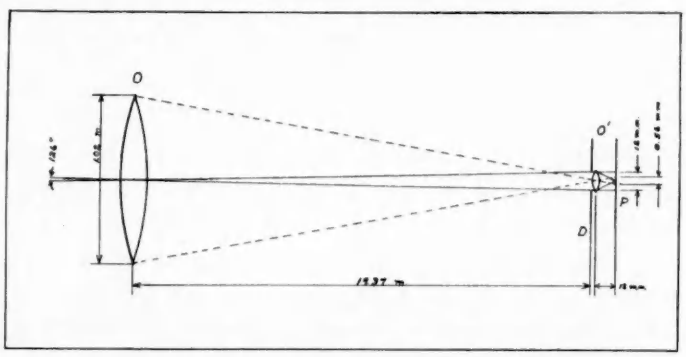

FIG. 1.—Optical arrangement of Fabry photometer

The plates were standardized with a tube sensitometer, and the measures were made with a Hartmann microphotometer. The wedge readings of the sensitometer spots gave an interpolation curve by means of which all observations were expressed in terms of Δm. These were then calibrated by means of the photographic magnitudes of the comparison stars. All observations were made, as nearly as was possible, at the zenith-distance of the pole.

Since

$$B\omega = \frac{E}{1 - \frac{\omega'}{\omega}},$$

we find that all observations of $B\omega$ obtained directly from the reduction curves must be corrected by adding to the stellar magnitudes the quantity $\Delta m = 2.5 \log [1 - (\omega'/\omega)] = 0.02$ mag. Since this correc-

PLATE VI

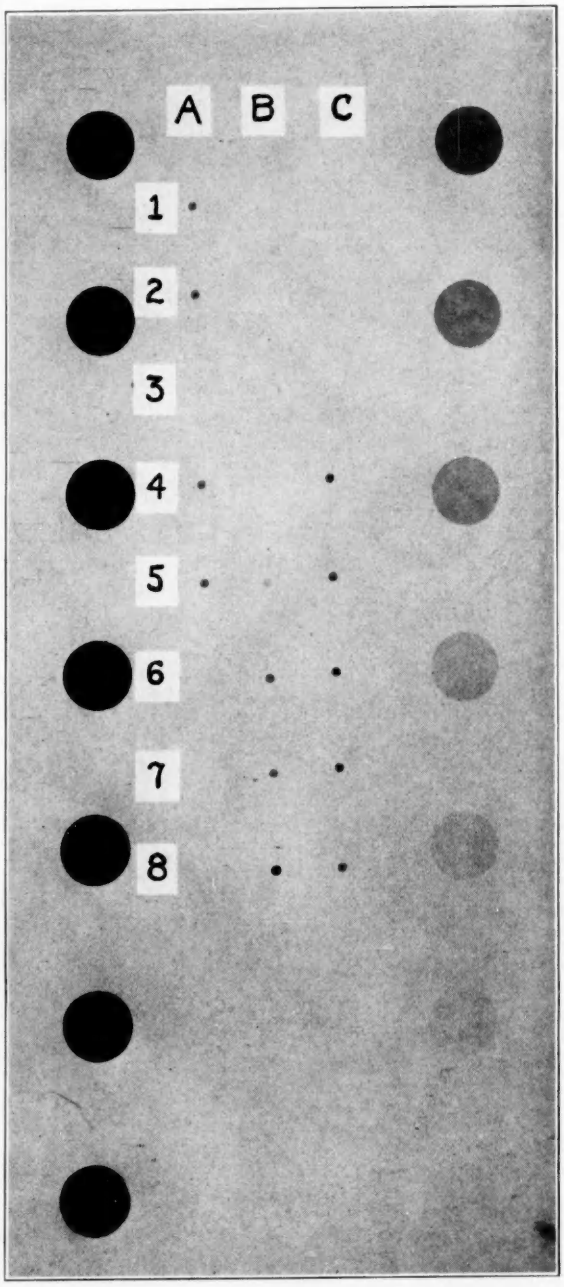

OBSERVATIONS OF B201 AND B15 WITH THE FABRY PHOTOMETER

tion is a constant for all observations, we have omitted it in the results given below. We have also disregarded another very small constant correction resulting from the fact that, on the average, the absorption in the glass of O' is slightly larger for the star than for the sky. This correction is probably negligible.

III

Plate VI is a reproduction from a photograph taken for dark nebulae B201 and B15. The various images are as follows:

Image	Object	Mag.	Image	Object	Mag.	Image	Object	Mag.
A1....	B201	11.49	B5....	N.P. Seq. 18	12.28	C8....	Sky (pole)	11.65
A2....	M.W. sky	11.51	B6....	Sky (pole)	11.59	C7....	B15	11.47
A4....	M.W. sky	11.51	B7....	N.P. Seq. 17	11.88	C6....	M.W. sky	11.40
A5....	B201	11.46	B8....	N.P. Seq. 13	10.52	C5....	B15	11.45
						C4....	M.W. sky	11.43

Means	Sky (pole).....	11.62
	B201−comp....	− 0.03
	B15−comp.....	+ 0.04

In order to obtain B per square degree, the observed magnitudes should be corrected by -7.54 mag. To express B per square second, the correction is $+10.24$ mag.

The advantage of our photometer lies in the small aperture of D and the great light-gathering power of O. In setting up the field, we were able to avoid all stars brighter than photographic magnitude 16. Even in dense regions of the Milky Way it was usually possible to find a comparison field in which there were no stars as bright as the 16th mag. It is well known that the stars of about the tenth magnitude are most effective in producing the stellar illumination of the whole sky.

Bottlinger's tables[14] can now be used to compute the effect of the unresolved faint stars. We find that for galactic latitude 0° there are the equivalent of 28 stars of apparent magnitude 10.0 per square degree, beginning from $15^{M}.5$, and the equivalent of 21 stars, beginning from $16^{M}.5$. The observed average magnitude of the sky is

[14] *Zs. f. Ap.*, **4**, 372, 1932.

almost exactly 4 mag., or 250 stars of magnitude 10. Hence, the correction for the stars is

$$b=0^\circ \begin{cases} \text{Beginning at } 15.5 \text{ mag.}: \Delta m = +0.11 \\ \text{Beginning at } 16.5 \text{ mag.}: \Delta m = +0.09 \end{cases}$$

$$b=15^\circ \begin{cases} \text{Beginning at } 15.5 \text{ mag.}: \Delta m = +0.06 \\ \text{Beginning at } 16.5 \text{ mag.}: \Delta m = +0.04 \end{cases}$$

In the absence of accurate star counts reaching below the limiting magnitude of the 40-inch telescope, we can correct all observations of the comparison fields by amounts computed as shown above.

If the dark nebulae are completely opaque, their observed brightnesses are directly comparable to the corrected results for the comparison fields. We neglect here the foregound stars fainter than the 16th mag. If, however, the nebula is not completely opaque, then the foregoing procedure would result in an overcorrection of the comparison fields. Suppose, for example, that the nebula absorbs three magnitudes. Then all entries of Bottlinger's tables should be shifted toward fainter apparent magnitudes by three steps, and each entry should be divided by num. log $3/2.5=16$. For $b=0$ we find that the nebula will contain approximately the equivalent of 4 stars of magnitude 10, beginning at 16 mag, so that the overcorrection would amount to 0.02 mag.

A summary of the observations is given in Table II. The mean deviation of the observations is only 0.02. Accordingly, the variation in the brightness of the sky at the pole is real. For example, on August 29 the sky at the pole was 0.16 mag. fainter than on August 24. The corresponding brightnesses of B201 and its comparison field show similar changes. We attribute these changes to rapid fluctuations of the atmospheric radiation. The average differences, *sky at pole minus nebula* and *sky at pole minus comparison field*, are of the order of +0.1 or +0.2 mag. This is due partly to the effect of unresolved stars in the comparison field and partly to the zodiacal light, which, on the average, was probably stronger in the Milky Way fields than at the pole. An attempt to correct the observations by means of Van Rhijn's table for the zodiacal light did not yield useful results: the observations are not sufficiently numerous and the table may not be sufficiently accurate.

The average uncorrected value for the difference, *nebula—comparison*, is +0.03. The corrected difference is −0.04. In spite of the uncertainty in the corrections, the latter value is probably preferable. It is surprising that this value is so much smaller than that computed by us from Seeliger's theory, viz., 0.15 mag. Two explanations may be advanced: (1) the albedo of the particles is smaller than that assumed in Schönberg's article; (2) the scattering in interstellar space is nearly as efficient as the scattering within the dark nebulae.

TABLE II

OBSERVATIONS WITH THE FABRY PHOTOMETER

Date 1935	Sky (Pole) Mag.	No.	Nebula			Comp. Field Mag.	Neb.—Comp. Mag.*	No.	Correction Mag.	Neb.—Comp. Corrected*
			Name	b	Mag.					
Aug. 4...	11.38	5	.....	.....	.....	.....	.....	.....	.....	.....
7...	11.90	5	.....	.....	.....	.....	.....	.....	.....	.....
22...	11.60	1	B316	0°	11.45	11.46	−0.01	1	−0.08	−0.09
23...	11.40	2	B139	− 8	11.26	11.17	+ .09	2	.06	+ .03
24...	11.46	2	B201	− 3	11.22	11.22	.00	2	.07	− .07
29...	11.62	2	B201	− 3	11.48	11.51	− .03	2	.07	− .10
30...	.....	.....	B15	0	11.46	11.42	+ .04	2	.08	− .04
Sept. 29...	.....	.....	B5	−15	.....	.....	.00	2	.04	− .04
Oct. 2...	11.62	4	B15	0	11.55	11.47	+ .08	6	.08	.00
25...	.....	.....	B15	0	11.55	11.48	+0.07	5	−0.08	−0.01
Mean	.....	.....	.....	.....	.....	.....	+0.03	.....	.....	−0.04

* A positive sign indicates that the nebula is fainter than the comparison field.

There is good reason to think that the second explanation, at least, holds true. Struve has shown[15] that theoretically we may expect a considerable amount of scattering from the material which produces the space-reddening of distant stars. Dufay[16] has pointed out that if the medium is sufficiently dense, the interstellar scattering in the galactic plane may at best double the amount of light received by us from the stars. For such a medium, the scattered light from interstellar space and from the dark nebulae would be identical, provided the particles have similar albedoes.

[15] *Ap. J.*, **77**, 152, 1933; see also *ibid.*, **82**, 271, 1935.

[16] *Op. cit.*, p. 41.

A special study was made of B15, which on Barnard's original photograph shows a large opaque area with a central core that is appreciably blacker than the—also opaque—outer portions. The latter do not appreciably differ in surface brightness from the uncorrected surface brightness of the sky in the comparison fields. The results of the observations are given in Plate VII. Within the nebula proper the correction for unresolved stars is zero. Consequently, we are here dealing with real differences in the surface brightness of an interstellar object. These differences amount to about 0.08 mag., the central parts of the nebula being by that amount darker than the outer regions.

A careful inspection of many dark nebulae listed by Barnard shows that a considerable number of them—but by no means all—contain such dark centers. The conclusion is obvious that the increased brightness of the outer regions of the dark nebulae and of the Milky Way comparison fields is produced by interstellar scattering. If the inner cores of these nebulae are intrinsically black (which is not probable), we have a minimum value for the interstellar illumination which is equivalent to about thirteen stars of magnitude 10. This is approximately one-third of the value computed for the dark nebulae.

The existence of black cores is not easy to explain. If the nebulae are composed of particles of similar properties, photometric theory would predict that the nebulae should be brightest near their centers, provided the general illumination by starlight is reasonably uniform. The fact that dark cores exist may mean that the central portions of the dark nebulae are composed of material having a lower albedo than the outer portions.

Dr. C. Hetzler and Dr. S. Arend have assisted in some of the computations, and Dr. F. W. Cooke has participated in the observations. Mr. O. C. Collins has taken the photograph reproduced in Plate VIII.

YERKES OBSERVATORY
November 26, 1935

PLATE VII

PLATE VII

S

E

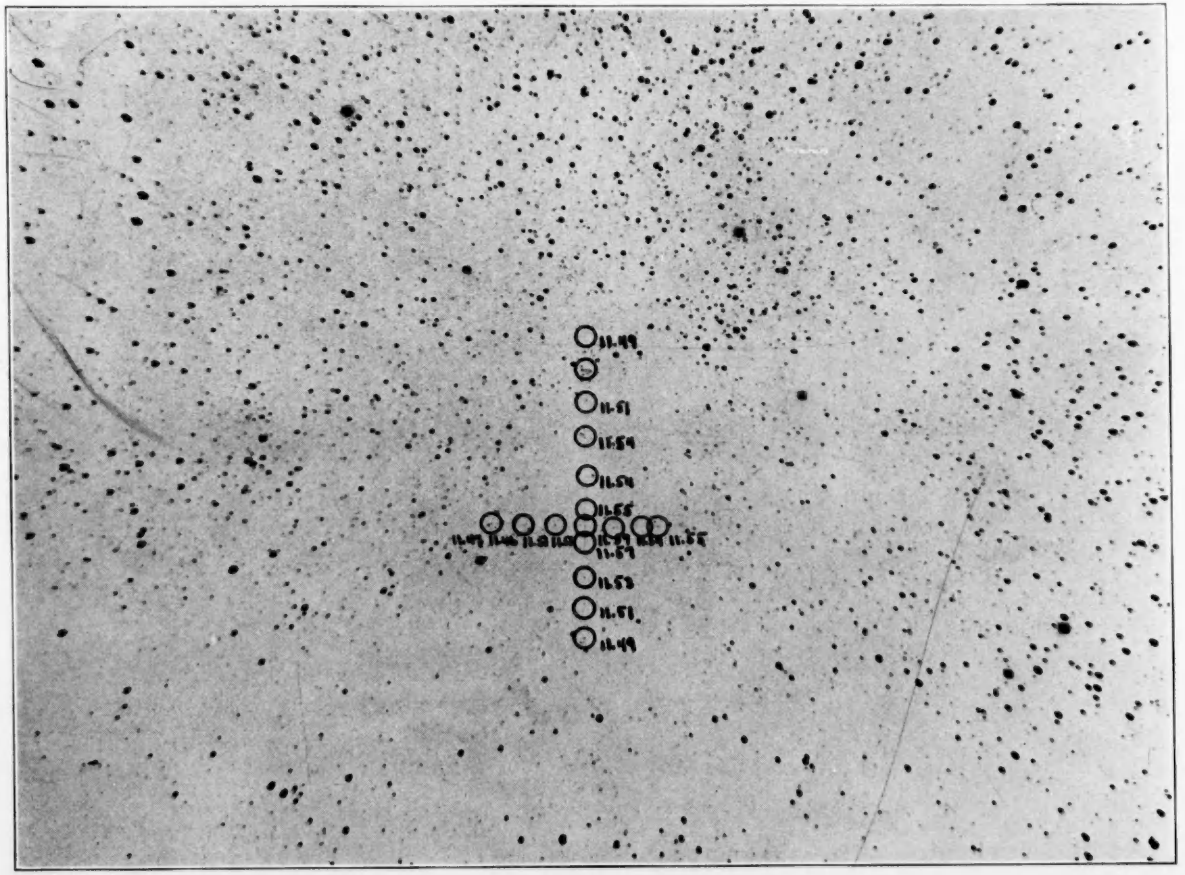

W

N

SURFACE BRIGHTNESSES IN B15

PLATE VIII

N

N

E

W

S

REFLECTOR PLATE OF B15 TAKEN BY O. C. COLLINS

NOTE ON THE SPECTRUM OF Z CENTAURI

CECILIA PAYNE GAPOSCHKIN

ABSTRACT

The spectrum of the supernova Z Centauri can be interpreted as that of a nova in the "4640" stage with abnormally wide bright lines. Since Nova Aquilae No. 4 appears not to be a nova at all, this observation removes from the lists all the supposed novae that showed only absorption spectra after maximum.

The spectrum of Z Centauri, one of the very few photographed spectra of supernovae, has long presented a puzzle, not only because spectral class R is usually assigned to it, but also because of the conflicting nature of most of the spectroscopic observations concerning it. In the light of present knowledge it seems that some of the conflict can be removed and the nature of the object better understood than has hitherto been possible.

The existing observations must first be reviewed. The discovery, from the spectral peculiarity, is announced in *Harvard Circular*, **4**, 1895, where the spectrum is likened to that of the nebula surrounding 30 Doradus (class Pd) and to that of AGC 20937 = HD 137613, now known to be of class Ro. In spite of this apparent contradiction, Pickering stated that "the star appears to have changed into a gaseous nebula." The spectroscopic observation was made on July 18, 1895, at least ten days but not more than thirty-five days after the star attained its maximum brightness.[1] On December 16, 1895, after the nova had faded four magnitudes, its spectrum was observed visually to be "monochromatic."[2]

On December 22 and 29, 1895, the spectrum of the star was examined visually by W. W. Campbell, who was

> reasonably certain that the spectrum was continuous . . . . certainly not nebular. . . . . The maximum visual intensity was in the yellow-green, the green-blue was very faint, while the blue was surprisingly strong. In fact, the blue

[1] *Harvard Circ.*, **4**, 1895.

[2] This rather peculiar and ambiguous description presumably means that most of the light was confined within a narrow spectral range. If the light had consisted of one narrow bright line, the observer would probably have said so. We suggest that the region seen at Harvard was Campbell's "yellow-green."

was very much brighter visually than the green-blue. The spectrum was relatively very faint from about λ 5200 to λ 4600. There was no trace of the nebular lines visible, nor of the *Hβ* line. There was some evidence of bright lines or of irregularities in the brightest portion of the spectrum, but the light was too weak to enable me to decide.[3]

A later classification of the Harvard photograph[4] inclined to give weight to the second identification of *Harvard Circular*, **4**, and estimated the spectrum as of class R.

It was noted in *Harvard Circular*, **4**, that Z Centauri appeared near to NGC 5253, and concerning this object also there has been considerable variety of opinion. Pickering did not comment upon its spectrum, but noted that on December 16, 1895, the spectrum of the star (then given as "monochromatic") resembled it. W. W. Campbell, however, observed on February 8, 1896:

> The nebula's spectrum was of the usual type, the lines at λλ 5007, 4959, and 4862 having their usual relative intensities. The line near λ 4690 seemed to be present, as in the case of NGC 7027. . . . . Is it not possible that the observed spectrum [at Harvard] was that of the nebula, and not that of the star?

In the Harvard catalogues of nebulae NGC 5253 is given as of class Sa and apparent magnitude 10.8.[5] Hubble and Lundmark, while not regarding the nebula as a typical spiral, described its spectrum as follows: "It seems to belong to the kind typical of spirals and other non-galactic nebulae; a strong continuous spectrum of approximately the type G, without bright lines or bands."[6] It seems to be the general opinion that NGC 5253 is an extra-galactic system, showing the not uncommon feature of localized bright lines. If this is admitted, we may conclude with fair confidence that Z Centauri is a typical supernova. It was regarded as such by Baade and Zwicky.[7]

If the star is regarded as a supernova, a spectrum of class R, at least ten days after maximum, is somewhat difficult to understand. Indeed, some investigators have sought refuge in the suggestion that the star may actually not be a nova, Lundmark[8] suggesting that it may possibly be a long-period variable of very long period, and

[3] *Ap. J.*, **5**, 234, 1897.

[4] *Harvard Ann.*, **76**, 37 and Plate 2, 1913.

[5] *Ibid.*, **88**, No. 4, p. 100, 1934.

[6] *Pub. A.S.P.*, **34**, 292, 1923.

[7] *Proc. Nat. Acad.*, **20**, No. 5, 1934.

[8] *Op. cit.*, **33**, 316, 1922.

Ludendorff[9] placing it tentatively with the R Coronae Borealis stars, in company with Nova Aquilae No. 4, which will be discussed later.

After repeated examinations of the spectrum, it occurred to the present writer that it might well be considered a bright-line spectrum with very wide lines. A reason for suspecting that it was not of class R lies in the great strength of the red end of the spectrum, which embraces within a couple of hundred angstroms more than half the total light of the object, and perhaps accounts for the description "monochromatic." It appears that the same impression of "a hazy bright line spectrum" had been independently received by Dr. Baade and Dr. Merrill at Mount Wilson.[10]

The crucial point is the wave-length of the intense portion of the spectrum at the redward end; if the spectrum is of class R, the center of this "bright" portion should lie at about 4800 A. Fortunately, the Harvard spectrum is on an objective-prism plate, so that the wave-length can be measured. Mr. Johnson has described the measures and results elsewhere.[11] He has established beyond doubt that the spectrum is not of class R. It could be interpreted as that of a nova in the "4640" stage, with bright lines perhaps five times as broad as those usually observed in the spectra of novae.

It may be noted that as the outburst of a supernova appears to be more violent than that of a normal nova, an interpretation of the spectrum suggesting radial velocities of the order of 10,000 km/sec is not impossible.

The spectrum of Z Centauri on the Harvard plate is clearly that of a seventh-magnitude object. As the nebula is of the eleventh magnitude, its spectrum cannot contribute to that observed on this plate. A search of all other spectrum plates of the region has revealed none that shows the spectrum of the nebula, so that W. W. Campbell's question can be answered in the negative, so far as the photographic observation is concerned. Concerning the Harvard visual observation of the spectrum of Z Centauri, a low-dispersion spectrograph would have given that impression visually if the spectrum resembled the one that was earlier photographed. There

[9] *A.N.*, **217**, 172, 1922.

[10] Private communication.

[11] *Harvard Bull.*, **902**, 1936.

is, of course, a possibility that the Harvard observation of a "monochromatic" spectrum refers to the nebula; but if it refers to the nova, there is no inconsistency.

Thus the class R spectra of Z Centauri and S Andromedae[12] resolve themselves on closer scrutiny into bright-line spectra. There remains the case of Nova Aquilae No. 4, for which Lundmark, two years after its discovery, obtained an excellent spectrum of class Ro.[13] The present writer, after collecting all the photometric observations, has concluded that this star is not a nova, but a long-period variable of the type of V Hydrae or W Orionis, which have spectra of class N. A similar conclusion was independently reached, on the basis of unpublished observations, by Graff.[14]

[12] *Ap. J.* (in press).

[13] *Op. cit.*, **33**, 316, 1921.

[14] *Beob. Zirk.*, **5**, 41, 29, 1932.

NOTES

A SEARCH FOR THE BANDS OF BORON COMPOUNDS IN STELLAR SPECTRA

In the course of an investigation of the SiF bands in late-type stellar spectra,[1] we found that a careful search for BH in the spot spectrum, with very high dispersion, would be valuable, as BH gives the only possibility of blending for the SiF band head at λ 4368. Such a search has been made by R. S. Richardson,[2] who has shown conclusively that the bands of BH are absent in the spot spectrum.

We have tried without success to find the BH bands in late-type stars. Advantage was taken of the fact that sixteen strong lines of the Q branch near λ 4332.7 should be superposed. We first used plates of K and M stars taken with the three-prism spectrograph of the Yerkes Observatory; afterward, we used coudé and other plates of the Mount Wilson Observatory for spectral types as far as M8.[3] No trace of BH appeared.

This absence seems rather surprising. The computation of the theoretical numbers of BH and BO molecules made according to Russell's theory[4] shows that the BH molecules should be much more abundant in M stars than BO is in the sun-spots. The absence of the BH bands is thus interesting in connection with the abundance of boron in stellar atmospheres. Owing to the fact that the boron atom has an unobservable ultra-violet spectrum, a careful search for BO in late-type spectra of sufficient dispersion would be valuable.[5] BO has been found in the spot spectrum by Nicholson and Perrakis,[6] but it has not been definitely observed in any late-type star. Theo-

[1] *Arkiv för Matem., Astr. och Fysik*, **25**, B, No. 2.

[2] *Pub. A.S.P.*, **47**, 275, 1935.

[3] We are indebted to Dr. Joy for these plates.

[4] *Ap. J.*, **79**, 317, 1934.

[5] Theoretically, BO is more abundant in M giants than in M dwarfs; the contrary is true for BH.

[6] *Ap. J.*, **68**, 327, 1928.

retically, the number of BO molecules must be more than a thousand times greater in M stars than in the sun-spots, and thus the BO bands should appear unless the sun is exceptionally rich in boron.

P. SWINGS

YERKES OBSERVATORY
December 17, 1935

A II IN THE SPECTRA OF B-TYPE STARS

In a recent note[1] we have given some evidence for the presence of *A* II in the spectra of B-type stars. A careful discussion showed that most of the strong *A* II lines are hopelessly blended with lines of other elements, but the presence of the *A* II line λ 4348 in γ Pegasi and β Orionis seems to manifest the presence of this element.

Recent investigations by B. Edlén[2] show that several lines which had been previously attributed to *N* II[3] (namely, λλ 6114.6, 4806.0, 4765.0, 4735.8, 4726.9, 4609.60,[4] 4426.05, etc.) are actually due to argon. Consequently, the stellar line λ 4425.95 which appears in γ Pegasi and β Orionis is not due to *N* II but has to be attributed to λ 4426.01, intensity 15 ($4s^4P_{3/2}-4p^4D^\circ_{5/2}$), of *A* II.

This supplementary result gives conclusive evidence for the presence of *A* II in normal stellar spectra.

M. NICOLET

DEPARTMENT OF ASTROPHYSICS
UNIVERSITY OF LIÉGE (BELGIUM)
November 28, 1935

[1] *Bull. Acad. Roy. Belg.*, **21**, 186, 1935.

[2] Private communication. To appear soon in *Zs. f. Phys.*

[3] A. Fowler and L. J. Freeman, *Proc. R. Soc.*, A, **114**, 662, 1927.

[4] Consequently, *N* II does not take part in the stellar line 4609.70.